Natural Products from Endophytic Fungus *Talaromyces wortmannii*: Their Structure Elucidation and Mechanism of Actions

(Naturstoffe aus dem Endophyten *Talaromyces wortmannii*, deren Strukturaufklärung und Wirkungsmechanismen)

Inaugural-Dissertation

zur

Erlangung des Doktorgrades

der Mathematisch-Naturwissenschaftlichen Fakultät

der Heinrich-Heine-Universität Düsseldorf

vorgelegt von

Robert Antonius Bara

Aus Manado , Indonesien

Düsseldorf, 12.11.2012

Aus dem Institut für Pharmazeutische Biologie und Biotechnologie

der Heinrich-Heine Universität Düsseldorf

Gedruckt mit der Genehmigung der
Mathematisch-Naturwissenschaftlichen Fakultät der
Heinrich-Heine-Universität Düsseldorf

Gedruckt mit der Unterstützung des
Deutscher Akademischer Austausch Dienst (DAAD)

Referent: Prof. Dr. Peter Proksch
Koreferent: Prof. Dr. Matthias Kassack
Tag der mündlichen Prüfung: 19.12. 2012

Erklärung

Hiermit erkläre ich ehrenwörtlich, dass ich die vorliegende Dissertation mit dem Titel „Naturstoffe aus dem Endophyten *Talaromyces wortmannii*, deren Strukturaufklärung und Wirkungsmechanismen“ selbst angefertigt habe. Außer den angegebenen Quellen und Hilfsmitteln wurden keine weiteren verwendet. Diese Dissertation wurde weder in gleicher noch in abgewandelter Form in einem anderen Prüfungsverfahren vorgelegt. Weiterhin erkläre ich, dass ich früher weder akademische Grade erworben habe, noch dies versucht habe.

Düsseldorf, den 12.11.2012

Robert A. Bara

To God Almighty!

and to my parents, Junus Bara and Suharningsih Sastra

Contents

= Chapter 1 =

General Introduction

Endophytes, from symbiosis (mutualism) to drug discoveries

Symbioses

Symbioses, intimate interactions between different species, are widespread. They range from being beneficial to one species at the cost of the other (parasitic) to being mutually beneficial (mutualistic). Mutualistic symbiosis often play dominant role in ecosystems, as the combined characteristics of two different organisms in a mutualism allow them to exploit previously inaccessible niches (Herre *et al.* 1999).

The word endophyte means "in the plant" (from gr. Endo = within, phyton = plant). The usage of this terminology is as broad as it is literal definition and spectrum of potential host inhabitants e.g. bacteria (Kobayashi and Palumbo 2000), fungi (Stone *et al.* 2000), parasitic plant endophytes (Marler *et al.* 1999) and insects in plants (Feller 1995), but also for algae within algae (Peters 1991), in latent developmental phases to mutualism, commensalism or parasitism to the plant itself (Sinclair and Cerkauskas 1996). Any organ of the host can be colonised. Equally variable is the usage of the term "endophyte" for variable life history strategies of the symbiosis, ranging from facultative saprobes to parasites, from exploitative to mutualistic organisms. Bacon and White (2000), give an inclusive and widely accepted definition of endophytes, "Microbes that colonize living, internal tissues of plants without causing any immediate, overt negative effects". While the symptomless nature of endophyte occupation in plant tissue has prompted focus on symbiotic or mutualistic relationships between endophytes and their hosts, the observed biodiversity of endophytes suggests that they can also be aggressive saprophytes or opportunistic pathogens.

Endophytes can be transmitted from one generation to the next through the tissue of host seed or vegetative propagules (Carroll 1988). Apparently, acquired chemical defense appears to be a common basis for endophytic association between a plant and its particular

endosymbiont (Carroll 1988; Clay 1988). They also play important roles in ecosystem processes such as decomposition and nutrient cycling, and have beneficial symbiotic relationships with roots of many plants (Christensen 1989).

They were relatively unstudied as potential sources of novel natural products for exploitation in medicine, agriculture, and industry. Among 300 thousand higher plant species, each individual plant is a host to one or more endophytes (Strobel *et al.* 2004). Recently, several new bioactive products were isolated and identified with unique core structures and potent biological activities (Debbab *et al.* 2009; Aly 2010; Proksch *et al.* 2010; Aly *et al.* 2011; Aly *et al.* 2011; Debbab *et al.* 2011; Debbab *et al.* 2012; Debbab *et al.* 2012; Ebrahim *et al.* 2012)

Ultimately, biological diversity implies chemical diversity due to the constant chemical innovation that exists in ecosystems where the evolutionary race to survive is the most active. Tropical rainforest are a remarkable example of this type of environment. In this type of ecosystem, the resistance of endophytes is great, resources are limited and selection pressure is at its peak. This gives rise to a high probability that rainforest endophytes are new sources of novel molecular structures with interesting biological activities.

In particular, the ability to produce a large number of chemically different secondary metabolites is associated mainly with the filamentous fungi for the eukaryotes (Donadio *et al.* 2002).

Drug discovery

Drug discovery and development has a long history and dates back to the early days of human civilization. In those ancient times, drugs were not just used for physical remedies but were also associated with religious and spiritual healing.

The nature itself, has constantly supplied mankind with a broad and structurally diverse array of pharmacologically active compounds that continue to be utilised as highly effective drugs to combat a multitude of deadly diseases or as lead structures for the development of novel synthetically derived drugs that mirror their models from nature (Proksch *et al.* 2002). These products have been exploited for human use for thousands of years, and plants have been the chief source of compounds used for medicine. China, for example, with more than

5,000 plants and plant products in its pharmacopeia, is the largest user of traditional medicines. In reality, aspirin (acetylsalicylic acid), which is derived from the glycoside salicin and is found in many species of the plant genera *Salix* and *Populus* is the world's best known analgesic used as a medicine. Examples abound of natural-product use, especially in small native populations in remote locations on earth. They include ethnic groups in the Amazon, mountain communities in Papua Island, spread all over west Papua, Indonesia and Papua New Guinea and the Aborigines population in Australia. All these mentioned populations have recognized definite plants to provide relief of symptoms that varying from a common cold, over fever to massive wounds and intestinal problems (Isaacs 2002). History also records that extinct civilizations had also discovered the benefits of medicinal plants. For example, around 1000 B.C., the Mayans used fungi grown on roasted green corn to treat intestinal sickness (Buss and Hayes 2000). Later, the Benedictine monks (800 AD) began to apply *Papaver somniferum,* which belongs to the poppy family (*Papaveraceae*), as an anesthetic and analgesic. While, the ancient Greeks, Romans and Egyptians had used it for centuries before as a medicine and sleeping aid. Its species name, *somniferum*, comes from the latin language meaning sleep bringing and was chosen because its seducing, relaxing and sleep-forcing effects. Centuries ago, people realized that leaves, roots, and stems of particular plants had the potential of enhancing quality of life, reducing pain and suffering, and providing relief, even though an understanding of the chemical nature of bioactive compounds in these complex mixtures and how they acted remained unknown. It wasn't until Pasteur discovered that fermentation caused by living cells that people is started to investigate microbes as a source for bioactive natural products (Strobel and Daisy 2003).

Then, by fortune, in 1928, Alexander Fleming, a Scottish scientist, found penicillin (figure 1) from the mold *Penicillium notatum*. He observed that colonies of the bacterium *Staphylococcus aureus* could be destroyed by the mold *Penicillium notatum*. Although this result was the milestone of the beginning of the antibiotic era, at that time, the importance of Alexander Fleming's discovery was not known (Bellis 2012). Up till the 1940s when Howard Florey and Ernst Chain isolated the active component and developed a powdery form of the medicine, due to the outbreak of the Second World War which increased the urgency with which the development was carried on to a success. The yield of penicillin had

been increased, which resulted in a breakthrough in the treatment of bacterial infections (Bellis 2012).

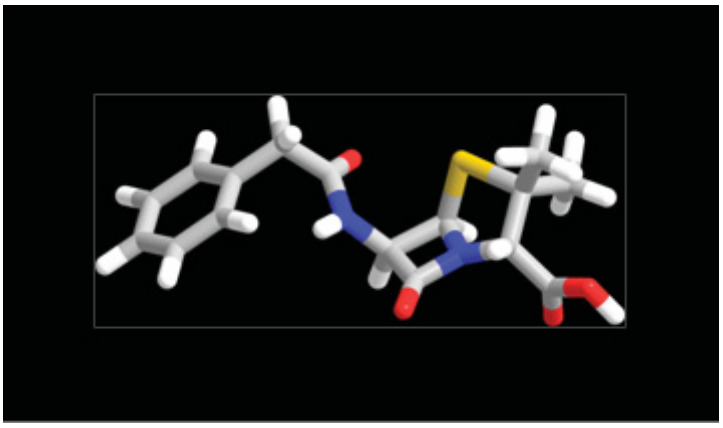

Figure 1. 3D-structure of benzyl-penicillin

The emerge of antibiotic resistance in bacteria

The introduction of antimicrobials transformed human and animal health systems by revolutionizing our weaponry in the war against infectious diseases, resulting in improved survival for both humans and their live stocks. Nevertheless, this health achievement was immediately overshadowed by the fact that bacterial populations can modify themselves to resist against antimicrobials, spread these resistance traits, and even share resistance genes with other bacteria. Such abilities have severely compromised the usefulness of antibiotics in the war against microbes and warn of a future when antimicrobials may have very limited usefulness to control diseases caused by bacteria (Alekshun and Levy 2007).

Antimicrobial resistance is the ability of a microorganism to survive and multiply in the presence of an antimicrobial agent that usually is able to inhibit or kill this organism. Antimicrobial resistance is just one of the many adaptive traits that resilient bacterial subpopulations may possess or acquire, enabling them to outcompete and survive their microbial neighbors and overcome host strategies aimed against them. The first antibiotic resistance mechanism described was that of penicillinase. Its presence and activity was first reported by (Abraham and Chain 1940) shortly after its discovery (table 1). At that time, the incidence of bacterial resistance was getting worse, penicillin-resistant *Staphylococcus aureus* was observed in the majority of Gram-positive infections in the population. The

initial response by the pharmaceutical industry was to develop beta-lactam antibiotics that were unaffected by the specific beta-lactamases secreted by *S. aureus*. However, bacterial strains producing beta-lactamases with different properties began to emerge, as well as those with other resistance mechanisms (Bush 1988).

The same things happened to other antibiotics, very soon after their introduction in the late 1940s, resistance to streptomycin, chloramphenicol and tetracycline was noted (Schofield 2011) . By 1953, during a *Shigella* outbreak in Japan, a strain of the dysentery bacillus (*Shigella dysenteriae*) was isolated which has multiple drug resistant, exhibiting resistance to chloramphenicol, tetracycline, streptomycin and the sulfonamides (Todar 2012). This cycle of resistance continues even today. In 1983 after a Multi Resistant *Staphylococcus aureus* infection outbreak in major western Australia hospitals it was recorded that about 5 % of those multi resistant *S. aureus* could only be treated with vancomycin (Dailey *et al.* 2005). Now, even that last line of defense is looking insecure. In 1997, a *S. aureus* strain partially resistant to vancomycin was found in Japan which was called Vancomycin intermediate *Staphylococcus aureus* (VISA). In USA, only eight cases of infection caused by VISA are known (Michigan 1997, New Jersey 1997, New York 1998, Illinois 1999, Minnesota 2000, Nevada 2000, Maryland 2000, and Ohio 2001) while, for vancomycin resistant *Staphylococcus aureus* (VRSA), eleven cases of infection (eight in Michigan 2002-2009, one in Pennsylvania 2002, one in New York 2004 and three in Detroit from 2010-2012) have been reported (CDC 2012). Although the incidence is categorized as rare, it seems to increase in number

What is most alarming these days is the rate at which antibiotic resistance often develops and how quickly it spreads across the world and among different species of bacteria. Furthermore, as a result of sequential, cumulative acquisition of resistance traits against different antibiotics, more bacterial pathogens with multiple-drug resistance are being reported worldwide and as a consequence, many bacterial organisms, including major human and animal pathogens such as Mycobacterium and Salmonella species, have become resistant to antibiotics which were before quite efficacious (Alekshun and Levy 2007).

Table 1. Antibiotic vs. bacterial resistance in timeline (Giguère 2006)

1929	Discovery of penicillin (1929)	
1930-1940	Introduction of sulfonamide	Efficacy of penicillin in humans shown; sulfonamides introduced in food animal use
1941 to 1950	Introduction of streptomycin (1944), chloramphenicol (1946) and chlortetracycline (1948)	Penicillin made available to the public; widespread use in animals by 1950.
1951 to 1960	Introduction of erythromycin, vancomycin, tylosin and methicillin	Penicillin-resistant infections become clinically significant
1961 to 1970	Introduction of gentamicin (1963), ampicillin (1966), cephalothin (1966), amikacin (1970)	Emergence of gentamicin-resistant Pseudomonas (1968); emergence of methicillin-resistant staphylococcal infections (1968)
1971 to 1980	Introduction of carbenicillin (1973), cefoxitin (1978), cefaclor (1979)	Increasing trend of nosocomial infections due to opportunistic pathogens; Ampicillin-resistant infections become frequent
1981 to 1990	Introduction of cefotaxime (1981), clavulanic acid-amoxicillin (1983), imipenem-cilastatin (1985), norfloxacin (1986), aztreonam (1986)	Spread of methicillin-resistant Staphylococcus infections; emergence of AIDS-related bacterial infections
1991 to 2000	Introduction of oral extended spectrum cephalosporins (1998), Quinupristin-dalfopristin (1999), linezolid	Emergence of vancomycin-resistant enterococci; emergence of multi-drug resistant *Mycobacterium tuberculosis*; global emergence of multi-drug resistant *Salmonella* enteric serovar *typhimurium* DT 104
2001 to date	Introduction of broader spectrum fluoroquinolones (2001), Telithromycin (2002), Tigecycline (2006)	Emergence of vancomycin-resistant staphylococcal infections; Spread of extended-spectrum beta-lactamase among Gram-negative bacteria; Emergence of more multi-drug resistant organisms

Horizontal gene transfers of antibiotic resistance genes

There is a mechanism beyond spontaneous mutation which is responsible for the acquisition of antibiotic resistance. Horizontal gene transfer is a process whereby genetic entities in small packets of DNA can be transferred between individual bacteria not only of the same species but also between different species (Todar 2012).

Many of the antibiotic resistance genes are carried on plasmids, transposons or integrons that can act as vectors that transfer these genes to other members of the same bacterial species, as well as to bacteria of another genus. This is thought to be the main mechanisms of horizontal gene transfer (Todar 2012). This may occur via three main mechanisms: transformation, transduction or conjugation. Transformation involves uptake of short fragments of exogenous DNA by naturally transformable bacteria. It occurs when the lysed bacteria which carry the particular resistance gene releases the gene and other bacteria are able to gather such genes and incorporate them into their genome. This system is also quite rich in extracellular DNA, either secreted or derived from dead cells. An uptake of foreign DNA has been suggested to play an important role in acquiring antibiotic resistance or increasing pathogenicity of bacteria. Transduction involves the transfer of DNA from one bacterium into another *via* bacteriophages, virus particles which only attack bacteria. Conjugation involves the transfer of DNA *via* a “sexual pilus” a channel made by certain bacteria where small entities of DNA can be passed through and cell-to-cell contact is needed (figure 2) (Slonczewski and Foster 2011). Figure 3 illustrates horizontal gene transfers. DNA fragments that contain resistance genes from resistant donors can then make previously susceptible bacteria become resistant.

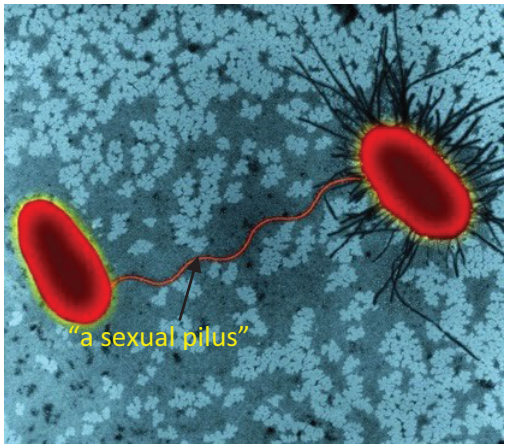

Figure 2. A conjungation between two *E. coli* form a sexual pilus (© (Slonczewski and Foster 2011)

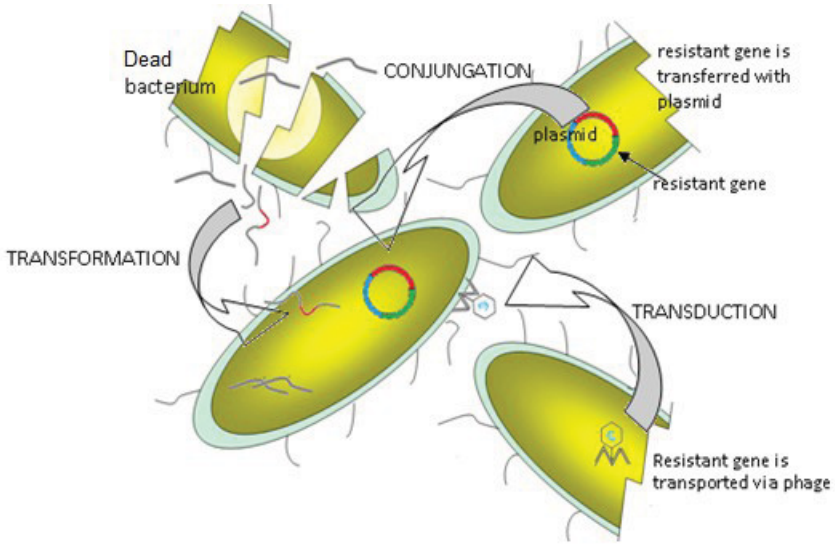

Figure 3. An illustration, horizontal gene transfers (Todar 2012)

What does it all mean for science?

One way of answering to bacterial resistance is developing new classes of antibiotics. The now existing classes of antibiotics were first identified in nature, for example, penicillin, as was mentioned previously. The term "antibiotic" originally referred to a natural compound made by one microorganism which inhibits the growth of another. Since then, scientists

have discovered that all organisms make compounds to fend off bacterial invasion. Up until now, vast numbers of organisms including protista, fungi, plants and animals have been screened in an attempt to discover novel antibiotics or other bioactive compounds to combat selective diseases.

Cytotoxic metabolites and other bioactive compounds

After the discovery of penicillin, the attention of pharmaceutical companies and research laboratories was focused more on fungi as a source of lead compounds. Since then, people have been engaged to search and discover new microbial metabolites with activity against plant, animals and human pathogens. Microbial secondary metabolites represent a vast source of compounds endowed with ingenious structures and potent biological activities (Meenupriya and Thangaraj). Many of the products currently used for human or animal therapy, in animal husbandry and in agriculture are either produced by microbial fermentation, or derived from chemical modification of a microbial product (Donadio *et al.* 2002).

Furthermore, the discovery of an excess of microbes for applications that span a broad spectrum of value in medicine, agriculture and industry is now becoming realistic since the development of novel and cutting-edge screening technologies in both medicine and agriculture.

These processes use individual organisms, cells, enzymes, and site-directed techniques, many times in automated arrays, resulting in the rapid detection of promising leads for product development. In reality, paclitaxel (taxol) (figure 1.4.1) which is very profitable in medicine, was a natural product originally derived from the North American yew tree *Taxus brevifolia* (Wani *et al.* 1971). It is used in chemotherapy for ovarian cancer, breast cancer and certain lung cancers, with a mechanism of action that involves binding to polymerized tubulin thus promoting microtubule formation and microtubule stabilization against disassembly which leads to an inhibition of mitosis. This drug was discovered by the US National Cancer Institute in the 1960s. Later on, after several years of effort, a novel paclitaxel-producing endophytic fungus, *T. andreanae*, was discovered in the plant *T. brevifolia* (Strobel *et al.* 1993). This was the first indication that endophytes were producing

paclitaxel. Therefore, a specific screening was carried out for paclitaxel producing endophytes on continents not known for any indigenous *Taxus* spp. This included an examination of the prospects that paclitaxel-producing endophytes exist in different parts of the globe such as in South America and Australia. From the extremely rare, and previously thought to be extinct, Wollemi pine (*Wollemia nobilis*), the endpophyte *Pestalotiopsis guepinii* was isolated, which was shown to produce paclitaxel (Strobel *et al.* 1997). Unpredictably, *Seimatoantlerium tepuiense,* a novel fungus from a rubiaceous plant, *Maguireothamnus speciosus*, was also shown to produce paclitaxel (Strobel and Daisy 2003). This endemic plant grows in the highland of the Venzuelan-Guyana area in southwest Venezuela. Furthermore, paclitaxel was also produced by *Periconia* sp. (Li *et al.* 1998) and *Seimatoantlerium nepalense*, another novel endophytic fungal species (Bashyal *et al.* 1999). It appears that the distribution of those fungi producing paclitaxel is worldwide and not confined to endophytes of Yews. The fungicide effect of paclitaxel against common plant pathogens, *Pythium* spp. and *Phytophthora* spp might be the best explanation why the particular compound is well distributed and produced by various types of endophytic fungi (Young *et al.* 1992).

Cryptocin (Figure 4.2), a tetramic acid, is also produced by *C. quercina* is an unusual compound which possesses potent activity against *Pyricularia oryzae* and other plant pathogenic fungi (Li and Strobel 2001). It was ineffective against a general array of human pathogenic fungi. Nevertheless, with the minimum inhibitory concentration of 0.39 μg/ml against *P. oryzae*, it is being examined as a natural chemical control agent for rice blast. Given the general interest on behalf of the public and of the industry to develop safer and more environmentally compatible plant disease control agents, endophytic fungi do serve as a reservoir of untapped biologically based compounds that may also be applicable in agriculture.

Another example can be named from our work group, an inseparable mixture of the alterporriol G/H (figure 4.5/6), which are new atropisomers belonging to the bianthracene group which is derived from *Stemphylium globuliferum* (Pleosporaceae), an endophytic fungus from medicinal plant *Mentha pulegium* (Lamiacae) growing in Marroco, exhibited considerable cytotoxicity against L5178Y lymphoma cells with an EC50 value of 3.7 μM

(kahalalide F = 4.3 µM,positive control). These compounds were also tested for protein kinase inhibitory activity in an assay involving 24 different human protein kinases which showed potent inhibitor effects and displayed EC_{50} values between 1.9 and 4.0 µM toward individual kinases. Among the 24 different enzymes tested, kinases Aurora B and CDK4/CycD1 proved most susceptible toward the tested compounds (Debbab *et al.* 2009).

Another example, *Pestalotiopsis jesteri*, isolated from an endemic plant of the Sepik River area of Papua New Guinea, produces jesterone (Figure 4.3) and hydroxy-jesterone, which exhibit antifungal activity against a variety of plant-pathogenic fungi (Li and Strobel 2001). Isopestacin (Figure 4.4), has been obtained from liquid culture of *P. microspora*, an endophyte isolated from a combretaceaous plant, *Terminalia morobensis*, growing in the same place mentioned above (Strobel *et al.* 2002; Harper *et al.* 2003). Isopestacin displays antimicrobial as well as antioxidant activity. Isopestacin is known for its antioxidant activity which is based on its structural similarity to the flavonoids.

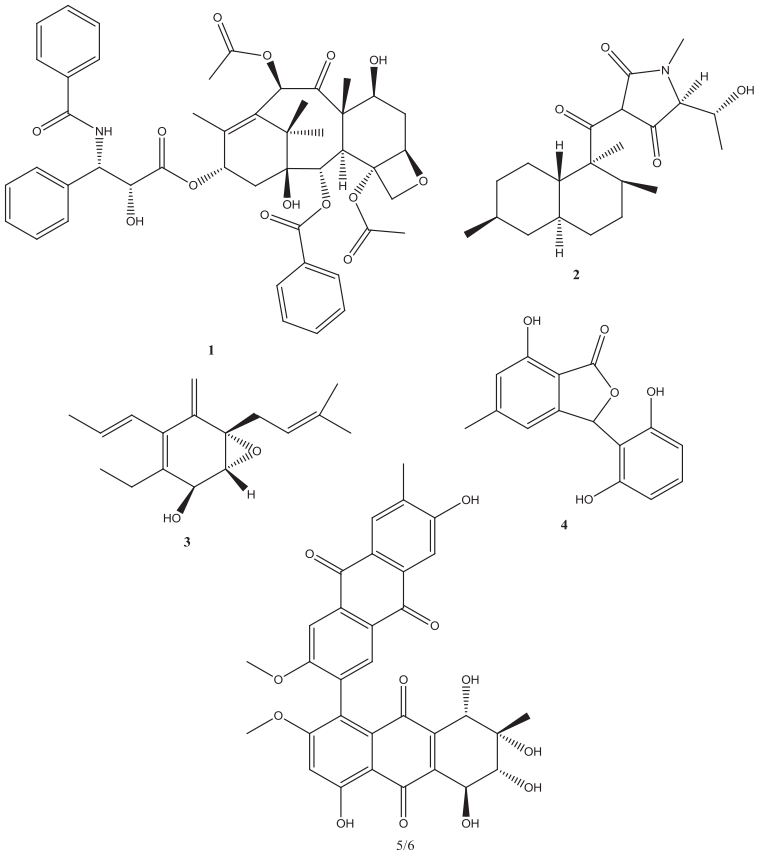

Figure 4. Various types of compounds produced by endophytic fungi, 1. Paclitaxel; 2. Cryptocin; 3. Jesteron; 4. Isopestacin; 5/6. Alterporriol G and H

Scope and outline of this thesis

Since fungal endophytes represent a rich source of bioactive metabolites which have not yet been fully exploited, the aim of this thesis is focused on this matter. The plant material *Aloe vera* collected in Alexandria, Egypt, yielded the fungal endophyte *Talaromyces wortmannii* that was analyzed for its bioactive constituents. The extract which exhibited antibacterial, antifungal or cytotoxic activities was separated using different chromatographic techniques.

In chapter two, six new bisdihydroantracene atropisomers are described. Five of them are new natural products named as flavomannins B-D (**2**-**4**) and talaromannins A (**5**) and B (**6**), together with a known compound flavomannin A (**1**). Their structures were determined on the basis of spectroscopic methods including 1D (^{1}H, ^{13}C and DEPT) and 2D (COSY, HMQC, HMBC, ROESY) NMR experiments, by mass spectrometry as well as CD spectroscopy. These atropisomers are interesting for further studies since they not only have interesting structures but also show activity against pathogenic bacteria including multi-resistant clinical isolates. Among all isolated atropisomers, flavomannin B exhibited a broad spectrum of antibacterial activity against multi-resistant clinical isolates of pathogenic bacteria including *Staphylococcus aureus* and *Pseudomonas aeruginosa*, but was considered inactive when it was tested against pathogenic fungi, the mouse lymphoma cell line (L5178Y), the human leukemic monocyte cell line (THP-1) and the mouse embryonic fibroblast cell line (BALB/3T3) suggesting that it is specifically acting against prokaryotes. The presumable mechanism of action of these atropismers is also presented in this chapter.

In chapter three, a new pure atropisomer named biemodin (**1**) and three wortmannin derivatives (**2**-**4**) reported previously only as synthetic compounds, in addition to eight known compounds (**5**-**11**) are presented. From the isolated compounds only biemodine (**1**) showed an inhibition to several Gram-positive bacteria including the clinical resistant ones.

In chapter four, two other compounds from *T. wortmanni* which are two cyclic peptides named Talaromarin A and B containing six amino acids are presented. The absolute configuration of their amino acids was determined by using Marfrey's Methods. Both compounds are cyclic peptides containing a ring system with 6 amino acids linked to anthranilic acid. The only difference of both peptides is the exchange of D-Val in one compound for D-Ile in the second peptide. Even though no biological activities have been

recorded so far for both peptides after they have been tested against pathogenic bacteria as well as against the mouse lymphoma cell line (L5178Y), both represent new structures and are still interesting for further studies.

Chapter five finally presents comprehensive overview and discusses possible future prospects of this work.

References

Abraham, E. P. and Chain, E. An enzyme from bacteria able to destroy penicillin. Rev Infect Dis. **1940**. 10. 677-8.

Alekshun, M. N. and Levy, S. B. Molecular mechanisms of antibacterial multidrug resistance. Cell.**2007**. 128**:** 1037-1050.

Aly, A. H. Protein kinase inhibitors and other cytotoxic metabolites from the fungal endophyte Stemphylium botryosum isolated from Chenopodium album. Mycosphere. **2010**. 1. 153.

Aly, A. H., Debbab, A., Clements, C., Edrada-Ebel, R., Orlikova, B., Diederich, M., Wray, V., Lin, W. and Proksch, P. NF kappa B inhibitors and antitrypanosomal metabolites from endophytic fungus Penicillium sp. isolated from Limonium tubiflorum. Bioorganic & Medicinal Chemistry. **2011**. 19. 414-421.

Aly, A. H., Debbab, A. and Proksch, P. Fungal endophytes: unique plant inhabitants with great promises. Applied Microbiology and Biotechnology. **2011**. 90. 1829-1845.

Bacon, C. W. and White, J. F. Microbial endophytes.**2000**. New York, Marcel Dekker, Inc.

Bashyal, B., Li, J. Y., Strobel, G. A. and Hess, W. M. Seimatoantlerium nepalense, an endophytic taxol producing coelomycete from Himalayan yew (Taxus wallichiana). Mycotaxon **1999**. 72. 33-42.

Bellis, M. The History of Penicillin; Alexander Fleming, John Sheehan and Andrew J Moyer, http://inventors.about.com/od/pstartinventions/a/Penicillin.htm. **2012**.

Bush, K. Beta-lactamase inhibitors from laboratory to clinic. Clin Microbiol Rev. **1988**. 1. 109-23.

Buss, T. and Hayes, M. A. Mushrooms, microbes and medicines.**2000**. Cambridge, United Kingdom, The Royal Society of Chemistry.

Carroll, G. Fungal endophytes in stems and leaves: from latent pathogen to mutualistic symbiont. Ecology. **1988**. 69.2-9.

CDC. CDC Reminds Clinical Laboratories and Healthcare Infection Preventionists of their Role in the Search and Containment of Vancomycin-Resistant Staphylococcus aureus (VRSA), Centers for Disease Control and Prevention, Atlanta, GA 30333, USA. **2012**.

Christensen, M. A view of fungal ecology. Mycologia. **1989**. 81. 1-19.

Clay, K. Fungal endophytes of grasses: a defensive mutualism between plants and fungi. Ecology. **1988**. 69.b10-16.

Dailey, L., Coombs, G. W., O'Brien, F. G., Pearman, J. W., Christiansen, K., Grubb, W. B. and Riley, T. V. Methicillin-resistant Staphylococcus aureus, Western Australia. Emerging Infectious Diseases. **2005**. 11. 10.

Debbab, A., Aly, A. and Proksch, P. Bioactive secondary metabolites from endophytes and associated marine derived fungi. Fungal Diversity. **2011**. 49.1-12.

Debbab, A., Aly, A. and Proksch, P. Endophytes and associated marine derived fungi-ecological and chemical perspectives. Fungal Divers. **2012**. 57. 45-83.

Debbab, A., Aly, A. H., Edrada-Ebel, R., Wray, V., Müller, W. E. G., Totzke, F., Zirrgiebel, U., Schälchtele, C., Kubbutat, M. H. G., Lin, W. H., Mosaddak, M., Hakiki, A., Proksch, P. and Ebel, R. Bioactive metabolites from the endophytic fungus Stemphylium globuliferum isolated from Mentha pulegium. J Nat Prod. **2009**. 72. 626-631.

Debbab, A., Aly, A. H., Edrada-Ebel, R., Wray, V., Pretsch, A., Pescitelli, G., Kurtan, T. and Proksch, P. New Anthracene Derivatives – Structure Elucidation and Antimicrobial Activity. Eur J Org Chem. **2012**. 1351-1359.

Donadio, S., Monciardini, P., Alduina, R., Mazza, P., Chiocchini, C., Cavaletti, L., Sosio, M. and Puglia, A. M. Microbial technologies for the discovery of novel bioactive metabolites. J Biotechnol. **2002**. 99. 187-198.

Ebrahim, W., Aly, A. H., Mándi, A., Totzke, F., Kubbutat, M. H. G., Wray, V., Lin, W.-H., Dai, H., Proksch, P., Kurtán, T. and Debbab, A. Decalactone derivatives from Corynespora cassiicola, an endophytic fungus of the mangrove plant Laguncularia racemosa. Eur J Org Chem. **2012**. 2012. 3476-3484.

Feller, I. C. Effects of Nutrient Enrichment on Growth and Herbivory of Dwarf Red Mangrove (Rhizophora Mangle). Ecological Monographs. **1995**. 65. 477-505.

Giguère, S. Antimicrobial Drug Action and Interaction: An Introduction. **2006**. Ames Iowa, USA.

Harper, J. K., Ford, E. J., Strobel, G. A., Arif, A., Grant, D. M., Porco, J., P.Tomer, D. and Oneill, K. Pestacin: a 1,3-dihydro isobenzofuran from Pestalotiopsis microspora possessing antioxidant and antimycotic activities. Tetrahedron. **2003**. 59. 2471-2476.

Herre, E. A., Knowlton, N., Mueller, U. G. and Rehner, S. A. The evolution of mutualisms: exploring the paths between conflict and cooperation. Trends in Ecology & amp; Evolution. **1999**. 14. 49-53.

Isaacs, J. Aboriginal food and herbal medicine.**2002**. Sydney, Australia, New Holland Press.

Li, J. Y., Sidhu, R. S., Ford, E., Hess, W. M. and Strobel, G. A. The induction of taxol production in the endophytic fungus Periconia sp. from Torreya grandifolia. J. Ind. Microbiol . **1998**. 20. 259-264.

Li, J. Y. and Strobel, G. A. Jesterone and hydroxy-jesterone antioomycetcyclohexenenone epoxides from the endophytic fungus Pestalotiopsis jesteri. Phytochem. **2001.** 57. 261-265.

Marler, M. J., Zabinski, C. A. and Callaway, R. M. Mycorrhizae indirectly enhance competitive effects of an invasive forb on a native bunchgrass. Ecology. **1999**. 80. 1180-1186.

Meenupriya, J. and Thangaraj, M. Analytical characterization and structure elucidation of metabolites from Aspergillus ochraceus MP2 fungi. Asian Pac J Trop Biomed. **2011**. 1. 376-380.

Peters, A. F. Field and culture studies of Streblonema-Macrocystis new species Ectocarpales Phaeophyceae from Chile, a sexual endophyte of giant kelp. Phycologia. **1991**. 30. 365-377.

Proksch, P., Edrada, R. and Ebel, R. Drugs from the seas - current status and microbiological implications. Appl Microbiol Biotechnol. **2002**. 59.125.

Proksch, P., Putz, A., Ortlepp, S., Kjer, J. and Bayer, M. Bioactive natural products from marine sponges and fungal endophytes. Phytochem Rev. **2010**. 9. 475-489.

Schofield, C. B. The anarchy of antibiotic resistance: mechanisms of bacterial resistance http://www2.mlo-online.com/features/201105/cover-story/the-anarchy-of-antibiotic-resistance-the-mechanisms-of-bacterial-resistance.aspx. **2011.**

Sinclair, J. B. and Cerkauskas, R. F. Latent infection vs. endophytic colonization by fungi.**1996**. St. Paul, MN, APS Press.

Slonczewski, J. L. and Foster, J. W. Microbiology : an evolving science. **2011**.

Stone, J. K., Bacon, C. W. and White Jr, J. F. An overiew of endophytic microbes: endophytism defined. **2000**. 14. 3.

Strobel, G. and Daisy, B. Bioprospecting for microbial endophytes and their natural products. Microbiol Mol Biol Rev. **2003**. 67. 491-502.

Strobel, G., Daisy, B., Castillo, U. and Harper, J. Natural Products from endophytic microorganisms. J Nat Prod. **2004**. 67. 257-268.

Strobel, G., Ford, E., Worapong, J., Harper, J. K., Arif, A. M., Grant, D. M., Fung, P. C. W. and Chan, K. Isopestacin, an isobenzofuranone from Pestalotiopsis microspora, possessing antifungal and antioxidant activities. Phytochemistry. **2002**. 60. 179-183.

Strobel, G. A., Hess, W. M., Li, J.-Y., Ford, E., Sears, J., Sidhu, R. S. and Summerell, B. Pestalotiopsis guepinii, a taxol-producing endophyte of the Wollemi pine, Wollemia nobilis. Aust J Bot. **1997**. 45. 1073-1082.

Strobel, G. A., Stierle, A., Stierle, D. and Hess, W. M. Taxomyces andreanae a proposed new taxon for a bulbilliferous hyphomycete associated with Pacific yew. Mycotaxon. **1993**. 47. 71-78.

Todar, K. Bacterial resistance to antibiotics. Online textbook of bacteriology. **2012**.

Wani, M. C., Taylor, H. L., Wall, M. E., Coggon, P. and McPhail, A. T. Plant antitumor agents. VI. The isolation and structure of taxol, a novel antileukemic and antitumor agent from Taxus brevifolia. J Am Chem Soc. **1971**. 93. 2325-7.

Young, D. H., Michelotti, E. L., C. S.Swindell and E.Krauss, N. Antifungal properties of taxol and various analogues. Experientia. **1992**. 48. 882-5.

= Chapter 2 =

Dihydroanthracenones from the Endophytic Fungus *Talaromyces wortmannii* with Activity against Multi-Resistant *Staphylococcus aureus*

Robert Bara,[†+] Ilka Zerfass,[†+] Amal H. Aly,[†] Heike Goldbach-Gecke,[†] Vijay Raghavan,[‡] Peter Sass,[†] Attila Mándi,[§] Victor Wray,[‖] Prasad L. Polavarapu,[‡] Alexander Pretsch,[⊥] WenHan Lin,[○] Gennaro Pescitelli,[□] Tibor Kurtàn,[§] Abdessamad Debbab,[†] Heike Brötz-Oesterhelt,[†]* Peter Proksch[†]*

[†] Institut für Pharmazeutische Biologie und Biotechnologie, Heinrich-Heine-Universität Düsseldorf, Universitätsstrasse 1, Geb. 26.23, 40225 Düsseldorf, Germany

[‡] Departments of Chemistry and Biochemistry, Vanderbilt Institute of Chemical Biology, Vanderbilt University, Nashville, Tennessee 37235, United States

[§] Department of Organic Chemistry, University of Debrecen, POB 20, 4010 Debrecen, Hungary

[‖] Helmholtz Centre for Infection Research, Inhoffenstraße 7, D-38124 Braunschweig, Germany

[⊥] SeaLife Pharma GmbH, 3430 Tulln, Austria

[○] National Research Laboratories of Natural and Biomimetic Drugs, Peking University, Health Science Center, 100083 Beijing, People's Republic of China

[□] Dipartimento di Chimica e Chimica Industriale, Università degli Studi di Pisa, I-56126 Pisa, Italy

This chapter is adapted from a manuscript which submitted to the *Journal of Medicinal Chemistry* as: R. Bara, I. Zerfass, A. H. Aly, H. Goldbach-Gecke, V. Raghavan, P. Sass, A. Mándi, V. Wray, P. L. Polavarapu, A. Pretsch, W. H. Lin, G. Pescitelli, T. Kurtàn, A. Debbab, H. Brötz-Oesterhelt, P. Proksch. 2012. Dihydroanthracenones from the endophytic fungus *Talaromyces wortmannii* with activity against multi-resistant *Staphylococcus aureus.*

The impact factor of related journal is 5.248, overall participation on the paper is 70% as the first author. The first author involved to all laboratory works as well as the manuscript preparation.

ABSTRACT

Chemical investigation of the fungus *Talaromyces wortmannii*, an endophyte of *Aloe vera*, yielded four bisdihydroanthracenone atropisomers, including the homodimers flavomannin A (**1**) and its previously unreported atropisomer flavomannin B (**2**), two heterodimers (**3** and **4**), as well as two new mixed dihydroanthracenone/anthraquinone dimers (**5** and **6**). The planar structures of the new compounds (**2**-**6**) were elucidated on the basis of one and two dimensional NMR spectroscopy as well as mass spectrometry. All six compounds exhibited antibacterial activity, predominantly directed against *Staphylococcus aureus*, including even high-level (multi)drug-resistant isolates. Further Gram-positive genera (*Streptococcus*, *Enterococcus*, *Bacillus*) were only moderately affected. Reporter gene analyses in *Bacillus subtilis* indicated induction of the SOS response for some of the isolated derivatives suggesting interference with DNA structure or metabolism. Accordingly, fluorescence microscopy demonstrated defective segregation of the bacterial chromosome and DNA degradation. Noteworthy, the compounds showed no activity when tested against eukaryotic THP-1 cells (leukemia cell line) and BALB cells (mouse embryonic fibroblasts), making those putative new starting points for antibacterial drug development.

Keywords

Aloe vera, endophyte, *Talaromyces wortmannii*, dihydroanthracenones, atropisomers, structure elucidation, antibiotic activities, MRSA, *Staphylococcus aureus*.

INTRODUCTION

Bacterial resistance to clinically applied antibiotics has been recognized as a serious threat worldwide and necessitates the search for new drugs that can overcome bacterial resistance mechanisms. An important example of a multi-drug resistant pathogen is *Staphylococcus aureus*, the leading cause of nosocomial infections among Gram-positive bacteria (Klevens et al. 2007). Today, resistance rates for antibiotics that have been the mainstay of anti-staphylococcal therapy for decades (e.g. methicillin or fluoroquinolones) have reached values that preclude their use in intensive care units in several countries (MacDougal et al. 2005; Knight et al. 2012). Moreover, these methicillin-resistant *S. aureus* isolates (MRSA) are now successfully spreading within the community, infecting young children and even healthy adults (Delero et al. 2010). Only few antibiotics like vancomycin, linezolid, daptomycin and ceftaroline represent the last resort for the therapy of infections caused by MRSA. However, vancomycin-intermediate (VISA, MIC 2 to 8 μg/mL) and vancomycin-resistant (VRSA, MIC ≥16 μg/mL) *S. aureus* strains have already been reported as well as clonal spread of linezolid-resistance and clinical failures caused by daptomycin-resistant isolates (Ruef 2004, Cui et al. 2006, Tenover and Moellering 2007, Tenover 2009, Gould et al. 2012). Thus, there is a constant and high demand for new drugs that might help to overcome this alarming scenario of resistance development and spread.

Endophytic fungi constitute a relatively unstudied and promising source for such new antibacterial agents (Aly et al. 2010, 2011, Debbab et al. 2010, 2011). Atropisomers form a particularly interesting class of fungal secondary metabolites, because their axial chirality represents an additional level of specificity, which contributes to their biological activity, pharmacodynamics, pharmacokinetics and toxicity (Eichelbaum and Gross 1996, Evans et al. 1998, Shah et al. 1998, Wagenaar et al. 2002, LaPlante et al. 2011a, 2011b). Several natural atropisomers, including the glycopeptide antibiotic vancomycin, in addition to other examples as marinopyrrole A, alterporriols D and N, were reported to be selectively active against several pathogenic microorganisms including MRSA (Lloyd-Williams and Giralt 2001, Li et al. 2008, Nicolaou et al. 2011, Debbab et al. 2012). Moreover, atropisomeric antiretroviral pairs were reported to differ in their potency as HIV-1 entry inhibitors in the treatment of AIDS (Muniz-Medina et al. 2009).

As part of our ongoing search for new bioactive secondary metabolites from terrestrial endophytic fungi (Aly et al. 2011, Debbab et al. 2012, Ebrahim et al. 2012, Hammerschmidt et al. 2012), we investigated in the current study *Talaromyces wortmannii* isolated from *Aloe vera* (Asphodeloideae) growing in Egypt. The plant genus *Aloe* includes several species, such as *A. vera*, that are important medicinal plants used mainly for their laxative anthracene derivatives (Dewick 2006). Even though *Aloe* species were already a subject of intensive research, chemical studies on their endophytic fungi are still lacking. The present study represents the first comprehensive investigation of natural products produced by *T. wortmannii* from *A. vera* and reports on new antibacterial agents which retain full activity against multi-resistant bacterial clinical isolates.

RESULTS AND DISCUSSION

Structure Elucidation of Isolated Compounds. Compound **1** was isolated as a brown amorphous powder. The UV spectrum of **1** showed three absorption maxima λ_{max} (MeOH) at 236, 278 and 408 nm. ESIMS indicated a molecular weight of 546 g/mol, and its molecular formula was determined as $C_{30}H_{26}O_{10}$, on the basis of the prominent signal detected at *m/z* 547.1618 $[M+H]^+$ in the HRESIMS. In contrast, inspection of the ^1H and ^{13}C NMR spectra of **1** (Table 1) showed signals corresponding only to 13 protons and 15 carbons, indicating that **1** is a symmetrical dimer consisting of two identical monomers. ^1H and ^{13}C NMR spectra of **1** (Table 1) revealed the presence of a tertiary methyl group resonating at δ_H 1.35 ppm, two methylene groups CH_2-2/2' and CH_2-4/4' (δ_H 2.80/2.71 and 3.00/ 2.95 ppm, respectively), and two aromatic methine groups appearing as singlets at δ_H 6.80 and δ_H 6.61 ppm and attributed to H-10/10' and H-5/5', respectively. In addition, analysis of ^{13}C NMR and DEPT spectra disclosed signals for 10 quaternary carbons, one of which was attributed to the carbonyl group C-1/1' (δ_C 203.3 ppm), one to the oxygen-bearing aliphatic carbon C-3/3' (δ_C 71.2 ppm), and eight aromatic carbons (C-4a/4a', C-6/6', C-7/7', C-8/8', C-8a/8a', C-9/9', C-9a/9a', C-10a/10a'). The deshielded signals for C-6/6', C-8/8' and C-9/9' (δ_C 161.7, 158.6, and 167.0 ppm, respectively) indicated their oxygenated nature. Comparison of the NMR data of **1** with those reported previously for flavomannin (Atherton *et al.* 1968; Ren *et al.* 2006), as well as for related derivatives such as atrovirins B1 and B2 (Antonowitz *et al.* 1994; Gill and Morgan 2004) and austrocolorins A1 and B1 (Beattie *et al.* 2004), suggested that the

isolated compound is flavomannin comprising two atrochrysone subunits. The structure of **1** was confirmed by thorough inspection of COSY, ROESY and HMBC correlations (Figure 1A). The latter showed that H-10/10' correlated with C-4/4', C-5/5', C-8a/8a' and C-9a/9a', whereas H-5/5' correlated to C-7/7', C-8a/8a' and C-10/10', thus establishing the link between the two monomers to reside between C-7 and C-7′. For further evidence of the planar structure and the assignment of exchangeable protons, the ^{1}H NMR, ROESY and HMBC spectra of **1** were measured in DMSO-d_6. The ^{1}H NMR showed three additional sharp signals (9.86, 10.01 and 16.50 ppm) and one broad signal at δ_H 4.80 ppm, which were attributed to 8/8'-OH, 6/6'-OH, 9/9'-OH, which forms a hydrogen bond with the keto-group at C-1/1', and the aliphatic hydroxyl group 3/3'-OH, respectively. Finally, ROESY correlations between 6/6'-OH, H-5/5', H-10/10' and CH_2-4/4' confirmed that the respective protons are located in neighboring positions with the same spatial orientation in both aromatic monomers.

Compound **2** was obtained as a brown amorphous powder. Both **1** and **2** shared the same molecular formula as indicated by HRESIMS ($C_{30}H_{26}O_{10}$). The UV spectrum of **2** showed almost identical absorption maxima to those observed for **1** (235, 279 and 410 nm), yet **2** eluted ca. 3.5 min earlier than **1** upon HPLC analysis (R_t 27.0 and 23.6 min for **1** and **2**, respectively). Moreover, ^{1}H and ^{13}C NMR spectra of both compounds were almost superimposable (Table 1), and analysis of 2D NMR spectra of **2** established the same planar structure as for **1**. Thus, **1** and **2** were assumed to be stereoisomers differing either in the configuration of the biaryl axis or in the C-3/3' chirality centers. It has been reported earlier for related natural biaryl derivatives having both central and axial chirality elements that it is the axial chirality that determines the ECD features (Elsässer *et al.* 2005; Polavarapu *et al.* 2009; Debbab *et al.* 2012). Thus the mirror image ECD spectra of **1** and **2** suggested that they are atropodiastereomeric homodimers with the same C-3/3' absolute configuration. As the $[\alpha]_D$ value of **1** (–82) corresponds to that reported for flavomannin A (Atherton *et al.* 1968), **2** was thus identified as the atropodiastereomer of **1** and given the name flavomannin B.

In order to determine the axial chirality of **1** and **2**, a TDDFT ECD calculation protocol was carried for the gas-phase and solution geometries. The ECD spectrum of **1** is dominated by a negative exciton couplet centered at 277 nm (Figure 2A), while **2** has a mirror image positive couplet in that region (Figure 2B). The initial 20 MMFF conformers of the arbitrarily chosen

(a*R*,3*R*,3'*R*) stereoisomer of **1** were reoptimized by DFT at the B3LYP/6-31G(d) in vacuo and B3LYP/TZVP with PCM solvent model for acetonitrile. Three identical conformers were identified in both cases, which differed only in their populations (Figure 3A). Due to the two hydrogen bonding interactions of phenolic hydroxyls of the two dihydroanthracenone moieties, the $\omega_{C6',C7',C7,C8}$ dihedral angle was around +53° in all the three conformers, a much smaller value than the usual near 90° dihedral angle of biaryls lacking hydrogen bondings. In the lowest-energy conformer (conformer A), both the C-3 and C-3' hydroxyl groups adopted axial orientation, while one of the hydroxyls in conformer B and both of them in conformer C were equatorial. TDDFT ECD calculations of the gas-phase and solution conformers of (a*R*,3*R*,3'*R*)-**1** using various functionals (B3LYP, BH&HLYP, PBE0) and TZVP basis set reproduced well the main features of the experimental ECD, especially the intense negative exciton couplet, allowing the determination of axial chirality as (a*R*)-**1** (Figure 2A). A similar ECD calculation protocol was carried out on the atropodiastereomeric (a*S*,3*R*,3'*R*)-**2** having negative $\omega_{C6',C7',C7,C8}$ dihedral angle, and the computed ECD spectra calculated for the gas-phase and solution conformers corroborated well the experimental ECD (Figures 2B and 3B), which allowed the determination of axial chirality as (–)-(a*S*). Since the ECD data of (+)-(a*R*)-**1** and (–)-(a*S*)-**2** were governed by the axial chirality, which were reflected in their near mirror image ECD spectra, the absolute configuration of the C-3 and C-3' chirality centers could not be determined by the ECD calculations.

VCD analysis had been successfully used in the past to determine the absolute configuration of central chirality elements in cephalochromin (Polavarapu *et al.* 2009), a homodimeric naphthopyranone natural product, containing both axial and central chirality. In order to explore the applicability of VCD for the determination of axial and/or central chirality of flavomannin A (**1**), its VA and VCD spectra were measured and calculated for the computed solution conformers with (a*R*,3*R*,3'*R*) and (a*S*,3*R*,3'*R*) configuration.

Experimental VCD and VA spectra of **1** matched well with those calculated for (a*R*,3*R*,3'*R*)-**1** (Figure 4). The prominent bisignate VCD couplet (positive at 1412 and negative at 1392 cm^{-1}) in the experimental spectrum is reproduced in the calculated spectrum (with corresponding locations at 1473 and 1458 cm^{-1}) for (a*R*,3*R*,3'*R*) stereoisomer reflecting the (a*R*) axial chirality. VCD calculated for (a*S*,3*R*,3'*R*) stereoisomer was found to be nearly a mirror image to that calculated for the (a*R*,3*R*,3'*R*) stereoisomer (Figure 4B). However, the calculated VCD

spectrum for (a*R*,3*S*,3'*S*) stereoisomer [obtained by multiplying the VCD spectrum of (a*S*,3*R*,3'*R*) with -1] also matched with the experimental VCD spectrum of **1**. Thus, VCD features in the 1700-1200 cm^{-1} region are clearly dominated by the axial chirality element in **1**, and contributions from central chirality elements are quite small. The average between VCD spectra of (a*R*,3*R*,3'*R*) and (a*S*,3*R*,3'*R*) diastereomers is expected to pull out the contribution from central chirality elements, but this contribution as seen in Figure 4B is almost negligible. VA spectra for diastereomers can also be different, but in the present case calculations at B3LYP/TZVP/PCM (acetonitrile) indicated no significant differences between the VA spectra of (a*R*,3*R*,3'*R*) and (a*S*,3*R*,3'*R*) stereoisomers in the spectral region investigated. The difference between VA spectra of (a*R*,3*R*,3'*R*) and (a*S*,3*R*,3'*R*) diastereomers, as seen in Figure 4B is nearly a baseline curve. As a result, VCD and VA spectra cannot discriminate between (a*R*,3*R*,3'*R*) and (a*R*,3*S*,3'*S*) diastereomers based on the analysis of experimental VCD and VA spectra of **1**, unlike the case of cephalochromin (Polavarapu *et al.* 2009).

Compound **3** was isolated as a brown amorphous powder. It showed very similar UV absorption maxima (λ_{max} MeOH 234, 279 and 407 nm) to those of **1** and **2**, indicating that all compounds share a similar core structure. The HRESIMS exhibited a prominent peak at 561.1754 $[M+H]^+$, with a 14 mass unit increase (CH_2) compared to **1** and **2**, which established a molecular formula of $C_{31}H_{28}O_{10}$. In the ^{1}H NMR spectra of compounds **1** and **2**, all resonances originated from pairs of magnetically equivalent protons due to the symmetry of the molecules. However, in the ^{1}H NMR spectrum of **3** (Table 2), the proton signals of the two building blocks of the molecule appeared as two sets rather than one indicating that this molecule is a heterodimer. Thus, it was possible to assign the ^{1}H NMR signals of both subunit structures, which were found to correspond to one atrochrysone and one torosachrysone monomeric building blocks. These included two tertiary methyl groups resonating at δ_H 1.41 and 1.42 ppm assigned for 3-CH_3 and 3'-CH_3, respectively, four well separated methylene groups at δ_H 2.80-2.89 ppm for CH_2-2, 2.82-2.92 ppm for CH_2-2', 3.04-3.08 ppm for CH_2-4, and 3.08-3.14 ppm for CH_2-4', as well as four aromatic singlets at δ_H 6.73, 6.84, 6.88 and 7.05 ppm for H-5, H-5', H-10 and H-10', respectively. In contrast to **1** and **2**, the ^{1}H NMR spectrum showed an additional methoxy group of the torosachrysone moiety at δ_H 3.82 ppm. The position of the methoxy group was established by a ROESY experiment showing correlation of the extra OCH_3 to the aromatic proton H-5', while the

latter showed a cross peak to H-10' which in turn correlated to CH_2-4'. This was confirmed by HMBC correlations of H-5' and 6'-OCH_3 to C-6' confirming the attachment of the methoxy group to C-6'. The complete planar structure of **3** was corroborated by careful analysis of HMBC correlations as well as comparison with NMR data of **1** and **2** (Figure 1B). Hence, **3** was identified as a new natural heterodimer for which the name flavomannin C is proposed. Flavomannin C (**3**) showed a similar ECD pattern to that of flavomannin A (**1**) including the negative exciton couplet at 276 nm, which suggested that it has also a positive $\omega_{C6',C7',C7,C8}$ dihedral angle. Since the presence of the C-6' methoxy group changed the priority assignment, **3** has (a*S*) axial chirality, although it has the same axial geometry as **1**.

Compound **4** was isolated as a brown amorphous powder. Both HRESIMS and molecular formula of **4** were identical to those of **3**, indicating that **4** is a stereoisomer of **3**. As discussed for the atropisomers **1** and **2**, **4** showed almost identical absorption maxima (λ_{max} MeOH) to those observed for **3** (234, 279 and 407 nm). However, **4** eluted ca. 2 min earlier than **3** upon HPLC analysis (R_t 28.3 and 26.5 min for **3** and **4**, respectively). Moreover, ^{1}H and ^{13}C NMR spectra of both **3** and **4** were almost superimposable (Table 2). In addition, analysis of 2D NMR spectra of **4** established the same planar structure as for **3**. Thus, **3** and **4** were assumed to be a pair of stereoisomers differing either in the configuration of the biaryl axis or in the chiral center at C-3/3'. This assumption was confirmed by measuring their $[\alpha]_D$ values (–170 and +110 for **3** and **4**, respectively). Thus, **4** was identified as a new natural product, for which the name flavomannin D is proposed. Flavomannin D (**4**) showed a positive ECD exciton couplet at 276 nm and similar ECD features to that of flavomannin B (**2**), which are derived from negative $\omega_{C6',C7',C7,C8}$ dihedral angle and (a*R*) absolute configuration.

Compound **5** was isolated as a brown amorphous powder. It showed similar UV spectral pattern (λ_{max} MeOH 223, 277, and 420 nm) to those of **1**-**4**. However, the bathochromic shift observed for the absorption band at 420 nm (ca. 10 nm) indicated an extended conjugation in the structure **5** compared to **1**-**4**. Its HRESIMS exhibited a dominant peak at *m*/*z* 543.1286 $[M+H]^+$ and 565.1102 $[M+Na]^+$, indicating a molecular formula of $C_{30}H_{23}O_{10}$. Comparison of ^{1}H and ^{13}C NMR data of **5** with those of **1**-**4** showed that **5** is a heterodimer consisting of an atrochrysone moiety and an emodin residue. ^{1}H NMR spectrum of **5** (Table 3) revealed the presence of all characteristic signals of the atrochrysone moiety, including a tertiary methyl group at δ_H 1.42 ppm (3-CH_3), two methylene groups at δ_H 2.79-2.93 and 3.04-3.11 ppm

(CH_2-2 and CH_2-4, respectively) and two aromatic singlets at δ_H 6.76 and 6.87 ppm (H-5 and H-10). In addition, signals corresponding to the emodin building block included one aromatic methyl group at δ_H 2.47 ppm (3'-CH_3), three aromatic methine groups appearing at δ_H 7.14, 7.43 and 7.60 ppm (H-2', H-5' and H-4', respectively), as well as two sharp chelated hydroxyl groups at δ_H 12.14 and 12.55 ppm (1'-OH and 8'-OH, respectively). ^{13}C NMR and DEPT spectra disclosed signals for 21 quaternary carbons, three of which were attributed to carbonyl groups at δ_C 203.8, 182.3 and 191.8 ppm (C-1, C-10' and C-9', respectively), one to the oxygen-bearing aliphatic carbon at δ_C 70.7 ppm (C-3), six to oxygen-bearing aromatic carbons at δ_C 158.4, 166.4, 160.8, 163.0 ppm including two overlapping signals at δ_C 164.5 ppm (C-6, C-8, C-9, C-1', C-6' and C-8', respectively), and finally eleven to aromatic carbons (Table 3). Absence of one aromatic proton of emodin in the ^{1}H NMR spectrum of **5** indicated that the atrochrysone moiety is attached to the emodin moiety either in position C-2', C-4', C-5' or C-7'. Analysis of COSY spectrum showed correlations of 3'-CH_3 to the *meta*-coupled protons H-2' and H-4' confirming its position between both protons (Figure 1C). Furthermore, H-4' and H-5' revealed strong HMBC correlations to the *keto* group C-10' resonating at δ_C 182.3 ppm. Thus, the emodin moiety is attached to the atrochrysone part at position C-7'. The planar structure of **5** was confirmed by further 2D NMR data including COSY and HMBC (Figure 1C). Accordingly, **5** was identified as a new natural product and named talaromannin A.

Compound **6** was isolated as a yellow brown amorphous powder. This compound shared the same molecular formula with compound **5** ($C_{30}H_{26}O_{10}$) as indicated by identical HRESIMS (*m/z* 543.1286 $[M+H]^+$). The UV spectrum of **6** showed almost identical absorption maxima as those observed for **5** (224, 277 and 421 nm), yet **6** eluted ca. 1.4 min earlier than **5** upon HPLC analysis (R_t 32.42 and 31.01 min for **5** and **6**, respectively). Moreover, ^{1}H and ^{13}C NMR spectra of both compounds were almost superimposable (Table 3), and analysis of 2D NMR spectra of **6** established the same planar structure as for **5**. The near mirror image ECD spectra of **5** and **6** and their opposite $[\alpha]_D$ values (–124 and +111 for **5** and **6**, respectively) suggested that they are atropodiastereomers. Compound **6** was hence identified as a new natural atropodiastereomer of **5**, for which the name talaromannin B is proposed.

Since one of the dihydroanthracene-1-one moiety is replaced by an anthracene-9,10-dione unit in **5** and **6**, their ECD spectra could not be correlated with those of **1**-**4**. Thus TDDFT ECD calculation was applied to the (a*S*,3*R*) and (a*R*,3*R*) atropodistereomers to determine the

axial chirality (central chirality was arbitrarily chosen as *R*). The DFT reoptimization of the initial MMFF conformers resulted in two major conformers above 5% population, which differed in the axial/equatorial orientation of the 3-OH group governed by the helicity of the fused cyclohexenone ring (Figure 5). The ECD calculations reproduced well the ECD bands of **5** and **6** allowing the assignment of axial chirality as (−)-(a*R*)-**5** and (+)-(a*S*)-**6** (Figure 6). Similar to flavomannins A and B, the negative ECD exciton couplet around 278 nm derived from (a*R*) and positive one from (a*S*) axial chirality, although the high-energy band of the couplet was overlapping with more transitions in talaromannins A and B.

The known anthraquinone skyrin (**7**) was likewise isolated and identified by comparison of its spectral characteristics to published data (Gill *et al.* 1988). Efforts to determine the absolute configuration at C-3/C-3' in **1**-**4** and at C-3 in **5** and **6** by reductive cleavage of the compounds with alkaline sodium dithionite (Takeda *et al.* 1973; Elsworth *et al.* 1999) or with alkaline sodium bisulfate (Arai *et al.* 1989) proved unsuccessful. HPLC analysis revealed that the compounds remained unchanged and no monomers were detected. As both 3*R* and 3*S* configurations are reported for atrochrysone and torosachrysone monomers in literature (Gill *et al.* 1989; Gill *et al.* 1990; Gill *et al.* 2000; Gill and Morgan 2001; Müller *et al.* 2004), experiments to determine the central chirality of the compounds by further chemical or biochemical methods are presently in progress.

Further dimeric dihydroanthracene derivatives structurally related to **1**-**4** were previously reported from several higher plants including *Bulbine abyssinica* (Asphodelaceae) (Wanjohi *et al.* 2005), *Cassia torosa* (Fabaceae),(Takahashi *et al.* 1977) *C. singueana* (Endo and Naoki 1980), *C. occidentalis* (Kitanaka and Takido 1989), *Karwinskia humboldtiana* (Dreyer *et al.* 1975), and *K. parvifolia* (Rhamnaceae) (Rivas *et al.* 2005; Salazar *et al.* 2006). The biosynthesis of diverse natural products, originally only characterized from plants, by endophytic fungi was repeatedly reported in the past decades. Well known examples include paclitaxel, originally obtained from *Taxus brevifolia* and later reported from endophytic *Taxomyces andreanae*, and hypericin, reported from *Hypericum perforatum* and endophytic *Thielavia subthermophila* (Stierle *et al.* 1993; Kusari *et al.* 2008; Kusari *et al.* 2009; Aly 2010). Hence, it is intriguing to speculate on the true origin of fungal dimeric dihydroanthracene derivatives, as those reported in this study, based on the close structural resemblance of these natural products to known plant metabolites. This remains to be investigated.

Cytotoxicity Assays. As part of our biological profiling compounds **1**-**6** were tested for putative cytotoxic activity against THP-1 human leukemic monocyte cells and BALB/3T3 mouse embryonic fibroblast cells. The IC_{50} value for both cell lines was >32 μg/mL, indicating that the compounds did not interfere with growth and viability of the eukaryotic cells in the concentration range tested. Emodin and skyrin (**7**) did also not show cytotoxicity for these cell linees (IC_{50} >32 μg/mL), although an inhibitory effect of emodin and skyrin on particular tumor cell lines had been reported previously (Parker *et al.* 2000; Lin *et al.* 2001; Lee *et al.* 2005; Tan *et al.* 2006; Liu *et al.* 2010).

Determination of Antibacterial Activity. The isolated compounds were also evaluated for their antibacterial activity against a spectrum of Gram-positive and Gram-negative bacterial species, including antibiotic-susceptible reference strains and multi-resistant clinical isolates and their minimal inhibitory concentrations (MIC) were determined by broth microdilution assays (Table 4). Compounds **1**-**6** were predominantly active against staphylococci, with MIC values from 4 to 8 μg/mL for the most active compounds. Surprisingly, the investigated natural products displayed even better antibacterial activity against the high-level (multi)-resistant staphylococcal isolates present in the panel than against the susceptible reference strain recommended by the Clinical Laboratory Standards Institute (CLSI) for sensitive antibiotic testing (CLSI 2008). Although the number of strains investigated so far is still small, this is a strong indication that the compounds are not affected by conventional resistance mechanisms. In general, all six compounds displayed moderate MICs in a comparable concentration range for *S. aureus* and **5** and **3** represented the most and least active congeners, respectively. In addition, MIC values in the range of 32 to 64 μg/mL were observed for streptococcal and enterococcal species.

Due to the structural similarity to **1**-**6**, the two known anthraquinones emodin and skyrin (**7**) (Scheme 1) were also included in the MIC determination assay. Emodin forms one half of **5** and **6**, and **7** is an emodin dimer. Both compounds also showed antibacterial activity and addressed the same Gram-positive strain panel as **1**-**6** including *B. subtilis* (Table 4). Thus, we included emodin and **7** in the mechanism of action studies outlined below in parallel with the new compounds. Preceding literature on the antibacterial activity of emodin and skyrin is somewhat inconsistent. One report described MIC values in the range of 6.25 to 25

*µ*g/mL for *S. aureus*, *Escherichia coli* and *Pseudomonas aeruginosa* for both compounds (Liu et al. 2010), while in an independent study emodin yielded considerably higher MIC values for *S. aureus* and *P. aeruginosa* (90 and 70 *µ*g/mL, respectively) and low single digit MICs for *Bacillus* species (Basu *et al.* 2005).

According to the guidelines the MIC is defined as the lowest concentration of an antibacterial agent required for prevention of visible bacterial growth after overnight incubation. From this value it is not possible to judge, if an antibiotic exhibits a bactericidal or bacteriostatic effect. Therefore, we determined the number of viable cells after treatment with different concentrations of **2** or **5**. We selected these particular compounds, because **2** played a prominent role in the mechanism of action studies (see below) and **5** was the most active derivative of the flavomannins/talaromannins in the MIC studies. For **2** and **5**, 4 x 10^6 colony forming units (CFU) and 6.14 x 10^6 CFU, respectively, were recorded at 64 *µ*g/mL compared to 10^9 in the growth control. Considering the inoculum used for seeding the plates (5x 10^5 CFU/mL) this result points to a bacteriostatic effect of the compound in this concentration range and under the assay conditions applied. It is noteworthy, that we observed precipitation of all flavomannin/talaromannin derivatives at concentrations of 16 *µ*g/mL and above in aqueous Mueller-Hinton broth, the test medium recommended for standard MIC determinations (CLSI M7-A8, 2008). The effect started approximately 2 hours after dilution of the compound stock solution (prepared in DMSO) into aqueous solution. The final DMSO concentration in the serial two-fold compound dilution series did not exceed 0.64% to avoid interference with bacterial growth, limiting the solubilizing potential of the solvent. Hence, we cannot exclude a potential for bactericidal activity at higher concentrations, which we could not reach in this assay setup. Solubilizing the compounds in other solvents like DMF or DMSO/ethylene glycol monomethyl ether (EGME) did not reduce precipitation significantly.

In addition, we followed the growth of the multi-resistant MRSA and VISA strain *S. aureus* Mu50 with increasing flavomannin/talaromannin concentrations by recording the optical densities of untreated *versus* antibiotic-treated cultures at 600 nm over a period of 16 hours (Figure 7). Corresponding growth curves for the therapeutically applied reference antibiotics vancomycin and tetracycline generated in the same assay setup are provided as supporting online material (Figure S1). All flavomannin/talaromannin derivatives showed concentration dependent growth inhibition, starting from 0.5 to 4 *µ*g/mL, depending on the respective

derivative. The fact that complete growth inhibition could not be achieved is probably a consequence of the limited solubility of the rather hydrophobic compounds. For the curves representing the 16 μg/mL concentration, compound precipitation is obvious from the elevated A_{600} values and occurred already at a time, when the bacterial culture was still in its lag phase (Figure 7).

Studies on the Mechanism of Antibacterial Action. For orienting studies on the mode of action of the flavomannin/talaromannin derivatives, we chose *B. subtilis* as a model organism, since it is still the best characterized Gram-positive species and its response to diverse classes of antibiotics is known from broad expression profiling studies (Bandow *et al.* 2003; Freiberg *et al.* 2006). *B. subtilis* had also proven instrumental in previous investigations on the mechanisms of action of several structurally unrelated antibacterial agents (Brotz-Oesterhelt *et al.* 2005; Freiberg *et al.* 2005; Sass *et al.* 2011; Wenzel *et al.* 2011). Although most flavomannin/talaromannin derivatives did not yield an MIC for *B. subtilis* up to 64 μg/mL using the standard MIC testing method (Table 4), growth kinetic studies in lysogeny broth indicated that the compounds nonetheless reduced its growth rate (Figure S2). As these results demonstrated that *B. subtilis* reacted to the compounds, we started our mode of action studies using this species.

To get a first hint on the metabolic area affected by **1**-**6**, reporter gene assays were performed using *B. subtilis* strains that carry the firefly luciferase or β-galactosidase reporter gene fused to six different antibiotic-inducible promoters. Previous whole genome mRNA profiling of *B. subtilis* after treatment with a broad range of antibiotic classes had identified these promoters as particularly responsive to DNA-, RNA-, protein- or cell envelope damage (Freiberg *et al.* 2006; Urban *et al.* 2007). Promoter induction can be readily measured in the reporter strains by a luminescence or fluorescence signal (Cheo *et al.* 1992; Urban *et al.* 2007) and is often in line with current knowledge on the function of their corresponding genes. The gene *helD* (synonym *yvgS*) encodes a DNA 3'-5'-helicase type IV, which is involved in DNA repair and recombination and which interacts with the RNA polymerase (Delumeau *et al.* 2011). Accordingly, the *helD* promoter was shown to respond preferentially to inhibitors of transcription (Urban *et al.* 2007). The *liaI* promoter (synonym *yvqI*) regulates expression of a small membrane protein and is controlled by the LiaRS two-component system. In previous studies the Lia response had been elicited, when the

bacteria experienced cell envelope stress by agents interfering with membrane-associated steps of peptidoglycan synthesis or disturbing the integrity of the cytoplasmic membrane (Mascher *et al.* 2004; Pietiäinen *et al.* 2005; Wolf *et al.* 2010). The product of the *bmrC* gene (synonym *yheI*) was recently shown to be part of a multidrug ABC transporter, which, however, seems to be rather specifically induced by antibiotics that block translation (Urban *et al.* 2007; Torres *et al.* 2009). The particular signaling cascade that causes this mechanism of action related specificity of the efflux pump is still unknown. None of the reporter strains mentioned so far was induced by the flavomannin/talaromannin derivatives up to concentrations of 64 µg/mL (Figure 8). In contrast, two promoters indicative of interference with DNA structure or metabolism were reproducibly induced, although only by a subset of the compounds. Among them the *yorB* promoter (Figure 8), which had previously been shown to respond to 1) inhibitors of DNA processing enzymes (gyrase, ligase or DNA polymerase), to 2) compounds that interfere with the syntheses of DNA building blocks (purine or pyrimidine) as well as to 3) DNA binding, crosslinking or strand-breaking agents (Urban *et al.* 2007). Notably, when exposed to a 14,000-membered collection of pure natural products in a previous study, the *yorB* promoter had not responded to non-covalent DNA binder (Urban *et al.* 2007). *YorB* was recently suggested to be part of the LexA regulon in *B. subtilis*, a global transcriptional network in bacteria that mediates the so-called SOS response in reaction to different sorts of DNA damage (Lazarevic *et al.* 1999; Au *et al.* 2005). In the presence of intact DNA the LexA repressor suppresses all genes within the SOS regulon. Single-stranded DNA activates the system (Cheo *et al.* 1992). When the RecA protein encounters single-stranded DNA regions, it assists the LexA repressor in autoproteolysis followed by derepression of more than 30 proteins involved in different sorts of error-prone DNA repair and inhibition of cell division (Yasbin 1977; Yasbin 1977; Yasbin and Andersen 1982; Au *et al.* 2005). The biological function for the bacterial cell is to gain time to attempt chromosomal repair prior to daughter cell separation. Interestingly, all three compounds with negative $\omega_{C6',C7',C7,C8}$ dihedral angles, **2**, **4** and **6**, induced the *yorB* promoter (Figure 8), whereas no effect was repeatedly observed for the three atropisomers with positive $\omega_{C6',C7',C7,C8}$ dihedral angles, **1**, **3** and **5** (Figure 8). Among the different congeners, **2** demonstrated the strongest promoter induction, with a 5-fold increase of reporter gene expression compared to the untreated control, followed by **4** and **6** in that order. The maximal luminescence signal was reached at concentrations of 2 to 4 µg/mL for **2**

and **4** and 8 μg/mL for **6**. As positive controls for the *yorB* reporter strain we employed two agents that are known to induce DNA-strand breaks, the quinolone ciprofloxacin trapping the gyrase in a state, where the enzyme has cut but not resealed the DNA (Love and Yasbin 1984; Drlica and Zhao 1997) and the DNA-crosslinking agent mitomycin C. Both controls led to a 20 to 25-fold increase of the *yorB* signal (Figure S3). In order to confirm the effect of the flavomannins/talaromannins on the SOS-response of *B. subtilis*, we measured the impact of all six compounds on the *recA* promoter that acts upstream of *yorB* in the regulating hierarchy of the SOS response (Figure 9). In addition, we changed the strain background and the reporter protein, in order to exclude potential false positive effects on any component of our assay system. While all promoter strains discussed so far had been generated in *B. subtilis* IS34 using firely luciferase, we now used *B. subtilis* YB3001 and β-galactosidase as reporter of the *recA* gene. **2**, **4** and **6** did also induce the *recA* promoter (Figure 9) and again **2** appeared to be the most strongly inducing congener, with an amplitude of induction that matched those of ciprofloxacin and mitomycin C (Figure S4), while **4** and **6** showed weaker effects in comparison (Figure 9). Interestingly, **1** also led to a slight *recA* induction (less than 2-fold) at elevated concentrations, although this effect was too weak to elicit the *recA*-dependent *yorB* induction. Emodin and **7**, which were tested in parallel with the **1-6** for *yorB* and *recA* induction, did not induce the promoters at all (Figures S3 and S4).

A prominent phenotypical consequence of the SOS response in rod-shaped cells is the formation of filaments due to the inhibition of cell division. Indeed, microscopic investigation of *B. subtilis* 168 trpC2 treated with **2** showed substantial and reproducible cell elongation. Staining of cells with the DNA-specific fluorescent dye 4',6'-diamidino-2-phenylindole (DAPI) revealed diffuse distribution of the nucleoid followed by considerable DNA degradation (Figure 10). The effect was more pronounced with higher concentrations of the compound and at longer incubation times. The phenotype induced by **2** resembled the one observed in the presence of ciprofloxacin. Hence, three independent experimental approaches suggest that *B. subtilis* experiences DNA damage in the presence of **2** that elicits the SOS response and probably involves the formation of single stranded DNA. Such an effect could for instance be caused by structural distortions within the DNA due to compound binding or a direct interference of the agent with one or more DNA synthesizing or processing enzymes.

Although it is likely that such severe effects on the bacterial nucleoid as demonstrated by fluorescence microscopy contribute to the growth inhibitory effect of **2** on *B. subtilis* and although **4** and **6**, which also have negative $\omega_{C6',C7',C7,C8}$ dihedral angles, probably cause similar damage to a lesser degree, the DNA related effect cannot be the sole basis of the antibacterial activity of this class of compounds. Among the three atropisomers with positive $\omega_{C6',C7',C7,C8}$ dihedral angles only **1** led to a slight induction of *recA* and neither **1**, nor **3** nor **5** induced *yorB*. All the same they inhibited the growth of *B. subtilis* to a comparable extent as the compounds with negative $\omega_{C6',C7',C7,C8}$ dihedral angles (Figure S2). Along the same line, the two structurally related anthraquinones emodin and **7**, which surpassed the flavomannin/talaromannin derivatives in antibacterial activity, did not yield an effect in the reporter gene assays. In summary, our exploratory investigations on the mode of action of the flavomannin/talaromannin derivatives demonstrate some potential of particular congeners of this compound class to interfere with DNA structure or metabolism, but do also suggest that there is yet another, probably dominant and novel mechanism of antibacterial action that will be subject of further studies.

EXPERIMENTAL SECTION

General Experimental Procedures. Optical rotations were determined on a Perkin-Elmer-241 MC polarimeter. 1D and 2D NMR spectra were recorded on a Bruker ARX 500 or Avance DMX 600 NMR spectrometer. Mass spectra were measured with a LCMS HP1100 Agilent Finnigan LCQ Deca XP Thermoquest and high-resolution electrospray ionization mass spectroscopy (HRESIMS) spectra were recorded with an UHR-TOF maXis 4G (Bruker Daltonics, Bremen) mass spectrometer. HPLC analysis was performed using a HPLC (Dionex P580) system coupled to a photodiode array detector (UVD340S). Routine detection was at 235, 254, 280, and 340 nm. The separation column (125 × 4 mm, L × ID) was prefilled with Eurospher-10 C18 (Knauer, Germany) using a linear gradient of MeOH and 0.02% H_3PO_4 in H_2O and a flow rate of 1 mL/min. UV data (λ_{max}) for individual compounds were extracted from the online UV spectra provided by the instrument software. Column chromatography was performed on Silica gel 60M (230-3400 mesh ASTM, Macherey-Nagel GmbH & Co.KG, Dueren, Germany), Sephadex LH-20 (Sigma), or HP20 (Mitsubishi). TLC was carried out on

precoated silica gel plates (silica gel 60 F-254, Merck KGaA, Darmstadt, Germany) for monitoring of fractions using EtOAc/MeOH/H_2O (30:5:4) and CH_2Cl_2/MeOH (9:1) as solvent systems. Detection was at 254 and 366 nm or by spraying the plates with anisaldehyde reagent. Semi-preparative HPLC was carried out with Merck Hitachi L-7100 pump and L-7400 UV detector on an Eurosphere 100-10 C18 column (300 x 8 mm, L x ID, Knauer, Germany). Emodin (Sigma) was used in the antibacterial assays. Solvents were distilled before use, and spectral grade solvents were used for spectroscopic measurements.

ECD spectra were recorded on a J-810 spectropolarimeter. Vibrational circular dichroism (VCD) and absorption (VA) spectra were measured on a commercial ChiralIR spectrometer, modified to reduce the spectral artifacts by adding a second photoelastic modulator and associated electronics (Polavarapu and Shanmugam 2011). A 2 mg sample of flavomannin A (**1**) was dissolved in 0.100 mL CD_3CN solvent and the solution was equilibrated for 1 hr. Some portion of the sample was insoluble and the solution remained turbid. The solution was centrifuged and the supernatant liquid was transferred to a 200 micron path length infrared cell equipped with BaF_2 windows for the VCD measurements. The spectra were collected at 8 cm^{-1} resolution with 1 hr data collection time. Because of the use of saturated solutions, concentration is not known and for this reason, the experimental spectra are presented in absorbance units (instead of converting to molar extinction units).

Fungal Material. The endophytic fungus was isolated from inner tissues of *A. vera*, collected from the coastal region of Alexandria, Egypt, in June 2009, using a protocol previously described.(Debbab *et al.* 2009) The fungus (strain designation AVE 3.2) is kept in the authors' laboratory (P.P.).

Identification of Fungal Cultures. Fungal cultures were identified according to a molecular biological protocol by DNA amplification and sequencing of the ITS region as described previously.(Kjer *et al.* 2010) BLAST search revealed 95-97% similarity to *Talaromyces* sp. (AF285115.1). The fungal strain was sent in parallel to the Deutsche Sammlung von Mikroorganismen und Zellkulturen GmbH (DSMZ), Braunschweig, Germany, and was identified as *Talaromyces wortmannii* (Kloecker) C.R. Benj. The sequence data has been submitted to GenBank with accession number HM807532.1.

Cultivation. Mass growth of the fungus for the isolation and identification of new metabolites was carried out in Erlenmeyer flasks (1 L each). The fungal strain was cultivated on rice solid medium (100 mL of distilled water was added to 100 g commercially available rice and kept overnight prior to autoclaving) for 14 days at 22 °C under static conditions.

Extraction and Purification. Cultures were exhaustively extracted with EtOAc and the crude extract (3.5 g) was subjected to chromatographic separation over HP-20 using water/methanol/acetone gradient elution. The fraction eluted with 100% methanol was further fractionated by vacuum liquid chromatography (VLC) using mixtures of *n*-hexane/EtOAc/CH_2Cl_2/MeOH as eluting solvents. Fraction 4 (174 mg), eluted with 100% EtOAc**,** was further purified by semi-preparative HPLC using MeOH/H_2O gradient as the mobile phase to yield compounds **1** (20 mg) and **2** (5 mg). Fraction 8 (125 mg), eluted from VLC with CH_2Cl_2:MeOH (6:2), was further purified using sephadex LH-20 followed by semi-preparative HPLC with the same gradient mentioned above to yield **3** (14 mg), **4** (8 mg), **5** (7 mg) and **6** (3 mg).

Flavomannin A (1). Brown amorphous powder (MeOH); $[\alpha]_D^{20}$ –82 (*c* 0.02, MeOH); UV (MeOH/H_2O) λ_{max} (PDA) 236, 278 and 408 nm. ECD (MeCN, λ_{max} [nm] ($\Delta\varepsilon$), *c* = 3.02×10^{-4}): 442 (–0.64), 428 (0.24), 411sh (–2.43), 397 (–2.79), 316sh (–1.40), 285 (–24.53), 268 (35.87), 230 (3.86), 210 (–2.15), 195 (–3.74). ^{1}H and ^{13}C NMR data, see Table 1; ESIMS positive *m/z* 547.3 $[M+H]^+$ (100), 569.1 $[M+Na]^+$ (10), negative *m/z* 545.4 $[M-H]^-$ (100); HRESIMS *m/z* 547.1618 $[M+H]^+$ (calcd for $C_{30}H_{27}O_{10}$, 547.1599).

Flavomannin B (2). Brown amorphous powder (MeOH); $[\alpha]_D^{20}$ +72 (*c* 0.02, MeOH); UV (MeOH/H_2O) λ_{max} (PDA) 235, 279, 410 nm. ECD (MeCN, λ_{max} [nm] ($\Delta\varepsilon$), *c* = 1.55×10^{-4}): 462 (–1.34), 429 (–2.47), 409sh (4.04), 393 (5.59), 324sh (4.37), 286 (40.17), 266 (–67.25), 228 (–7.29), 211 (2.63), 195 (4.47). ^{1}H and ^{13}C NMR data, see Table 1. ESIMS positive *m/z* 547.4 $[M+H]^+$ (100), negative *m/z* 545.4 $[M-H]^-$ (100); HRESIMS *m/z* 547.1618 $[M+H]^+$ (calcd for $C_{30}H_{27}O_{10}$, 547.1599).

Flavomannin C (3). Brown amorphous powder; $[\alpha]_D^{20}$–170 (*c* 0.02, MeOH); UV (MeOH/H_2O) λ_{max} (PDA) 234, 279 and 407 nm. ECD (MeCN, λ_{max} [nm] ($\Delta\varepsilon$), *c* = 1.90×10^{-4}): 462 (–0.52), 443 (–0.79), 405 (–2.41), 349 (0.63), 316sh (–2.02), 286 (–16.99), 265 (18.45), 225 (5.51), 211 (–0.55), 192 (–2.59). ^{1}H and ^{13}C NMR data, see Table 2. ESIMS positive *m/z* 561.1

$[M+H]^+$ (100), negative *m/z* 559.3 $[M-H]^-$ (100). HREIMS *m/z* 561.1754 $[M+H]^+$ and 583.1569 $[M+Na]^+$ (calcd for $C_{31}H_{29}O_{10}$ 561.1761 and $C_{31}H_{28}O_{10}Na$ 583.1580, respectively).

Flavomannin D (4). Brown amorphous powder; $[\alpha]_D^{20}$ +110 (*c* 0.02, MeOH); UV (MeOH/H_2O) λ_{max} (PDA) 234, 279 and 407 nm. ECD (MeCN, λ_{max} [nm] ($\Delta\varepsilon$), *c* = 1.89×10^{-4}): 445sh (1.21), 412 (3.88), 394sh (2.68), 349 (–0.16), 323sh (2.62), 285 (52.08), 265 (–66.83), 229 (–10.46), 208 (3.23), 195 (4.58). ^1H and ^{13}C NMR data, see Table 2. ESIMS positive *m/z* 561.2 $[M+H]^+$ (100), negative *m/z* 559.2 $[M-H]^-$ (100). HREIMS *m/z* 561.1757 $[M+H]^+$ (calcd for $C_{31}H_{29}O_{10}$ 561.1761).

Talaromannin A (5). Brown amorphous powder; $[\alpha]_D^{20}$ –124 (*c* 0.02, MeOH); UV (MeOH/H_2O) λ_{max} (PDA) 223, 277 and 420 nm. ECD (MeCN, λ_{max} [nm] ($\Delta\varepsilon$), *c* = 1.86×10^{-4}): 456sh (–3.05), 434 (–3.90), 340 (–0.76), 308 (3.67), 288 (–33.25), 270 (25.88), 252sh (11.61), 225 (19.77), 209 (–8.81), 199 (1.09). ^1H and ^{13}C NMR data, see Table 3. ESIMS positive *m/z* 543.0 $[M+H]^+$ (100), negative *m/z* 541.2 $[M-H]^-$ (100). HREIMS *m/z* 543.1286 $[M+H]^+$ and 565.1102 $[M+Na]^+$ (calcd. for $C_{30}H_{23}O_{10}$ 543.1291 and for $C_{30}H_{22}O_{10}Na$ 565.1111, respectively).

Talaromannin B (6). Yellow brown amorphous powder; $[\alpha]_D^{20}$ +111 (*c* 0.02, MeOH); UV (MeOH/H_2O) λ_{max} (PDA) 224, 277 and 421 nm. ECD (MeCN, λ_{max} [nm] ($\Delta\varepsilon$), *c* = 1.81×10^{-4}): 463sh (1.16), 440 (2.03), 339 (0.69), 308 (–0.45), 289 (16.44), 270 (–13.85), 252sh (–6.98), 225 (12.12), 208 (4.42), 199 (–1.29). ^1H and ^{13}C NMR data, see Table 3. ESIMS negative *m/z* 541.3 $[M-H]^-$ (100). HREIMS *m/z* 543.1286 $[M+H]^+$ (calcd. for $C_{30}H_{23}O_{10}$ 543.1291).

Determination of Minimal Inhibitory Concentration. The MIC for the bacterial strains was determined by the broth microdilution method according to the recommendations of the Clinical and Laboratory Standards Institute (CLSI). (CLSI 2008) For preparation of the inoculum the direct colony suspension method was used. The strain panel included antibiotic-susceptible CLSI quality control strains: *S. aureus* ATCC 29213, *Streptococcus pneumoniae* ATCC 49619, *E. coli* ATCC 25922, *Klebsiella pneumoniae* ATCC 27799 (CLSI 2008), a standard laboratory strain (*B. subtilis* 168 trpC2) (Burkholder and Giles 1947), a high-level quinolone-resistant laboratory mutant (*E. coli* WT-3-1 MB2, Peter Heisig, University of Hamburg, Germany) and the following (multi)drug-resistant clinical isolates: *S. aureus* Mu50 (Hiramatsu et al. 1997), *S. aureus* 25697 (AiCuris, Wuppertal, Germany), *Streptococcus agalactiae* 013761 and *Streptococcus pyogenes* 014327 (Hans-Georg Sahl, University of

Bonn, Germany), *Enterococcus faecalis* UW 2689 (Wolfgang Witte, Robert Koch Institute, Wernigerode, Germany), *Enterococcus faecium* 6011 (Klare *et al.* 1995) and *P. aeruginosa* B 63230 (Henrichfreise *et al.* 2005).

Determination of Bacterial Cell Numbers. The number of viable bacterial cells was determined after performing the broth microdilution method as described above. Culture aliquots from each antibiotic concentration in the microtiter plate and from the growth control were serially diluted in fresh medium and plated on Mueller-Hinton agar. After incubation overnight at 37 °C visible colonies were counted.

Growth Curves. Bacterial growth was monitored by measuring the optical density in a microtiter plate reader (infinite M200, Tecan) at 600 nm in the absence and presence of the indicated antibiotic concentrations. For compound dilution and inoculating the plates the same conditions were used as described above for the broth microdilution method except for performing the assay in 96-well flat-bottom polystyrol microtiter plates in a total volume of 200 µL and shaking the plates between measurements. Plates were incubated at 37 °C and measured at 5 min intervals over 20 hours. Mueller-Hinton broth was used as growth medium for *S. aureus* Mu50 and lysogeny broth for *B. subtilis* 168 trpC2.

Reporter Gene Assays. For orienting mechanism of action studies five bacterial reporter strains were used, carrying the promoter of either *yorB*, *bmrC* (synonym *yheI)*, *helD* (synonym *yvgS)* and *liaI* (synonym *yvqI*) fused to the firefly luciferase reporter gene, or the promoter of the *recA* gene fused to the *β*-galactosidase reporter gene. *YorB*, *bmrC*, *helD*, and *liaI* strains were constructed in the genetic background of *B. subtilis* IS34 (Urban *et al.* 2007) and the *recA* strain in the background of *B. subtilis* YB3001 (Cheo *et al.* 1992). The luciferase assay was performed in white 96-well flat bottom polystyrol microtiter plates according to a previously described procedure (Stülke *et al.* 1993; Urban *et al.* 2007) and luciferase expression was measured in a Tecan microtiter plate reader (infinite M200, Tecan). For the *β*-galactosidase assay a serial twofold dilution of the compound in lysogeny broth in 96-well flat-bottom polystyrol microtiter plates was inoculated with a mid-exponential growing culture of the reporter strain. After an incubation period of 3 h at 37 °C, the microtiter plates were stored at -20 °C overnight. Then microtiter plates were thawed,

15 μL of a lysozyme solution (2.5 mg/mL in Z-buffer (Miller 1972)) was added and incubated for 30 min at 37 °C with shaking. After adding 15 μL of a Triton X-100 solution (0.5% in Z-buffer), black 96-well flat-bottom polystyrol microtiter plates containing 10 μL of the fluorogenic substrate 4-methylumbelliferyl β-D-galactopyranoside (MUG) were inoculated with 50 μL of the so treated culture and incubated for 1 h at 25 °C. Fluorescence was measured in a Tecan microtiter reader (infinite M200, Tecan) at an excitation wavelength of 360 nm and an emission wavelength of 450 nm.

Microscopy. For microscopy a *B. subtilis* 168 trpC2 culture was grown in lysogeny broth to early exponential growth phase (OD_{600} of 0.1-0.3) and treated with increasing concentrations of the test compound in 96-well flat-bottom polystyrol microtiter plates at 37 °C with shaking. At various time points (30 to 180 min after compound addition) culture aliquots of 6 μL were mixed with 2 μL of DAPI solution (Sigma-Aldrich, 1 μg/mL in H_2O) and incubated 60 s for DNA staining. 0.3 μL of the mixture was immobilized on microscope slides coated with 0.5 mL 1 % agarose (in H_2O) and analyzed by phase contrast and fluorescence microscopy using a Zeiss Axio Observer.Z1 microscope equipped with a Zeiss AxioCam camera. Image acquisition and analysis were performed with Zeiss ZEN 2011 software.

Cytotoxicity Assay. Cytotoxicity against the human leukemic monocyte cell line THP-1 and the mouse embryonic fibroblast cell line BALB/3T3 was measured using a fluorometric Alamar Blue assay. BALB/3T3 cells were grown in DMEM medium (PAN Biotech GmbH), containing 4.5 g/L glucose and 3.7 g/L $NaHCO_3$, supplemented with 10% fetal calf serum (v/v), 1% sodium pyruvate and 1% L-glutamine. THP-1 cells were cultured in RPMI-1640 medium (PAN Biotech GmbH) containing 2.0 g/L $NaHCO_3$, supplemented with 10% fetal calf serum (v/v), 1% L-glutamine and 1% penicillin-streptomycin (10,000 U/mL penicillin and 10 mg/mL streptomycin; PAN Biotech GmbH). Cells were seeded in 96-well plates at 10^4 cells/well in 190 μL of cell culture medium without penicillin-streptomycin. Test compounds were dissolved in DMSO (10 mg/mL) and twofold serial dilutions were prepared in DMSO. 10 μL sample of each compound dilution was added to the cells, resulting in final concentration of 0.016 - 32 μg/mL test compound per mL in cell culture medium plus 0.32% DMSO. Plates were incubated for 48 h at 5% CO_2 and 37 ^{o}C. Cell culture medium and cycloheximide (AppliChem) served as negative and positive controls, respectively. Then 10

μL Alamar Blue/well (Invitrogen) was added and the incubation was continued for another 24 h. After 72 h of total incubation time in the presence of test compound, fluorescence was read using a 96-well fluorometer (Tecan, infinite M200) with excitation at 560 nm and emission at 600 nm. Relative fluorescence units (RFU) were determined by the ratio of fluorescence emitted by treated cells vs. untreated cells and served for determination of the 50% inhibitory concentrations (IC_{50}). Experiments were carried out in duplicates.

Computational Section. Conformational searches were carried out by means of the Macromodel 9.7.211(Schrödinger 2009) software using Merck Molecular Force Field (MMFF) with implicit solvent model for chloroform. Geometry optimizations [B3LYP/6-31G(d) in vacuo and B3LYP/TZVP with PCM solvent model for acetonitrile and TDDFT calculations were performed with Gaussian 09 (Frisch *et al.* 2010) using various functionals (B3LYP, BH&HLYP, PBE0) and TZVP basis set. ECD spectra were generated as the sum of Gaussians (Stephens and Harada 2010) with 3000 and 2700 cm^{-1} half-height width (corresponding to 22 and 20 nm at 270 nm, respectively), using dipole-velocity computed rotational strengths. Boltzmann distributions were estimated from the ZPVE corrected B3LYP/6-31G(d) or the B3LYP/TZVP energies. The MOLEKEL (Varetto 2009) software package was used for visualization of the results.

20 conformations of (a*R*,3*R*,3'*R*) and 20 conformations of (a*S*,3*R*,3'*R*) stereoisomers optimized at B3LYP/TZVP level using PCM for representing acetonitrile solvent influence were used for VCD calculations at the same level using G09 program. Gibbs free energies were used to calculate the populations of individual conformers and population weighted VCD and VA spectra were generated for both stereoisomers. The spectral simulations were carried out with Lorentzian band shapes and 10 cm^{-1} half-width at half-peak height.

ACKNOWLEDGMENTS

We gratefully acknowledge Christoph Freiberg (Bayer Pharma AG, Wuppertal, Germany), Andreas Urban (AiCuris, Wuppertal, Germany) and David Cheo (Quanta Biosciences, Gaithersburg, USA) for generating and providing reporter strains. In addition, we thank Peter Heisig (University of Hamburg, Germany), Hans-Georg Sahl (University of Bonn, Germany), Wolfgang Witte (Robert-Koch Institute, Wernigerode, Germany) and AiCuris GmbH & Co. KG (Wuppertal, Germany) for providing clinical isolates. This study was supported by grants of the BMBF awarded to P.P. and A.D., of the state North Rhine-Westphalia and the European Union (European Regional Development Fund, Investing in your future) to I.Z., H.G.-G. and H.B.-O. T.K. and A.M. thank the Hungarian National Research Foundation for financial support (OTKA K105871) and the National Information Infrastructure Development Institute (NIIFI 10038). P.L.P. gratefully acknowledges NSF funding (CHE-0804301). This work was conducted in part using the resources of the Advanced Computing Center for Research and Education at Vanderbilt University, Nashville, TN.

REFERENCES

Aly, A. H. Protein kinase inhibitors and other cytotoxic metabolites from the fungal endophyte Stemphylium botryosum isolated from Chenopodium album. *Mycosphere*. **2010**, *1*(2): 153.

Aly, A. H., Debbab, A., Clements, C., Edrada-Ebel, R., Orlikova, B., Diederich, M., Wray, V., Lin, W. and Proksch, P. NF kappa B inhibitors and antitrypanosomal metabolites from endophytic fungus Penicillium sp. isolated from Limonium tubiflorum. *Bioorganic & Medicinal Chemistry*. **2011**, *19*(1): 414-421.

Antonowitz, A., Gill, M., Morgan, P. M. and Jin, Y. Coupled anthraquinones from the toadstool Dermocybe icterinoides. *Phytochemistry*. **1994**, *37*(6): 1679-1683.

Arai, K., Aoki, Y. and Yamamoto, Y. Asperinines A and B, dimeric tetrahydroanthracene derivatives from Aspergillus ruber.**1989**, Tokyo, JAPON, Chemical & pharmaceutical bulletin.

Atherton, J., Bycroft, B. W., Roberts, J. C., Roffey, P. and Wilcox, M. E. Studies in mycological chemistry. Part XXIII. The structure of flavomannin, a metabolite of Penicillium wortmanni Klock. *Journal of the Chemical Society C: Organic*. **1968**: 2560-2564.

Au, N., Kuester-Schoeck, E., Mandava, V., Bothwell, L. E., Canny, S. P., Chachu, K., Colavito, S. A., Fuller, S. N., Groban, E. S., Hensley, L. A., O'Brien, T. C., Shah, A., Tierney, J. T., Tomm, L. L., O'Gara, T. M., Goranov, A. I., Grossman, A. D. and Lovett, C. M. Genetic composition of the Bacillus subtilis SOS system. *J Bacteriol*. **2005**, *187*(22): 7655-66.

Bandow, J. E., Brotz, H., Leichert, L. I., Labischinski, H. and Hecker, M. Proteomic approach to understanding antibiotic action. *Antimicrob Agents Chemother*. **2003**, *47*(3): 948-55.

Basu, S., Ghosh, A. and Hazra, B. Evaluation of the antibacterial activity of Ventilago madraspatana Gaertn., Rubia cordifolia Linn. and Lantana camara Linn.: Isolation of emodin and physicon as active antibacterial agents. *Phytother. Res.* **2005**, *19*: 888-894.

Beattie, K., Elsworth, C., Gill, M., Milanovic, N. M., Prima-Putra, D. and Raudies, E. Austrocolorins A1 and B1: atropisomeric 10,10'-linked dihydroanthracenones from an Australian Dermocybe sp. *Phytochemistry*. **2004**, *65*(8): 1033-1038.

Brotz-Oesterhelt, H., Beyer, D., Kroll, H. P., Endermann, R., Ladel, C., Schroeder, W., Hinzen, B., Raddatz, S., Paulsen, H., Henninger, K., Bandow, J. E., Sahl, H. G. and Labischinski, H. Dysregulation of bacterial proteolytic machinery by a new class of antibiotics. *Nat Med*. **2005**, *11*(10): 1082-7.

Cheo, D. L., Bayles, K. W. and Yasbin, R. E. Molecular characterization of regulatory elements controlling expression of the Bacillus subtilis recA+ gene. *Biochimie*. **1992**, *74*(7-8): 755-62.

CLSI, M.-A. Methods for dilution antimicrobial susceptibility tests for bacteria that grow aerobically. Approved standard.**2008**, Clinical and Laboratory Standards Institute.

Debbab, A., Aly, A. and Proksch, P. Bioactive secondary metabolites from endophytes and associated marine derived fungi. *Fungal Diversity*. **2011**, *49*(1): 1-12.

Debbab, A., Aly, A. and Proksch, P. Endophytes and associated marine derived fungi-ecological and chemical perspectives. *Fungal Diversity*. **2012**, *57*(1): 45-83.

Debbab, A., Aly, A. H., Edrada-Ebel, R., Wray, V., Müller, W. E. G., Totzke, F., Zirrgiebel, U., Schälchtele, C., Kubbutat, M. H. G., Lin, W. H., Mosaddak, M., Hakiki, A., Proksch, P. and Ebel, R. Bioactive metabolites from the endophytic fungus Stemphylium

globuliferum isolated from Mentha pulegium. *Journal of Natural Products*. **2009**, *72*(4): 626-631.

Debbab, A., Aly, A. H., Edrada-Ebel, R., Wray, V., Pretsch, A., Pescitelli, G., Kurtan, T. and Proksch, P. New Anthracene Derivatives – Structure Elucidation and Antimicrobial Activity. *European Journal of Organic Chemistry*. **2012**, (7): 1351-1359.

Debbab, A., Aly, A. H., Edrada-Ebel, R., Wray, V., Pretsch, A., Pescitelli, G., Kurtan, T. and Proksch, P. New Anthracene Derivatives – Structure Elucidation and Antimicrobial Activity. *European Journal of Organic Chemistry*. **2012**, *2012*(7): 1351-1359.

Debbab, A., Aly, A. H., Lin, W. H. and Proksch, P. Bioactive compounds from marine bacteria and fungi. *Microb Biotechnol*. **2010**, *3*(5): 544-63. doi: 10.1111/j.1751-7915.2010.00179.x. Epub 2010 May 23.

Deleo, F. R., Otto, M., Kreiswirth, B. N. and Chambers, H. F. Community-associated meticillin-resistant Staphylococcus aureus. *Lancet*. **2010**, *375*(9725): 1557-68.

Delumeau, O., Lecointe, F., Muntel, J., Guillot, A., Guedon, E., Monnet, V., Hecker, M., Becher, D., Polard, P. and Noirot, P. The dynamic protein partnership of RNA polymerase in Bacillus subtilis. *Proteomics*. **2011**, *11*(15): 2992-3001.

Dewick, P. M. Medicinal natural products. A biosynthetic approach; 3rd ed.**2009**, Baffins Lane, Chichester, England, John Wiley & Sons, Ltd.

Dreyer, D. L., Arai, I., Bachman, C. D., Anderson, W. R. J. and Smith, R. G. D., G. D. Jr. . Toxins causing noninflammatory paralytic neuronopathy. Isolation and structure elucidation. *J. Am. Chem. Soc.* **1975**, *97*: 4985-4990.

Drlica, K. and Zhao, X. DNA gyrase, topoisomerase IV, and the 4-quinolones. *Microbiol Mol Biol Rev*. **1997**, *61*(3): 377-92.

Ebrahim, W., Aly, A. H., Mándi, A., Totzke, F., Kubbutat, M. H. G., Wray, V., Lin, W.-H., Dai, H., Proksch, P., Kurtán, T. and Debbab, A. Decalactone derivatives from Corynespora cassiicola, an endophytic fungus of the mangrove plant Laguncularia racemosa. *European Journal of Organic Chemistry*. **2012**, *2012*(18): 3476-3484.

Eichelbaum, M., Gross, A. S. and Bernard Testa and Urs, A. M. Stereochemical aspects of drug action and disposition. Advances in Drug Research, Academic Press.**1996**, *Volume 28***:** 1-64.

Elsässer, B., Krohn, K., Flörke, U., Root, N., Aust, H.-J., Draeger, S., Schulz, B., Antus, S. and Kurtán, T. X-ray Structure Determination, Absolute Configuration and Biological Activity of Phomoxanthone A. *European Journal of Organic Chemistry*. **2005**, *2005*(21): 4563-4570.

Elsworth, C., Gill, M., Gimenez, A., M. Milanovic, N. and Raudies, E. Pigments of fungi. Part 50.1 Structure, biosynthesis and stereochemistry of new dimeric dihydroanthracenones of the phlegmacin type from Cortinarius sinapicolor Cleland. *Journal of the Chemical Society, Perkin Transactions 1*. **1999**, (2): 119-126.

Endo, M. and Naoki, H. Antimicrobial and antispasmodic tetrahydroanthracenes from Cassia singueana. *Tetrahedron* **1980**, *36*: 2449-2452.

Evans, D. A., Dinsmore, C. J., Watson, P. S., Wood, M. R., Richardson, T. I., Trotter, B. W. and Katz, J. L. Nonconventional Stereochemical Issues in the Design of the Synthesis of the Vancomycin Antibiotics: Challenges Imposed by Axial and Nonplanar Chiral Elements in the Heptapeptide Aglycons. *Angewandte Chemie International Edition*. **1998**, *37*(19): 2704-2708.

Freiberg, C., Brunner, N., Macko, L. and Fischer, H. P. Discovering Antibiotic Efficacy Biomarkers. *Molecular & Cellular Proteomics*. **2006**, *5*(12): 2326-2335.

Freiberg, C., Fischer, H. P. and Brunner, N. A. Discovering the Mechanism of Action of Novel Antibacterial Agents through Transcriptional Profiling of Conditional Mutants. *Antimicrobial Agents and Chemotherapy*. **2005**, *49*(2): 749-759.

Frisch, M. J., G. W. Trucks, H. B. Schlegel, G. E. Scuseria, M. A. Robb, J. R. Cheeseman, J. A. Montgomery, J., T. Vreven, K. N. Kudin, J. C. Burant, J. M. Millam, S. S. Iyengar, J. Tomasi, V. Barone, B. Mennucci, M. Cossi, G. Scalmani, N. Rega, G. A. Petersson, H. Nakatsuji, M. Hada, M. Ehara, K. Toyota, R. Fukuda, J. Hasegawa, M. Ishida, T. Nakajima, Y. Honda, O. Kitao, H. Nakai, M. Klene, X. Li, J. E. Knox, H. P. Hratchian, J. B. Cross, C. Adamo, J. Jaramillo, R. Gomperts, R. E. Stratmann, O. Yazyev, A. J. Austin, R. Cammi, C. Pomelli, J. W. Ochterski, P. Y. Ayala, K. Morokuma, G. A. Voth, P. Salvador, J. J. Dannenberg, V. G. Zakrzewski, S. Dapprich, A. D. Daniels, M. C. Strain, O. Farkas, D. K. Malick, A. D. Rabuck, K. Raghavachari, J. B. Foresman, J. V. Ortiz, Q. Cui, A. G. Baboul, S. Clifford, J. Cioslowski, B. B. Stefanov, G. Liu, A. Liashenko, P. Piskorz, I. Komaromi, R. L. Martin, D. J. Fox, T. Keith, M. A. Al-Laham, C. Y. Peng, A. Nanayakkara, M. Challacombe, P. M. W. Gill, B. Johnson, W. Chen, M. W. Wong, C. Gonzalez and Pople, J. A. Gaussian 09, Revision B.01. *Gaussian, Inc., Pittsburgh PA,* . **2010**.

Gill, M., Gimenez, A., Jhingran, A. G. and Palfreyman, A. R. Pigments of fungi. Part 19. A degradative method for the determination of central chirality in naturally occurring 3-hydroxy-3-methyl-3,4-dihydroanthracen-1(2H)-ones: Application to pigments of the flavomannin type. *Tetrahedron*. **1990**, *1*: 621-634.

Gill, M., Gimenez, A., Jhingran, A. G. and Smrdel, A. F. Pigments of fungi. Part 10. Dihydroanthracenones from Dermocybe splendida and related fungi. *Phytochemistry*. **1989**, *28*: 2647-2650.

Gill, M., Gimenez, A. and McKenzie, R. W. Pigments of Fungi, Part 8. Bianthraquinones from Dermocybe austroveneta. *Journal of Natural Products*. **1988**, *51*(6): 1251-1256.

Gill, M. and Morgan, P. M. New fungal anthraquinones. *ARKIVOC*. **2001**, *7*: 145-156.

Gill, M. and Morgan, P. M. Absolute stereochemistry of fungal metabolites: icterinoidins A1 and B1, and atrovirins B1 and B2. *Arcivoc*. **2004**, *X*: 152-165

Gill, M., Saubern, S. and Yu, J. Pigments of fungi. LXVI. The gentiobiosides of (R)- and (S)-torosachrysone from Australian toadstools and methods for assaying the enantiomeric purity of natural torosachrysone. . *Aust. J. Chem.* **2000**, *53*: 213-220.

Gould, I. M., David, M. Z., Esposito, S., Garau, J., Lina, G., Mazzei, T. and Peters, G. New insights into meticillin-resistant Staphylococcus aureus (MRSA) pathogenesis, treatment and resistance. *International Journal of Antimicrobial Agents*. **2012**, *39*(2): 96-104.

Hammerschmidt, L., Wray, V., Lin, W., Kamilova, E., Proksch, P. and Aly, A. H. New styrylpyrones from the fungal endophyte Penicillium glabrum isolated from Punica granatum. *Phytochemistry Letters*. **2012**, *5*(3): 600-603.

Henrichfreise, B., Wiegand, I., Sherwood, K. J. and Wiedemann, B. Detection of VIM-2 metallo-beta-lactamase in Pseudomonas aeruginosa from Germany. *Antimicrob Agents Chemother*. **2005**, *49*(4): 1668-9.

Kitanaka, S. and Takido, M. Two new bitetrahydroanthracenes from roots of Cassia occidentalis L. *Chem. Pharm. Bull.* . **1989**, *37*: 511-512.

Kjer, J., Debbab, A., Aly, A. H. and Proksch, P. Methods for isolation of marine-derived endophytic fungi and their bioactive secondary products. *Nat. Protoc.* . **2010**, *5*: 479-490.

Klare, I., Heier, H., Claus, H., Bohme, G., Marin, S., Seltmann, G., Hakenbeck, R., Antanassova, V. and Witte, W. Enterococcus faecium strains with vanA-mediated high-level glycopeptide resistance isolated from animal foodstuffs and fecal samples of humans in the community. *Microb Drug Resist*. **1995**, *1*(3): 265-72.

Klevens, R. M., Morrison, M. A., Nadle, J., Petit, S., Gershman, K., Ray, S., Harrison, L. H., Lynfield, R., Dumyati, G., Townes, J. M., Craig, A. S., Zell, E. R., Fosheim, G. E., McDougal, L. K., Carey, R. B. and Fridkin, S. K. Invasive methicillin-resistant Staphylococcus aureus infections in the United States. *Jama*. **2007**, *298*(15): 1763-71.

Knight, G. M., Budd, E. L., Whitney, L., Thornley, A., Al-Ghusein, H., Planche, T. and Lindsay, J. A. Shift in dominant hospital-associated methicillin-resistant Staphylococcus aureus (HA-MRSA) clones over time. *J Antimicrob Chemother*. **2012**, *67*(10): 2514-22.

Kusari, S., Lamshöft, M., Zühlke, S. and Spiteller, M. An endophytic fungus from Hypericum perforatum that produces hypericin. *J. Nat. Prod.* **2008**, *71*: 159-162.

Kusari, S., Zühlke, S., Kosuth, J., Cellarova, E. and Spiteller, M. Light-independent metabolomics of endophytic Thielavia subthermophila provides insight into microbial hypericin biosynthesis. . *J. Nat. Prod.* **2009**, *72.*: 1825-1835.

LaPlante, S. R., D. Fader, L., Fandrick, K. R., Fandrick, D. R., Hucke, O., Kemper, R., Miller, S. P. F. and Edwards, P. J. Assessing Atropisomer Axial Chirality in Drug Discovery and Development. *Journal of Medicinal Chemistry*. **2011**, *54*(20): 7005-7022.

LaPlante, S. R., Edwards, P. J., Fader, L. D., Jakalian, A. and Hucke, O. Revealing Atropisomer Axial Chirality in Drug Discovery. *ChemMedChem*. **2011**, *6*(3): 505-513.

Lazarevic, V., Dusterhoft, A., Soldo, B., Hilbert, H., Mauel, C. and Karamata, D. Nucleotide sequence of the Bacillus subtilis temperate bacteriophage SPbetac2. *Microbiology*. **1999**, *145 (Pt 5)*: 1055-67.

Lee, N. J., Choi, J. H., Koo, B. S., Ryu, S. Y., Han, Y. H., Lee, S. I. and Lee, D. U. Antimutagenicity and cytotoxicity of the constituents from the aerial parts of Rumex acetosa. *Biol Pharm Bull*. **2005**, *28*(11): 2158-61.

Li, E., Jiang, L., Guo, L., Zhang, H. and Che, Y. Pestalachlorides A-C, antifungal metabolites from the plant endophytic fungus Pestalotiopsis adusta. *Bioorganic & Medicinal Chemistry*. **2008**, *16*(17): 7894-7899.

Lin, L.-C., Chou, C.-J. and Kuo, Y.-C. Cytotoxic Principles from Ventilago leiocarpa. *Journal of Natural Products*. **2001**, *64*(5): 674-676.

Liu, F., Cai, X.-L., Yang, H., Xia, X.-K., Guo, Z.-Y., Yuan, J., Li, M.-F., She, Z.-G. and Lin, Y.-C. The bioactive metabolites of the mangrove endophytic fungus Talaromyces sp. ZH-154 isolated from Kandelia candel (L.) Druce. *Planta Med*. **2010**, *76*(02): 185-189.

Lloyd-Williams, P. and Giralt, E. Atropisomerism, biphenyls and the Suzuki coupling: peptide antibiotics. *Chemical Society Reviews*. **2001**, *30*(3): 145-157.

Love, P. E. and Yasbin, R. E. Genetic characterization of the inducible SOS-like system of Bacillus subtilis. *J Bacteriol*. **1984**, *160*(3): 910-20.

MacDougall, C., Powell, J. P., Johnson, C. K., Edmond, M. B. and Polk, R. E. Hospital and community fluoroquinolone use and resistance in Staphylococcus aureus and Escherichia coli in 17 US hospitals. *Clin Infect Dis*. **2005**, *41*(4): 435-40.

Mascher, T., Zimmer, S. L., Smith, T. A. and Helmann, J. D. Antibiotic-inducible promoter regulated by the cell envelope stress-sensing two-component system LiaRS of Bacillus subtilis. *Antimicrob Agents Chemother*. **2004**, *48*(8): 2888-96.

Müller, M., Lamottke, K., Steglich, W., Busemann, S., Reichert, M., Bringmann, G. and Spiteller, P. Biosynthesis and Stereochemistry of Phlegmacin-Type Fungal Pigments. *European Journal of Organic Chemistry*. **2004**, *2004*(23): 4850-4855.

Muniz-Medina, V. M., Jones, S., Maglich, J. M., Galardi, C., Hollingsworth, R. E., Kazmierski, W. M., Ferris, R. G., Edelstein, M. P., Chiswell, K. E. and Kenakin, T. P. The Relative Activity of â€œFunction Sparingâ€□ HIV-1 Entry Inhibitors on Viral Entry and CCR5 Internalization: Is Allosteric Functional Selectivity a Valuable Therapeutic Property? *Molecular Pharmacology*. **2009**, *75*(3): 490-501.

Nicolaou, K. C., Simmons, N. L., Chen, J. S., Haste, N. M. and Nizet, V. Total synthesis and biological evaluation of marinopyrrole A and analogues. *Tetrahedron*. **2011**, *52*(17): 2041-2043.

Parker, J. C., McPherson, R. K., Andrews, K. M., Levy, C. B., Dubins, J. S., Chin, J. E., Perry, P. V., Hulin, B., Perry, D. A., Inagaki, T., Dekker, K. A., Tachikawa, K., Sugie, Y. and Treadway, J. L. Effects of skyrin, a receptor-selective glucagon antagonist, in rat and human hepatocytes. *Diabetes*. **2000**, *49*(12): 2079-2086.

Pietiäinen, M., Gardemeister, M., Mecklin, M., Leskelä, S., Sarvas, M. and Kontinen, V. P. Cationic antimicrobial peptides elicit a complex stress response in Bacillus subtilis that involves ECF-type sigma factors and two-component signal transduction systems. *Microbiology*. **2005**, *151*(5): 1577-1592.

Polavarapu, P. L., Jeirath, N., Kurtán, T., Pescitelli, G. and Krohn, K. Determination of the absolute configurations at stereogenic centers in the presence of axial chirality. *Chirality*. **2009**, *21*(1E): E202-E207.

Ren, X., Dong, Y., Zhang, H., Lu, X., Zheng, Z., Liu, M. and He, J. Study on aldose reductase inhibitor F01-195A produced from fermentation broth of microorganism. . *J Hebei Univ Nat Sci* **2006**, *26:*: 7-10.

Rivas, V., Cuevas, G., Garza, L. and Waksman, N. Isolation and evaluation of the cytotoxic properties of peroxisomicine isomers from Karwinskia parvifolia. *ARKIVOC*. **2005**: 224-233.

Ruef, C. Epidemiology and clinical impact of glycopeptide resistance in Staphylococcus aureus. *Infection*. **2004**, *32*(6): 315-27.

Salazar, R., Rivas, V., González, G. and Waksman, N. Antimicrobial activity of coupled hydroxyanthracenones isolated from plants of the genus Karwinskia. *Fitoterapia , ,*. **2006**, *77*: 398-400.

Sass, P., Josten, M., Famulla, K., Schiffer, G., Sahl, H. G., Hamoen, L. and Brotz-Oesterhelt, H. Antibiotic acyldepsipeptides activate ClpP peptidase to degrade the cell division protein FtsZ. *Proc Natl Acad Sci U S A*. **2011**, *108*(42): 17474-9.

Schrödinger, L. L. C. Macromodel 9.7.211 *http://www.schrodinger.com/Products/macromodel.html*. **2009**.

Shah, R. R., Midgley, J. M. and Branch, S. K. Stereochemical origin of some clinically significant drug safety concerns: lessons for future drug development. *Adverse drug reactions and toxicological reviews*. **1998**, *17*(2-3): 145-190.

Stephens, P. J. and Harada, N. ECD cotton effect approximated by the Gaussian curve and other methods. *Chirality*. **2010**, *22*(2): 229-33.

Stierle, A., Strobel, G. A. and Stierle, D. Taxol and taxane production by Taxomyces andreanae, an endophytic fungus of Pacific yew. *Science* **1993**, *260*: 214-216.

Stülke, J., Hanschke, R. and Hecker, M. Temporal activation of beta-glucanase synthesis in Bacillus subtilis is mediated by the GTP pool. *J Gen Microbiol*. **1993**, *139*(9): 2041-5.

Takahashi, S., Kitanaka, S., Takido, M., Sankawa, U. and Shibata, S. Phlegmacins and anhydrophlegmacinquinones: Dimeric hydroanthracenes from seedlings of Cassia torosa. *Phytochemistry*. **1977**, *14*: 999-1002.

Takeda, N., Seo, S., Ogihara, Y., Sankawa, U., Iitaka, I., Kitagawa, I. and Shibata, S. Studies on fungal metabolites XXXI: Anthraquinonoid colouring matters of Penicillium islandicum sopp and some other fungi (+)-luteoskyrin, (+)-rubroskyrin, (+)-rugulosin and their related compounds. *Tetrahedron*. **1973**, *29*(22): 3703-3719.

Tan, J. H., Zhang, Q. X., Huang, Z. S., Chen, Y., Wang, X. D., Gu, L. Q. and Wu, J. Y. Synthesis, DNA binding and cytotoxicity of new pyrazole emodin derivatives. *Eur J Med Chem*. **2006**, *41*(9): 1041-7.

Tenover, F. C. and Moellering, R. C. The Rationale for Revising the Clinical and Laboratory Standards Institute Vancomycin Minimal Inhibitory Concentration Interpretive Criteria for Staphylococcus aureus. *Clinical Infectious Diseases*. **2007**, *44*(9): 1208-1215.

Tenover, F. C., Sinner, S. W., Segal, R. E., Huang, V., Alexandre, S. S., McGowan Jr, J. E. and Weinstein, M. P. Characterisation of a Staphylococcus aureus strain with progressive loss of susceptibility to vancomycin and daptomycin during therapy. *International Journal of Antimicrobial Agents*. **2009**, *33*(6): 564-568.

Torres, C., GaliÃ¡n, C., Freiberg, C., Fantino, J.-R. l. and Jault, J.-M. The YheI/YheH heterodimer from Bacillus subtilis is a multidrug ABC transporter. *Biochimica et Biophysica Acta (BBA) - Biomembranes*. **2009**, *1788*(3): 615-622.

Urban, A., Eckermann, S., Fast, B., Metzger, S., Gehling, M., Ziegelbauer, K., Rabsamen-Waigmann, H. and Freiberg, C. Novel Whole-Cell Antibiotic Biosensors for Compound Discovery. *Applied and Environmental Microbiology*. **2007**, *73*(20): 6436-6443.

Varetto, U. MOLEKEL 5.4.0.8, Swiss National Supercomputing Centre, Manno, Switzerland. **2009**.

Wagenaar, M. M., Gibson, D. M. and Clardy, J. Akanthomycin, a New Antibiotic Pyridone from the Entomopathogenic Fungus Akanthomyces gracilis. *Organic Letters*. **2002**, *4*(5): 671-673.

Wanjohi, J. M., Yenesew, A., Midiwo, J. O., Heydenreich, M., Peter, M. G., Dreyer, M., Reichert, M. and Bringmann, G. Three dimeric anthracene derivatives from the fruits of Bulbine abyssinica. *Tetrahedron*. **2005**, *61*(10): 2667-2674.

Wenzel, M., Patra, M., Albrecht, D., Chen, D. Y., Nicolaou, K. C., Metzler-Nolte, N. and Bandow, J. E. Proteomic signature of fatty acid biosynthesis inhibition available for in vivo mechanism-of-action studies. *Antimicrob Agents Chemother*. **2011**, *55*(6): 2590-6.

Wolf, D., Kalamorz, F., Wecke, T., Juszczak, A., MÃ¤der, U., Homuth, G., Jordan, S., Kirstein, J., Hoppert, M., Voigt, B., Hecker, M. and Mascher, T. In-Depth Profiling of the LiaR Response of Bacillus subtilis. *Journal of Bacteriology*. **2010**, *192*(18): 4680-4693.

Yasbin, R. E. DNA repair in Bacillus subtilis. I. The presence of an inducible system. *Mol Gen Genet.* **1977**, *153*(2): 211-8.

Yasbin, R. E. DNA repair in Bacillus subtilis. II. Activation of the inducible system in competent bacteria. *Mol Gen Genet.* **1977**, *153*(2): 219-25.

Yasbin, R. E. and Andersen, B. J. DNA repair in Bacillus subtilis: the identification of a strain temperature inducible for SOS functions.**1982**, New York, Academic Press, Inc.

Table 1. NMR data of 1 and 2 (MeOH-d_4, δ in ppm, J in Hz)

Position	**1**[a]		**2**[b]	
	δ_C	δ_H	δ_C[c]	δ_H
1/1'	203.3		202.0	
2/2'	51.4	2.80 (d, 17.4)	51.0	2.90 (d, 17.3)
		2.71 (d, 17.4)		2.81 (d, 17.3)
3/3'	71.2		70.0	
4/4'	43.6	3.00 (d, 16.0)	43.0	3.11 (d, 16.2)
		2.95 (d, 16.0)		3.06 (d, 16.2)
4a/4a'	137.0		137.0	
5/5'	102.8	6.61 (s)	102.0	6.69 (s)
6/6'	161.7		162.0	
7/7'	108.8		108.0	
8/8'	158.6		159.0	
8a/8a'	108.0		108.0	
9/9'	167.0		167.0	
9a/9a'	107.9		107.0	
10/10'	117.8	6.80 (s)	118.0	6.90 (s)
10a/10a'	141.8		141.0	
11/11'	28.9	1.35 (s)	29.0	1.43 (s)

[a]500 (^{1}H) and 125 (^{13}C) MHz. [b]600 (^{1}H) and 150 (^{13}C) MHz. [c]Derived from HMBC spectrum.

Table 2. NMR data of 3 and 4 at 600 (^{1}H) and 150 (^{13}C) MHz (MeOH-d_4, δ in ppm, J in Hz)

Position	3		4	
	δ_C	δ_H	δ_C[a]	δ_H
1	203.1		204.0	
2	51.2	2.80 (d, 17.0)	51.6	2.81 (d, 17.0)
		2.89 (d, 17.0)		2.90 (d, 17.0)
3	70.7		71.4	
4	43.8	3.04 (d, 15.7)	43.9	3.05 (d, 15.0)
		3.08 (d, 15.7)		3.09 (d, 15.0)
4a	137.3		138.0	
5	102.7	6.73 (s)	103.0	6.66 (s)
6	157.8		162.0	
7	107.6		108.0	
8	161.3		163.6	
8a	108.8		109.0	
9	166.6		167.2	
9a	108.8		109.0	
10	118.4	6.88 (br. s)	118.0	6.89 (br. s)
10a	141.3		142.2	
1'	204.4		204.0	
2'	51.6	2.82 (d, 17.0)	51.9	2.90 (d, 17.0)
		2.92 (d, 17.0)		2.92 (d, 17.0)
3'	70.8		71.5	
4'	43.8	3.08 (d, 15.7)	43.9	3.10 (d, 15.0)
		3.14 (d, 15.7)		3.15 (d, 15.0)
4a'	138.0		138.0	
5'	98.8	6.84 (s)	99.0	6.82 (s)
6'	163.2		163.5	
7'	107.9		109.0	
8'	165.8		163.6	
8a'	108.8		109.0	
9'	167.9		168.2	
9a'	109.4		109.5	
10'	117.2	7.05 (br. s)	119.0	7.07 (br. s)
10a'	141.6		142.0	
3-CH_3	29.0	1.41 (s)	28.9	1.42 (s)
3'-CH_3	29.0	1.42 (s)	29.0	1.43 (s)
6'-OCH_3	56.5	3.82 (s)	56.2	3.86 (s)

[a]Derived from HMBC spectrum.

Table 3. NMR data of 5 and 6 at 600 (^{1}H) and 150 (^{13}C) MHz (Aceton-d_6, δ in ppm, J in Hz)

Position	**5**		**6**	
	δ_C	δ_H	δ_C[a]	δ_H
1	203.8		203.5	
2	51.5	2.79(d, 17.5)	51.6	Ov. Solvent
		2.93 (d, 17.5)		2.92 (d, 17.4)
3	70.7		70.0	
4	43.7	3.04 (d, 15.8)	43.1	3.05 (d, 15.8)
		3.11 (d, 15.8)		3.11 (d, 15.8)
4a	138.2		137.9	
5	102.8	6.76 (s)	108.0	6.77 (s)
6	158.4			
7	107.6		106.2	
8	166.4		165.0	
8a	105.3		105.4	
9	160.8		160.0	
9a	109.0		108.2	
10	117.3	6.87 (br. s)	117.0	6.90 (br. s)
10a	141.8			
1'	163.0		162.3	
2'	124.8	7.14 (s)	124.2	7.15 (s)
3'	149.3		148.6	
4'	121.3	7.60 (s)	120.6	7.61 (s)
4a'	134.3		134.6	
5'	109.5	7.43 (s)	108.8	7.44 (s)
6'	164.5		163.9	
7'	115.7		115.0	
8'	164.5		163.9	
8a'	110.1		109.4	
9'	191.8		191.1	
9a'	114.6		113.9	
10'	182.3		181.6	
10a	135.3		134.6	
3-CH_3	29.0	1.42 (s)	28.5	1.41 (s)
3'-CH_3	21.9	2.47 (s)	21.2	2.48 (s)
6-OH		10.08[b]		10.08[c]
8-OH		10.08[b]		10.20[c]
9-OH		16.70 (s)		16.71 (s)
1'-OH		12.14 (s)		12.15 (s)
6'-OH		10.20[b]		10.20[c]
8'-OH		12.55 (s)		12.54 (s)

[a]Derived from HMBC spectrum. [b,c]Assignments may be exchangeable.

Table 4. Minimal inhibitory concentrations [μg/mL] of the flavomannin/talaromannin derivatives (1-6), emodin and skyrin (7)

Tested organism	Resistance phenotype[a]	Flavomannin				Talaromannin		Emodin	Skyrin
Gram-positive		**A**	**B**	**C**	**D**	**A**	**B**		
Staphylococcus aureus ATCC 29213	susceptible	16	16	64	8-16	8	16	4(2)	4(2)
Staphylococcus aureus Mu50	CAZ^{R}[b], CLA^{R}, CIP^{R}, CLI^{R}, DOX^{R}, ERY^{R}, MET^{R}, MXF^{R}, KAN^{R}, TEL^{R}, RIF^{R} (MRSA[d], VISA[e])	16	16(8)[c]	16-32	8	4	8	4(2)	2
Staphylococcus aureus 25697	AMX^{R}, CHL^{R}, CIP^{R}, CLI^{R}, ERY^{R}, FOS^{R}, GEN^{R}, KAN^{R}, NIT^{R}, TET^{R} (MRSA)	8	8	32	8	8(4)	16(8)	2	4
Streptococcus pneumoniae ATCC 49619	susceptible	>64	>64	>64	64	32	32	1	4
Streptococcus agalactiae 013761	DOX^{I}[f]	>64	>64	>64	>64	>64	64	>64	>64
Streptococcus pyogenes 014327	DOX^{I}	>64	>64	>64	64	64	32	>64	>64
Enterococcus faecalis UW 2689	CLA^{R}, ERY^{R}, MXF^{R}, TEL^{R}, (VRE[g])	>64	>64	32	32	32	64	16	16
Enterococcus faecium 6011	CLA^{R}, ERY^{R}, TEL^{R} (VRE)	>64	>64	>64	>64	>64	>64	>64	32
Bacillus subtilis 168 trpC2	susceptible	>64	>64	>64	64	>64	>64	16(8)	4
Gram-negative									
Pseudomonas aeruginosa B 63230	CAZ^{R}, CIP^{R}, CPM^{R}, GEN^{R}, IMI^{R}, MER^{R}, PIP/TAZ^{R}	>64	>64	>64	>64	>64	>64	>64	>64
Escherichia coli ATCC 25922	susceptible	>64	>64	>64	>64	>64	>64	>64	>64
Escherichia coli WT-3-1 MB2	CIP^{R}	>64	>64	>64	>64	>64	>64	>64	>64
Klebsiella pneumoniae ATCC 27799	DOX^{R}, KAN^{R}	>64	>64	>64	>64	>64	>64	>64	>64

[a]Antibiotic abbreviations and breakpoints for resistance were applied according to the CLSI guidelines (CLSI M7-A8, 2008): AMX (amoxicillin), CAZ (ceftazidime), CHL (chloramphenicol), CIP (ciprofloxacin), CLA (clarithromycin), CLI (clindamycin), CPM (cefepime), DOX (doxycycline), ERY (erythromycin), FOS (fosmidomycin), GEN (gentamycin), KAN (kanamycin), LNZ (linezolid), MER (meropenem), MET (methicillin), MXF (moxifloxacin), NIT (nitrofurantoin), PIP/TAZ (piperacillin/tazobactam), RIF (rifampicin), TEL (telithromycin), TET (tetracycline). [b]R: Resistant. [c]Numbers in brackets indicate, that partial growth inhibition occurred at this concentration, while full growth inhibition was observed at the twofold higher concentration. [d]MRSA: Methicillin-resistant *Staphylococcus aureus*. [e]VISA: Vancomycin-intermediate *Staphylococcus aureus*. [f]I: Intermediate. [g]VRE: Vancomycin-resistant enterococci.

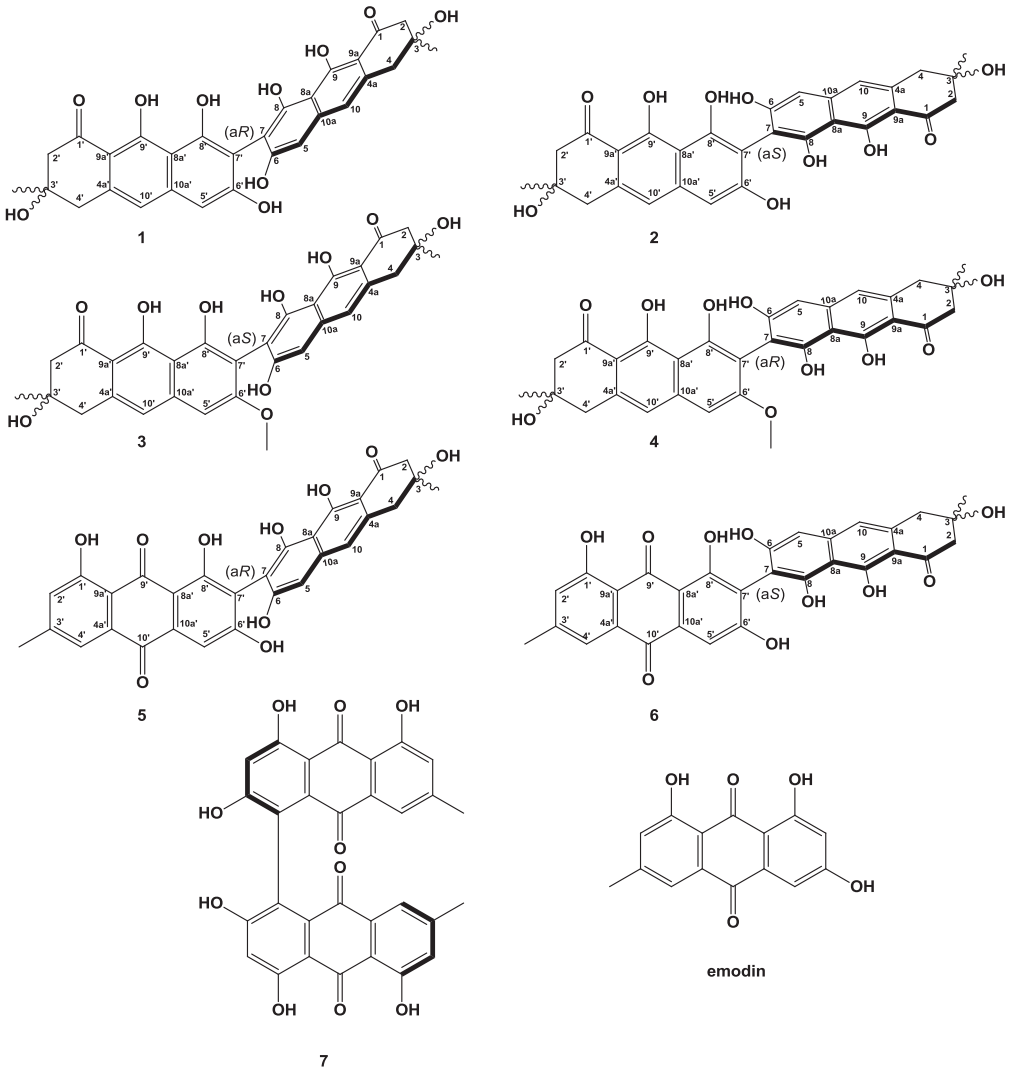

Scheme 1. The structures of **1**-**7** and emodin.

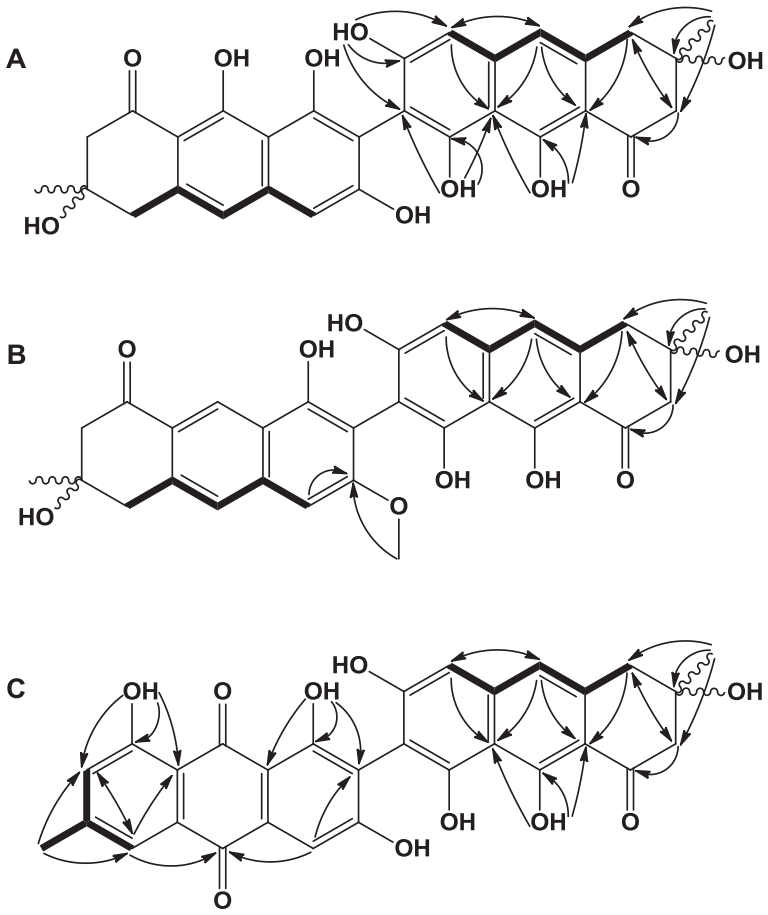

Figure 1. Important COSY (bold lines) and HMBC (arrows) correlations of atropisomers **1** and **2** (a), **3** and **4** (b), **5** and **6** (c).

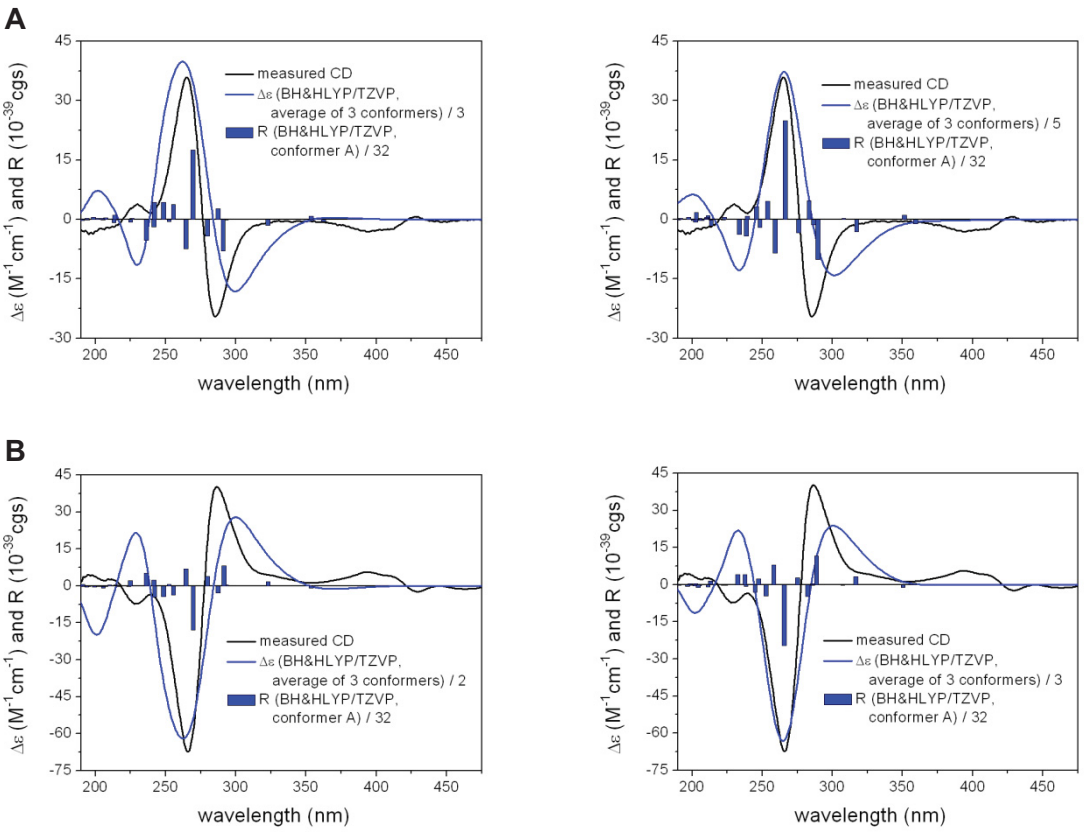

Figure 2. Comparison of experimentally measured ECD spectra of **1** (A) and **2** (B) in acetonitrile with the BH&HLYP/TZVP spectra calculated for the conformers of (a*R*,3*R*,3'*R*)-**1** and (a*S*,3*R*,3'*R*)-**2** in vacuo (left) and in acetonitrile (right). Bars represent rotational strength values.

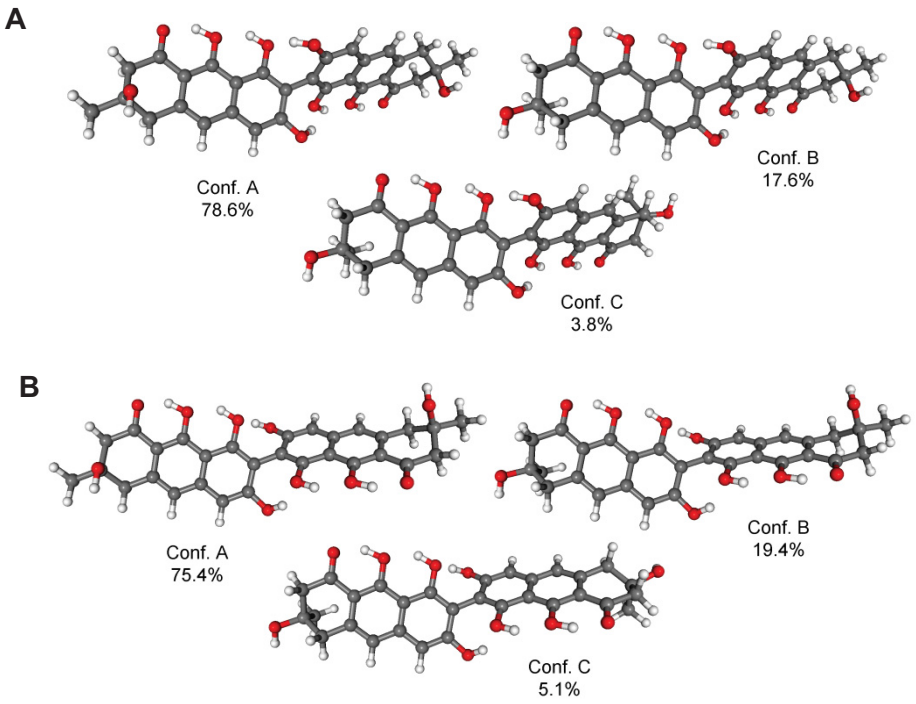

Figure 3. Low-energy conformers of (a*R*,3*R*,3'*R*)-**1** (A) and (a*S*,3*R*,3'*R*)-**2** (B) (B3LYP/TZVP level, PCM model for MeCN). (At B3LYP/6-31G(d) in vacuo the Boltzmann distributions of the corresponding conformers of (a*R*,3*R*,3'*R*)-**1** are 46.9%, 31.2% and 21.9%, respectively, and of (a*S*,3*R*,3'*R*)-**2** are 53.7%, 28.2% and 18.1%, respectively.)

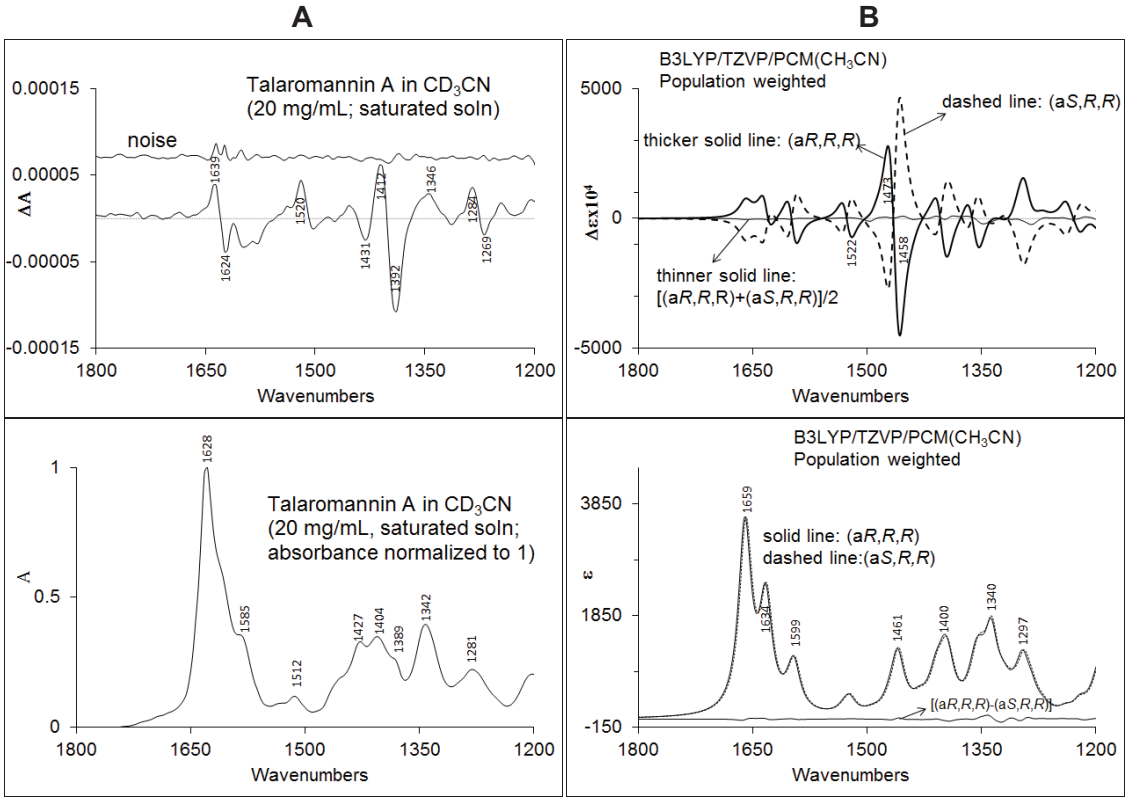

Figure 4. Experimental vibrational absorption (VA) and vibrational circular dichroism (VCD) spectra of **1** measured in 200 micron fixed path length cell for saturated solution in CD_3CN solvent (A). Calculated vibrational absorption (VA, bottom) and vibrational circular dichroism (VCD, top) spectra for (a*R*,3*R*,3'*R*) and (a*S*,3*R*,3'*R*) diastereomers of **1** (B). The average of VCD spectra of (a*R*,3*R*,3'*R*) and (a*S*,3*R*,3'*R*) diastereomers is expected to subtract out the contribution from axial chirality and yield the contribution of two central chiral centers.

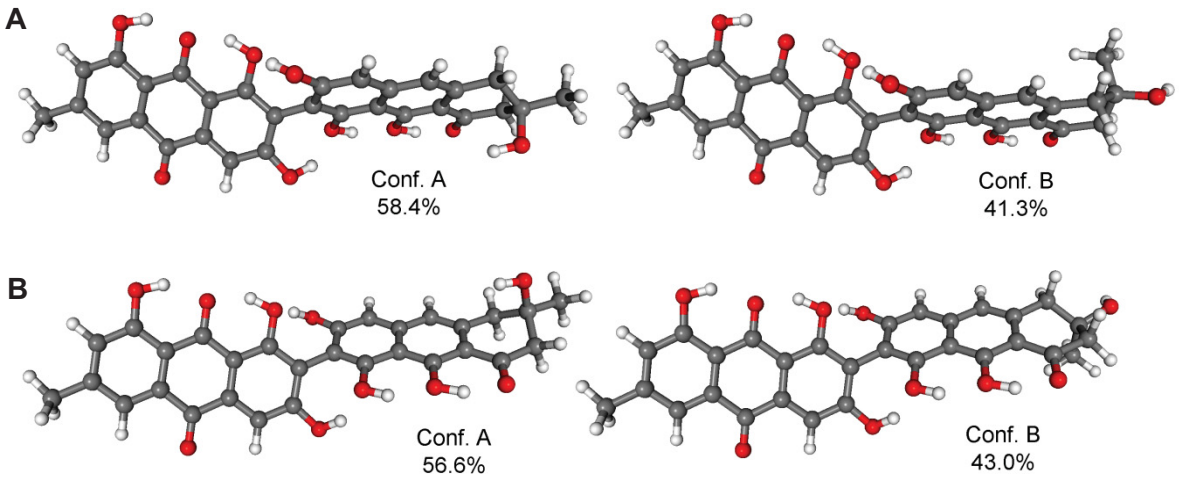

Figure 5. Low-energy conformers of (a*R*,3*R*)-**5** (A) and (a*S*,3*R*)-**6** (B) (B3LYP/6-31G(d) in vacuo).

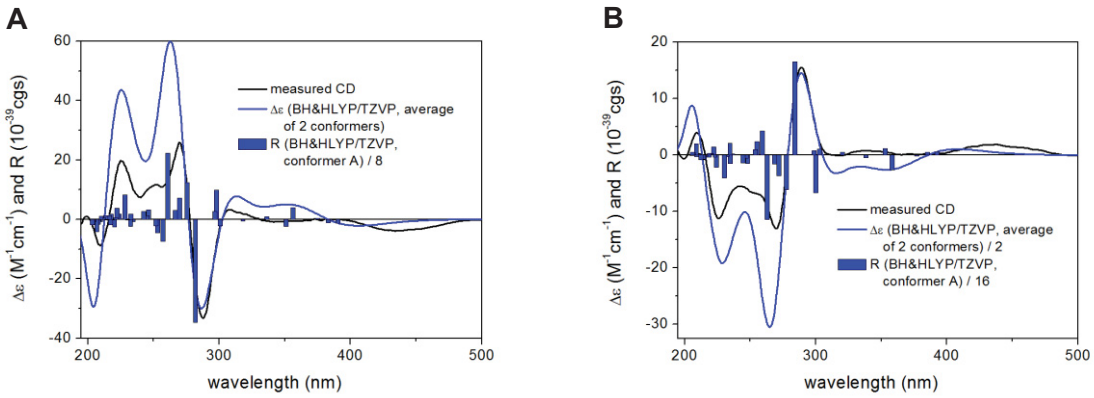

Figure 6. Comparison of experimentally measured ECD spectra of **5** (A) and **6** (B) in acetonitrile with the BH&HLYP/TZVP spectra calculated for the conformers of (a*R*,3*R*)-**5** and (a*S*,3*R*)-**6** in vacuo. Bars represent rotational strength values.

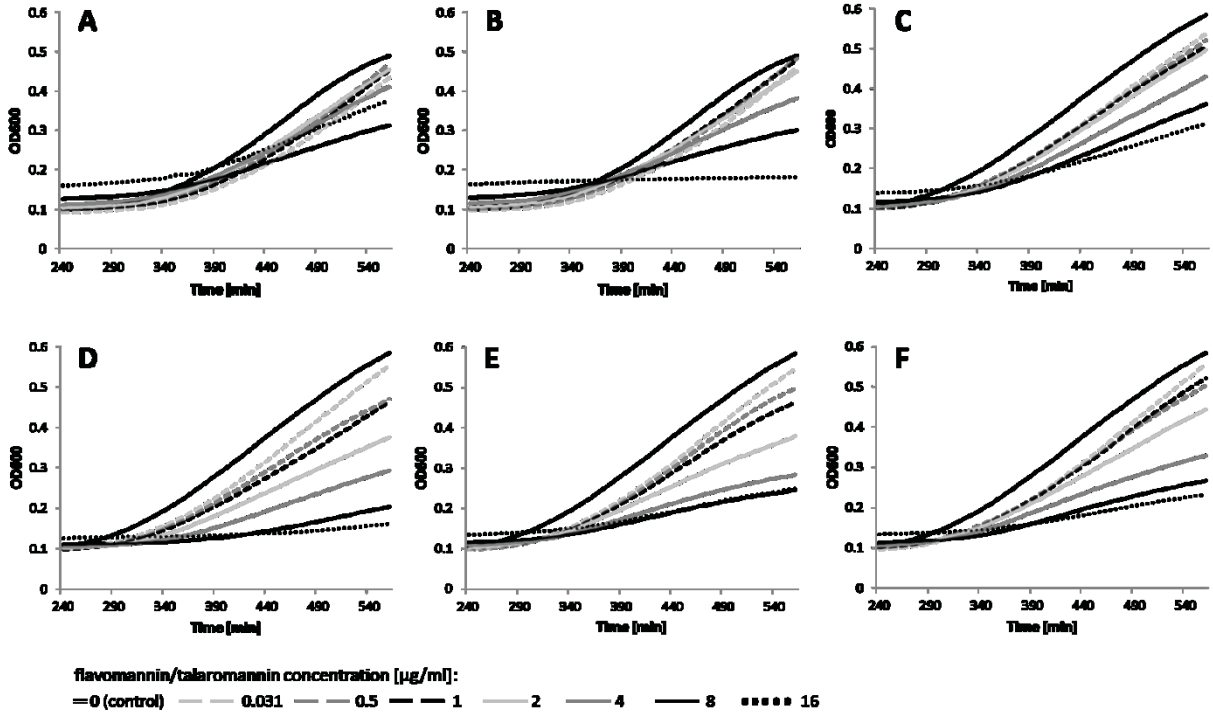

Figure 7. Effect of flavomannin/talaromannin derivatives on the growth of *S. aureus* Mu50. Growth was followed by measuring the optical density (OD_{600}) in the absence (control) or presence of increasing concentrations (0.031 to 64 µg/mL) of **1** (A), **2** (B), **3** (C), **4** (D), **5** (E) and **6** (F) in a microtiter plate reader for 20 h. The exponential growth phase at selected compound concentrations is shown. Growth experiments were performed in triplicate. The growth curves of two different experiments are shown: (A) and (B) derived from one experiment, (C), (D), (E) and (F) from another one.

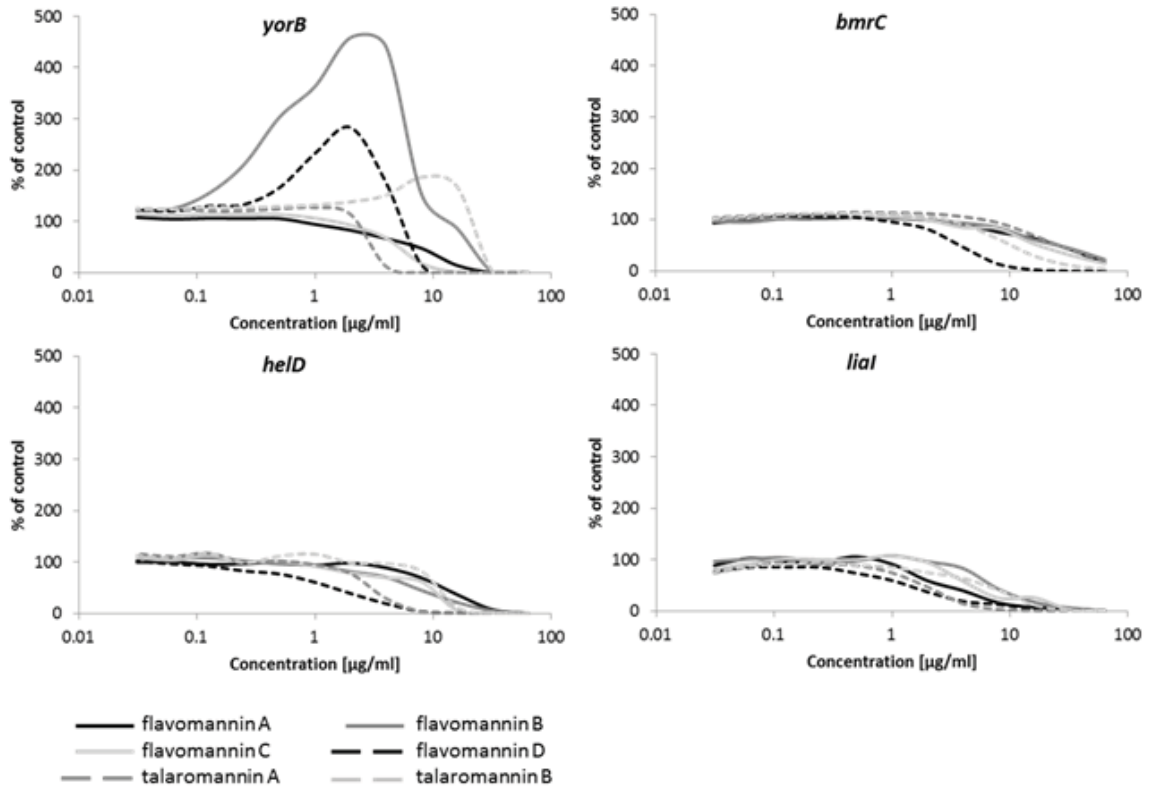

Figure 8. Induction of the biomarkers *yorB*, *helD*, *bmrC* and *lialI* in the presence of increasing concentrations of **1**-**6**. Promoter induction was visualized by detection of the corresponding luminescence signal and is depicted as percentage of the untreated control. Flavomannin B (**2**), D (**4**) and talaromannin B (**6**) specifically induced the *yorB* promoter. Results were confirmed in four independent experiments. The result of one representative experiment is shown.

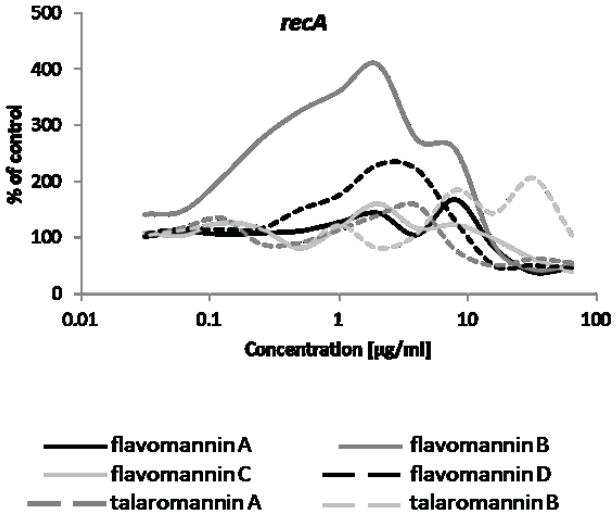

Figure 9. Induction of the biomarker *recA* in the presence of increasing concentrations of **1**-**6**. Promoter induction elicited a fluorescence signal and is depicted as percentage of the untreated control. The promoter was strongly induced by flavomannin B (**2**), and also in a decreasing order by flavomannin D (**4**) and talaromannin B (**6**). The experiment was performed six times. The result of one representative experiment is shown.

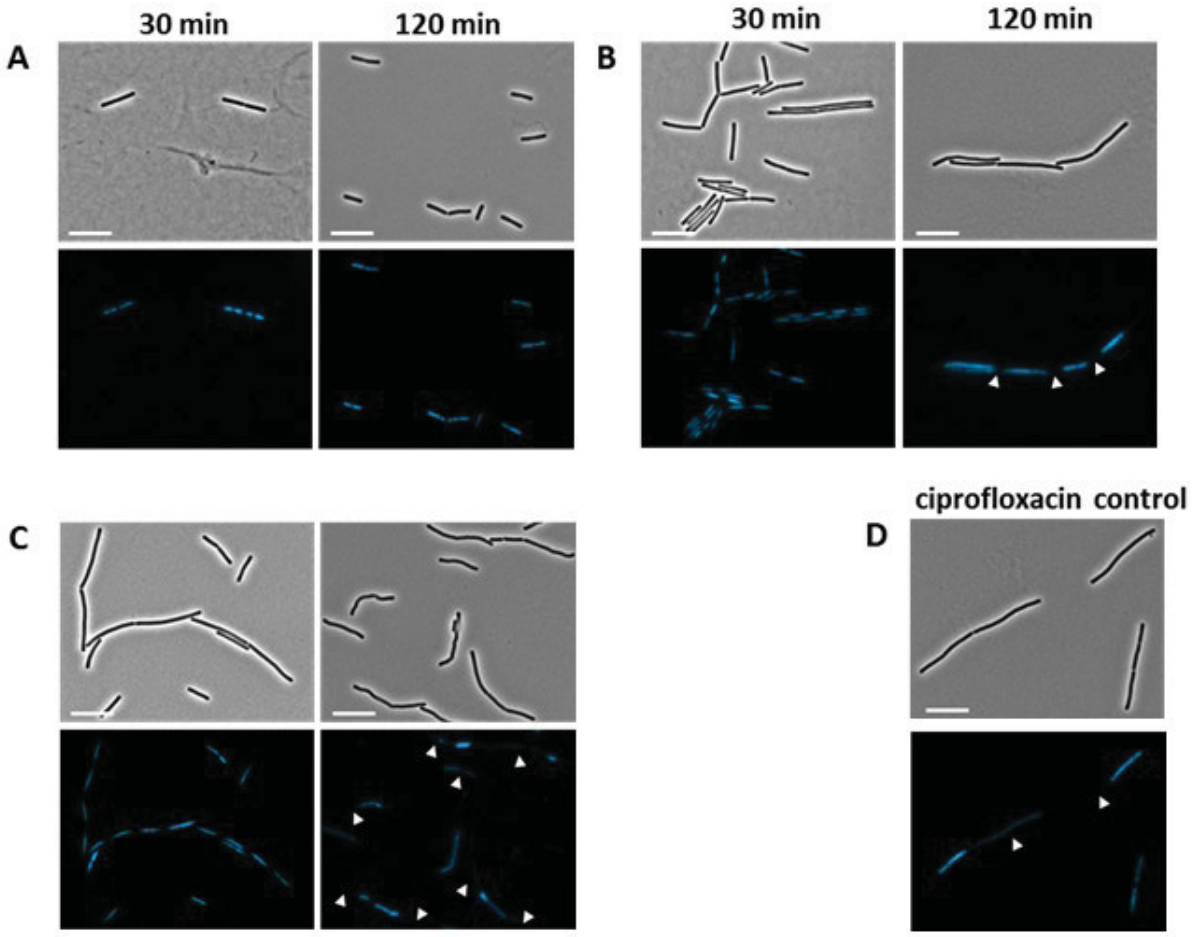

Figure 10. Effect of flavomannin B (**2**) on cell morphology and chromosomal organization of *B. subtilis* 168 trpC2. An exponentially growing culture was either treated with 1 μg/mL (B) or 8 μg/mL (C) of **2**, 0.125 μg/mL of ciprofloxacin (D) or left untreated (A). Cells were stained with the DNA-specific fluorochrome DAPI and examined by phase contrast (upper panels) or fluorescence (lower panels) microscopy. Images were taken at indicated time points (30, 120 min) after addition of the respective compound. Flavomannin B (**2**) and ciprofloxacin treatment resulted in filamentation of *B. subtilis* 168 trpC2, indicating cell division inhibition. DAPI staining revealed an imperfect chromosome segregation and DNA degradation. The experiment was performed twice with the same outcome. Exemplary representative pictures are shown. Scale bars represent 10 μm. Arrows mark cells, which have a considerably reduced DNA content.

Supporting Information

Dihydroanthracenones from the Endophytic Fungus *Talaromyces wortmannii* with activity against multi-resistant *Staphylococcus aureus*

Robert Bara,[†] Ilke Zerfass,[†] Amal H. Aly,[†] Heike Goldbach-Gecke,[†] Vijay Raghavan,[‡] Peter Sass,[†] Attila Mándi,[§] Victor Wray,[∥] Prasad L. Polavarapu,[‡] Bingui Wang,[⊥] Gennaro Pescitelli,[#] Tibor Kurtàn,[§] Abdessamad Debbab,[†] Heike Brötz-Oesterhelt,[†]* Peter Proksch[†]*

Table of Contents

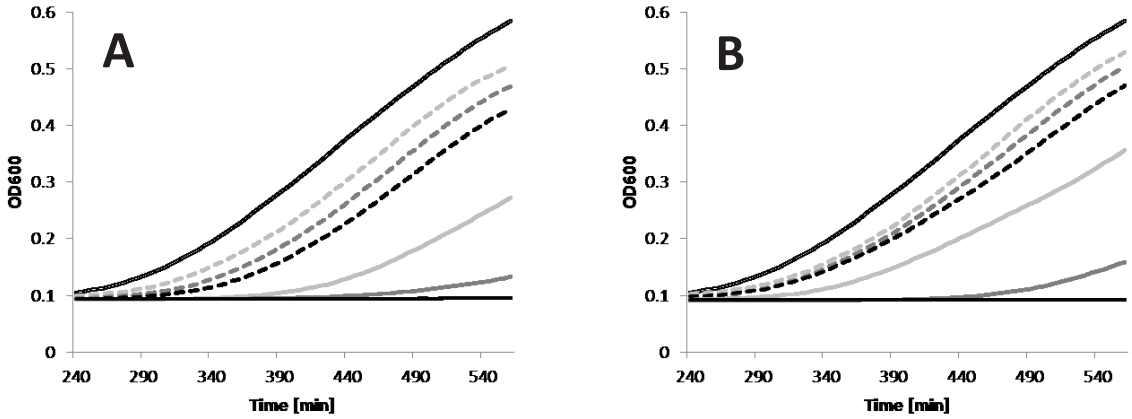

(A) 0 (control) 0.031 1 2 8 16 32 µg/ml tetracycline
(B) 0 (control) 0.031 0.125 0.25 0.5 1 2 µg/ml vancomycin

Figure S1. Effect of control antibiotics on the growth of *S. aureus* Mu50. Growth was followed by measuring the optical density (OD_{600}) in the absence (control) or presence of increasing concentrations (0.031 to 64 µg/ml) of tetracycline (A) and vancomycin (B) in a microtiter plate reader for 20 h. The exponential growth phase at selected compound concentrations is shown. Growth experiments were performed in triplicate. The growth curves of one representative experiment are shown.

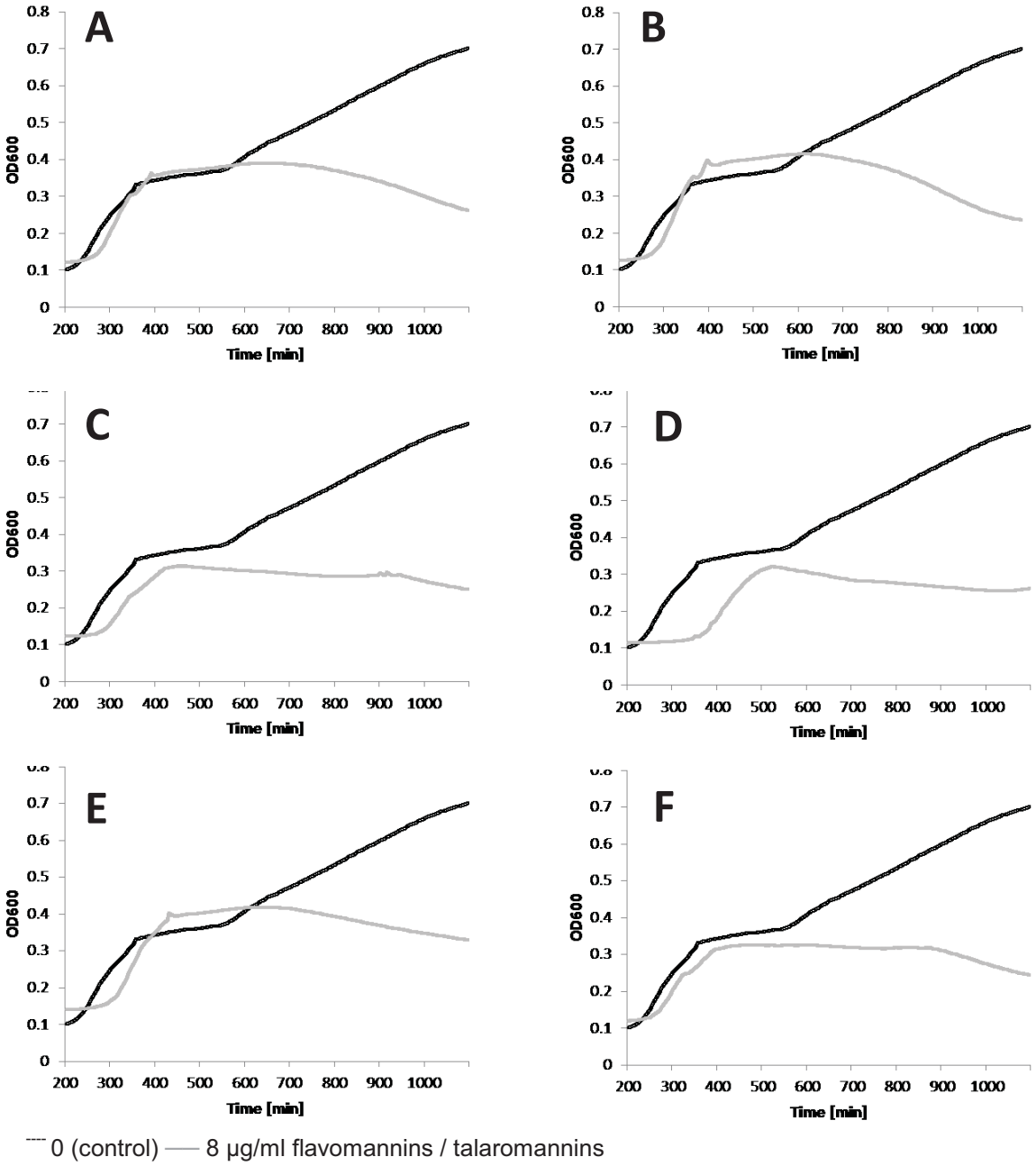

Figure S2. Effect of flavomannins and talaromannins on the growth of *B. subtilis* 168 trpC2. Growth was followed by measuring the optical density (OD_{600}) in the absence (control) or presence of increasing concentrations (0.031 to 64 µg/ml) of flavomannin A (A), B (B), C (C), D (D) or talaromannin A (E) and B (F) in a microtiter plate reader for 20 h. The exponential growth phase at selected compound concentrations is shown. Since *B. subtilis* is a strictly aerobic species and does not grow well in microtiter plates, which we had to use for the growth experiment due to compound limitation, the growth curves are somewhat heterogeneous. Nonetheless, growth inhibition is clearly visible for all compounds.

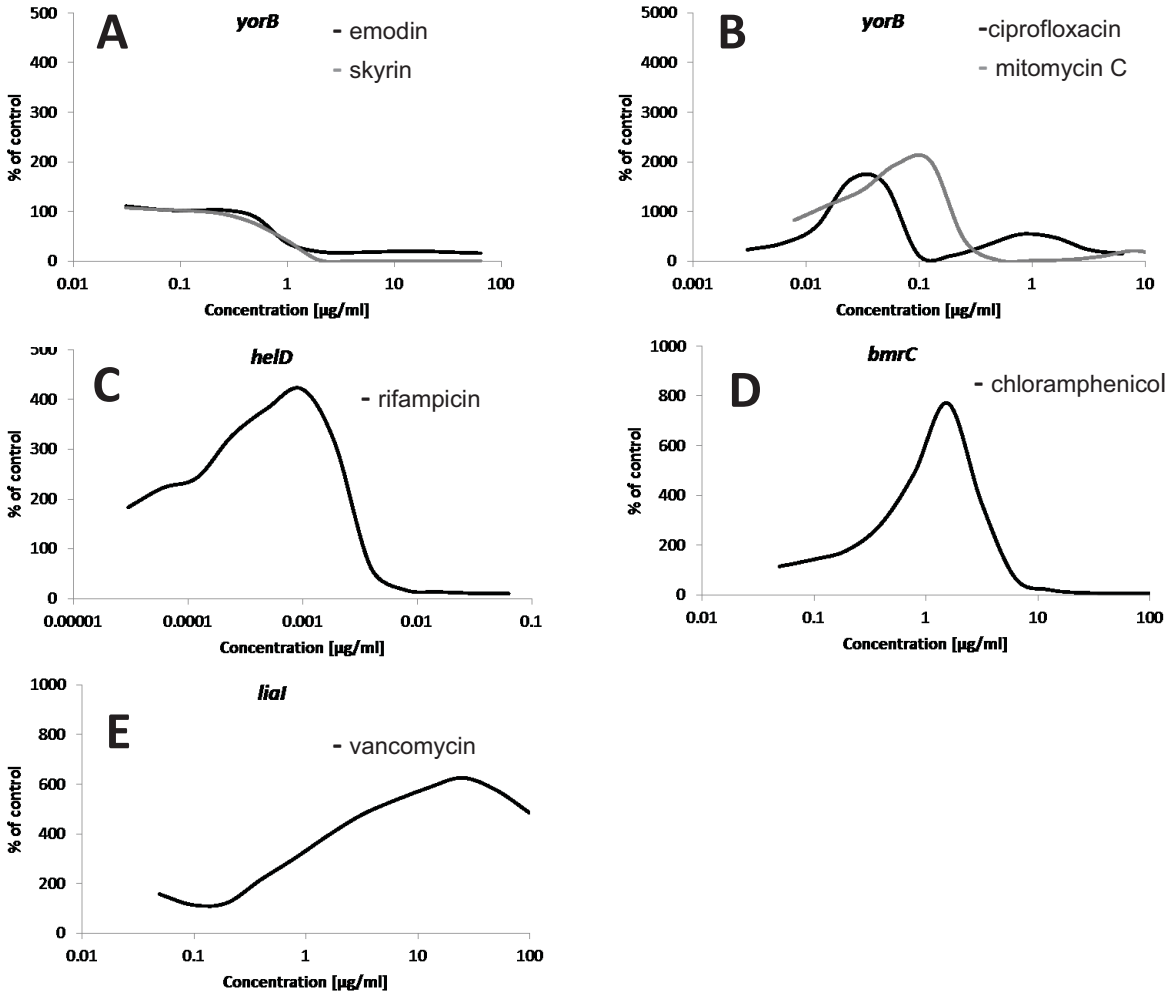

Figure S3. Induction of the biomarkers *yorB*, *helD*, *bmrC* and *liaI* in the presence of increasing concentrations of emodin and skyrin (A) as well as the reference antibiotics ciprofloxacin and mitomycin C (B), rifampicin (C), chloramphenicol (D) and vancomycin (E). Promoter induction was detected via the corresponding luminescence signal and is depicted as percentage of the untreated control. Results were confirmed in two independent experiments. The result of one representative experiment is shown.

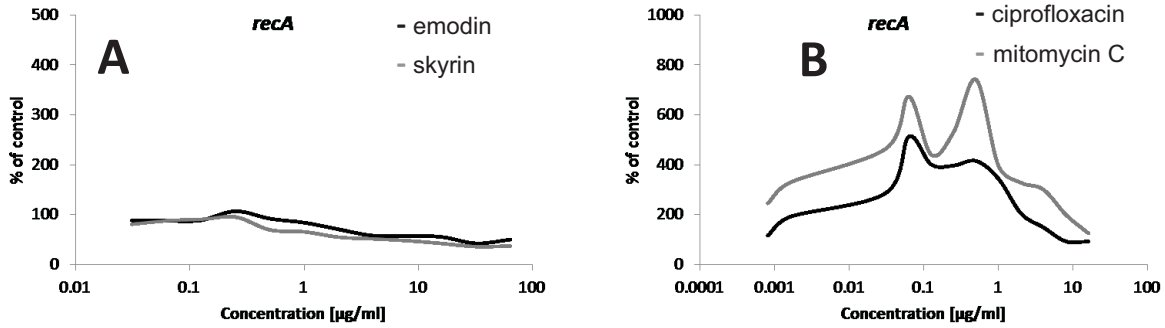

Figure S4. Induction of the biomarker *recA* in the presence of increasing concentrations of emodin and skyrin (A) as well as the reference antibiotics ciprofloxacin and mitomycin C (B). Promoter induction as detected via the corresponding fluorescence signal is depicted as percentage of the untreated control. Results were confirmed in three independent experiments. The result of one representative experiment is shown.

= Chapter 3 =

New Antibiotically Active Metabolites from *Talaromyces wortmannii*, an Endophyte of *Aloe vera*

Robert Bara,[a] Amal Hassan Aly,[a] Alexander Pretsch,[b] Victor Wray,[c] Bingui Wang,[d] , Peter Proksch,[a] Abdessamad Debbab[a]*

[a] Institut für Pharmazeutische Biologie und Biotechnologie,
Heinrich-Heine-Universität Düsseldorf
Universitätsstrasse 1, Geb. 26.23, 40225 Düsseldorf, Germany

[b] SeaLife Pharma GmbH,
3430 Tulln, Austria

[c] Helmholtz Centre for Infection Research,
38124 Braunschweig, Germany

[d] Laboratory of Experimental Marine Biology, Institute of Oceanology,
Chinese Academy of Science
Nanhai Road 7, 266071 Quindao, P.R. China

*Corresponding author, abdessamad.debbab@uni-duesseldorf.de

This chapter is adapted from a manuscript which has been submitted to *Journal of Antibiotics* as: R. Bara, A. H. Aly, B. G. Wang, A. Pretsch, W. H. Lin, P. Proksch, A. Debbab. 2012. Bioactive metabolites from *Talaromyces wortmannii*, an endophyte of *Aloe vera*.

Impact factor of the related journal is 1.651, overall participation on the paper is 70% as the first author. The first author involved to all laboratory works as well as the manuscript preparation.

Abstract

Chemical investigation of the EtOAc extract of *Talaromyces wortmanii*, an endophyte of *Aloe vera*, afforded one new biemodin atropsiomer (**1**) and a new wortmannin derivative (**2**). Two further wortmannin derivatives (**3** and **4**) were hitherto known only as synthetic compounds and are here reported as natural products for the first time. In addition, seven known compounds (**5**-**11**) were isolated. All structures were unequivocally determined on the basis of NMR spectroscopic methods including 1D (^{1}H , ^{13}C and DEPT) and 2D (COSY, HMQC, HMBC and ROESY) and by mass spectrometry data (ESI and HRESI-MS). The axial chirality of **1** was determined by CD. When tested against pathogenic bacteria, only **1**, **8** and **10** showed strong inhibition, especially against gram positive bacteria with MIC values between 4 and 16 μg/mL.

Keywords: *Aloe vera* / antibiotic activity / endophyte / structure elucidation / *Talaromyces wortmannii*

Introduction

Endophytes are microbes that colonize the internal tissues of plants without causing any immediate overt negative effects (Bacon and White 2000). Recently, it was reported that endophytic fungi of higher plants are a promising source of new natural drug leads that are of great potential for medicinal and agricultural applications (Proksch, Putz, Ortlepp, Kjer and Bayer 2010; Xu, Ebada and Proksch 2010; Aly, Debbab and Proksch 2011; Debbab, Aly and Proksch 2011; Debbab, Aly and Proksch 2012) Many of the products currently used for human or animal therapy, in animal husbandry and in agriculture are produced by microbial fermentation, or are derived from chemical modification of a microbial product (Donadio, Monciardini, Alduina, Mazza, Chiocchini, Cavaletti, Sosio and Puglia 2002). With increasing problems of drug resistance in humanpathogenic bacteria, which are among the major causes of deaths worldwide (MacDougall, Powell, Johnson, Edmond and Polk 2005; Klevens, Morrison, Nadle, Petit, Gershman, Ray, Harrison, Lynfield, Dumyati, Townes, Craig, Zell, Fosheim, McDougal, Carey and Fridkin 2007; Knight, Budd, Whitney, Thornley, Al-Ghusein, Planche and Lindsay 2012), there is still a great opportunity to find new secondary metabolites from poorly investigated sources, such as endophytes, which can be used in the near future to combat many life threatening diseases.

As part of our ongoing research focused on the discovery of structurally new bioactive natural products from terrestrial endophytic fungi (Aly 2010; Aly, Debbab, Clements, Edrada-Ebel, Orlikova, Diederich, Wray, Lin and Proksch 2011; Xu, Aly, Wray and Proksch 2011; Debbab, Aly, Edrada-Ebel, Wray, Pretsch, Pescitelli, Kurtan and Proksch 2012; Ebrahim, Aly, Mándi, Totzke, Kubbutat, Wray, Lin, Dai, Proksch, Kurtán and Debbab 2012), we studied the chemical constituents of the endophytic fungus *Talaromyces wortmanii*, which was isolated from healthy tissue of *Aloe vera* collected in Alexandria, Egypt. Fungi of the genus *Talaromyces* have been found as solitary or as endophytes in various climates worldwide from terrestrial to the marine-influenced environment (Shiozawa, Takahashi, Takatsu, Kinoshita, Tanzawa, Hosoya, Furuya, Takahashi, Furihata and Seto 1995; Yuesheng, Jie, Xinhua, Zhihui, Xiao, Hua, Jiangong and Junshan 2009). This genus has been investigated by many researchers since it produces a plethora of interesting compounds such as tetraene lactones (Yuesheng, Jie, Xinhua, Zhihui, Xiao, Hua, Jiangong and Junshan 2009), diphenyl ether derivatives and anthraquinones (Liu, Cai, Yang, Xia, Guo, Yuan, Li, She and Lin 2010)

which show various biological activities ranging from antibiotics to cytotoxins (Frisvad, Filtenborg, Samson and Stolk 1990; Wakelin, Warren, Harvey and Ryder 2004; Fan, Qing, Hong, Xiao-Ling, Xue-Kui, Sheng-Ping, Meng-Feng, Zhi-Gang and Yong-Cheng 2009; Yuesheng, Jie, Xinhua, Zhihui, Xiao, Hua, Jiangong and Junshan 2009; Liu, Cai, Yang, Xia, Guo, Yuan, Li, She and Lin 2010). In the present study, we report the isolation and structure elucidation of a new biemodin atropisomer (**1**), and a new wortmannin derivative (**2**) in addition to two wortmannin derivatives (**3-4**) that were hitherto known only as synthetic products. In addition seven known metabolites including wortmannin A (**5**), wortmin (**6**) emodic acid (**7**), skyrin (**8**), oxyskyrin (**9**), rugulosin A (**10**) and B (**11**) were likewise isolated. Furthermore, we evaluated the antibiotic activity of the isolated compounds against several pathogenic Gram-positive and negative bacteria.

Result and discussion

Compound **1** was obtained as orange amorphous powder. It showed UV absorption maxima at λ_{max} (MeOH) 223, 255, 291 and 450 nm, which resemble those of the known emodin (Rao, Hanumaiah, Rao and Rao 1986). ESIMS data of **1** showed the base peak at *m*/*z* 537.3 $[M-H]^-$ in the negative mode, which inferred that **1** has a molecular weight of 538 g/mol. The molecular formula was established as $C_{30}H_{18}O_{10}$ based on prominent signals detected at *m*/*z* 539.0971 $[M+H]^+$ and 561.0787 $[M+Na]^+$ in the HRESIMS. In contrast, the ^{13}C NMR spectra of **1** (Table 1) showed signals corresponding to only 15 carbons, indicating that **1** is a symmetrical dimer consisting of two identical monomers. ^1H NMR showed proton signals of one aromatic methyl group resonating at δ_H 2.49 ppm, one aromatic singlet at δ_H 7.47 ppm and two aromatic broad singlets resonating at δ_H 7.17 and 7.62 ppm. The ^{13}C NMR spectrum (Table 1) exhibited 15 carbon peaks attributable to one methyl, three methine carbons and eleven quaternary carbons atoms. Further analysis of ^{13}C spectrum disclosed signals for two carbonyl group resonating at δ_C 186.0 (C-9/9′) and δ_C 182.0 (C-10/10′), three oxygenated aromatic carbon atoms at δ_C 164.0 (C-1/1′), 156.0 (C-6/6′) and 163.5 (C-8/8′) and nine aromatic carbons at δ_C 124.9 (C-2/2′), δ_C 150.0 (C-3/3′), δ_C 121.5 (C-4/4′), δ_C 134.2 (C-4a/4a′), δ_C 109.0 (C-5/5′), δ_C 114.1 (C-7/7′), δ_C 110.1 (C-8/8a′), δ_C 115.0 (C-9a/9a′), δ_C 137.0 (C-10a/10a′). Comparison of NMR data and UV spectra of **1** with those for emodin as well as consideration of the molecular weight suggested that **1** is a symmetrical dimer of two emodin units. The linkage between the emodin building blocks is confirmed by 2D NMR

analysis, including ^{1}H-^{1}H COSY and J^{2}/J^{3} HMBC correlations (figure 1). ^{1}H-^{1}H COSY spectrum showed that the aromatic methyl signal was correlated to the *meta*-coupled protons H-2 and H-4. The absence of the second *meta*-coupled protons and the presence of one aromatic singlet in **1** compared to emodin, confirmed that **1** is a symmetrical dimer consisting of two emodin moieties inferring either a 5,5′ or a 7,7′-linkage. CH_3-11 was correlated to C-2, C-3 and C-4, whereas, the aromatic singlet proton observed at δ_H 7.47 ppm together with H-4/4′ showed strong J^{3} correlations to the carbonyl carbon C-10 (figure 1). Thus, proton resonating at δ_H 7.47 ppm is assigned to H-5/5′ indicating a 7,7′-linkage. Furthermore, analysis of NMR data of structurally related anthranoids, isolated in our previous studies (Debbab, Aly, Edrada-Ebel, Wray, Müller, Totzke, Zirrgiebel, Schälchtele, Kubbutat, Lin, Mosaddak, Hakiki, Proksch and Ebel 2009; Pretsch, Proksch and Debbab 2010; Pretsch, Proksch and Debbab 2010; Debbab, Aly, Edrada-Ebel, Wray, Pretsch, Pescitelli, Kurtan and Proksch 2012), revealed that in such systems the two *meta*-coupled aromatic protons H-5 (H-5′) and H-7 (H-7′) resonate considerably in different chemical shifts, with H-5 (H-5′) consistently appearing more downfield than H-7 (H-7′). In addition, the 5,5′-linkage of two emodin moieties forms the known skyrin (Vargas, Rivas, Zoltan, López, Ortega, Izzo, Pineda, Medina, Medina and Rosales 2008), which was likewise isolated from *T. wortmanii* in this study. These observations proved vital that both emodin building blocks are 7,7′-linked to form the new atropisomer **1**. Thus, the planar structure of **1** including the linkage of both monomers is confirmed. Compound **1** is an atropisomer resulting from hindered rotation of two symmetrical moieties (emodin) around the biaryl axis. The configuration of the axial chirality was determined by a CD experiment. The CD spectrum exhibited a positive Cotton effect at shorter wavelength and a negative one at longer wavelength, which is typical for *M*-conformer (known also as 'A-type' or a*R*) (Prelog and Helmchen 1982; Harada and Nakanishi 1983; Gill and Steglich 1987; Nakanishi, Kakita, Takahashi, Kawahara, Tsukuda, Sano, Yamada, Yoshida, Kase, Matsuda and et al. 1992; Nakanishi and Berova 1994; Gill and Morgan 2004), which is in agreement with its $[\alpha]_D$ value of -156. Accordingly, compound **1** is a new natural product consisting of two emodin moieties linked *via* 7,7′ for which the name biemodin is proposed.

Compound **2** was obtained as light brown amorphous powder with UV absorption maxima (MeOH) at λ_{max} 210, 259 and 300 nm, which are resemble those of wortmannin (**5**), likewise

isolated during this study. The HRESIMS exhibited a prominent peak at m/z 387.1436 $[M+H]^+$, with a 42 mass unit decrease compared to the molecular weight of **5**, which established the molecular formula $C_{21}H_{22}O_7$ for **2**. Comparison of the ^1H NMR spectra of **2** and **5** (Table 2) showed a close relationship between both compounds except for the presence of an additional hydroxy group and the absence of the O-acetyl group in **2**. Further comparison of 2D NMR data of **2** and **5** confirmed that both share similar skeletons as well as substituents except for the loss of the acetyl function of **5** and the attachment of the aliphatic methoxy group and the hydroxyl group in **2** (figure 2). Three spin systems, including $CH(1)CH_2(2)OH(3)$, $CH_2(12)CH(11)$ and $CH_2(16)CH_2(15)CH(14)$ were detected in the ^1H-^1H COSY spectrum of **2**, which are also observed in **5**. In addition, HMBC spectra confirmed the assignments of these spin systems. In contrast to **5** the signal of the aliphatic methoxy group of **2** exhibited a strong J^3 HMBC correlation to a carbon resonating at δ_C 53.7 ppm which was attributed to C-11. Comparison of the published data of known wortmannin derivatives as well as to those isolated in this study (Norman, Shih, Toth, Ray, Dodge, Johnson, Rutherford, Schultz, Worzalla and Vlahos 1996), (MacMillan, Vanstone and Yeboah 1972)) revealed that carbons C-1 and C-11 differ considerably with regard to their chemical shifts, with C-1 consistently resonating more downfield (ca. 82 ppm) than C-11 (ca. 66 ppm). Hence, CH_2-2 is connected to the additional hydroxyl group (confirmed by COSY) whereas the methoxy group is attached to C-11. Thus, the planar structure of **2** was accomplished. The relative configuration of **2** was deduced from analysis of the coupling constants and comparison to those of **5**. Comparison of the $[\alpha]_D$ values of **2** (+ 19) and **5** (+ 44) furthermore suggested that both compounds also share the same absolute configuration which is corroborated based on biogenetic considerations. Accordingly, compound **2** was identified as a new wortmannin derivative for which the name wortmannin B is proposed.

Compound **3** was obtained as a brown amorphous powder. It has UV absorption maxima at λ_{max} (MeOH) 244, 312 and 398 nm. The MS data showed two strong peaks at *m/z* 445.9 $[M+H]^+$ and 890.8 $[2M+H]^+$ (positive mode) and two strong peaks at *m/z* 443.8 $[M-H]^-$ and 887.8 $[2M-H]^-$ (negative mode), indicating a molecular weight of 445 g/mol. The molecular formula was determined as $C_{23}H_{27}NO_8$ on the basis of the prominent signals detected at *m/z* 446.1802 $[M+H]^+$ and 468.1623 $[M+Na]^+$ in the HRESIMS. ^1H spectrum and HMQC showed signals for three methyl groups, one methoxy, four methylenes, three aliphatic protons, one

methine and three exchangeable protons. This was further confirmed by ^{13}C NMR spectrum and DEPT experiment, which yielded eleven quaternary carbons. The planar structure of **3** was confirmed by 2D NMR analysis, including ^{1}H-^{1}H COSY and HMBC. Finally, the relative configuration of **3** was determined by a ROESY experiment. Comparison of the spectroscopic data and $[\alpha]_D$ of **3** with published data for the synthetic amino adduct **3a**, previously reported only as a synthetic compound (Norman, Shih, Toth, Ray, Dodge, Johnson, Rutherford, Schultz, Worzalla and Vlahos 1996), indicated that both compounds are identical. To the best of our knowledge, this is the first report of the amino addition product **3a** as a natural product, for which the name wortmannin C is proposed.

Compound **4** was obtained as light brown amorphous powder and shared similar UV (MeOH) absorption maxima with wortmannin C (**3**) (λ_{max} 242, 302 and 390 nm). MS data of **4** showed three major peaks at 446.8 $[M+H]^+$, 468.9 $[M+Na]^+$ and 914.9 $[2M+Na]^+$ in the positive ion mode and a strong peak at 444.9 $[M-H]^-$ in the negative ion mode, confirming the molecular weight 446 g/mol. Its molecular formula was determined as $C_{23}H_{26}O_9$ on the basis of the prominent signals detected at *m/z* 447.1648 $[M+H]^+$ and 469.1467 $[M+Na]^+$ in the HRESIMS. Comparison of NMR data, including 1D and 2D, and HRESIMS of **4** with those of **3** showed that the $-NH_2$ group of **3** is replaced by a hydroxyl function in compound **4**. The relative configuration of **4** was obtained by a ROESY experiment as shown in chart 1. A literature survey showed that the spectroscopic data as well as $[\alpha]_D$ of **4** are in accordance with published data for the hydrolysis product of wortmannin-diol (VIII), previously reported only as synthetic compound (MacMillan, Vanstone and Yeboah 1972). To the best of our knowledge, this is the first report of the compound **4** as a natural product, for which the name wortmannin D is given.

All compounds, except **7** and **9** due to the small amounts, were tested for their antibiotic activity against pathogenic Gram negative bacteria, including *Escherichia coli*, *Klebsiella pneumonia*, *Pseudomonas aeruginosa*, *Acinetobacter baumannii*, *Enterobacter* sp., *Enterococcus cloacae* and Gram positive bacteria, including Methicillin-resistant *Staphylococcus aureus*, *Staphylococcus epidermidis*, *Streptococcus pneumonia*, *Enterococcus faecalis* (table 4). Among the tested compounds, **8** and **10** exhibited considerable antibiotic activity against Gram positive pathogenic bacteria with MIC values ranging between 4 and 16 μg/mL. The new biemodin atropisomer (**1**) showed also strong activity against Gram

positive bacteria, especially against MRSA, but was less active compared to compounds **8** and **10.**

General experimental procedures

Optical rotations were determined on a Perkin-Elmer-241 MC polarimeter. 1D and 2D NMR spectra were recorded on a Bruker DPX-300 or Avance DMX 600 NMR spectrometer. HPLC analysis was performed using a HPLC (Dionex P580) system coupled to a UV-Vis detector (UVD340S). Routine detection was at 235, 254, 280, and 340 nm. The separation column (125 × 4 mm, L × ID) was prefilled with Eurospher-10 C18 (Knauer, Germany) using a linear gradient of MeOH and 0.1 % HCOOH in H_2O and a flow rate of 1 mL/min. UV data (λ_{max}) for individual compounds were extracted from the online UV spectra provided by the instrument software. ESI/MS was conducted on a LCMS HP1100 Agilent Finnigan LCQDecaXP Thermoquest. Column chromatography was performed on Silica gel 60M (230-3400 mesh ASTM, Macherey-Nagel GmbH & Co.KG, Düren, Germany), Sephadex LH-20 (Sigma), or HP20 (Mitsubishi). TLC was carried out on precoated silica gel plates (silica gel 60 F-254, Merck KGaA, Darmstadt, Germany) for monitoring of fractions using EtOAc/MeOH/H_2O (30:5:4) and CH_2Cl_2/MeOH (9:1) as solvent systems. Detection was at 254 and 366 nm or by spraying the plates with anisaldehyde reagent. Semi-preparative HPLC was carried out with Merck Hitachi L-7100 pump and L-7400 UV detector on an Eurosphere 100-10 C18 column (300 x 8 mm, L x ID, Knauer, Germany). Solvents were distilled before use, and spectral grade solvents were used for spectroscopic measurements.

Fungal material. The endophytic fungus was isolated from healthy inner tissues of *Aloe vera* (Xanthorrhoeaceae), collected from the coastal region of Alexandria, Egypt, in June 2009, using a protocol described previously (Debbab, Aly, Edrada-Ebel, Wray, Müller, Totzke, Zirrgiebel, Schälchtele, Kubbutat, Lin, Mosaddak, Hakiki, Proksch and Ebel 2009). The fungus (strain designation AVE 3.2) is kept in the authors' laboratory (P.P.).

Identification of fungal cultures. Fungal cultures were identified according to a molecular biological protocol by DNA amplification and sequencing of the ITS region as described previously (Wang, Li, Teuscher, Li, Diesel, Ebel, Proksch and Wang 2006). BLAST search revealed 95-97% similarity to *Talaromyces* sp. (AF285115.1). The fungal strain was sent in

parallel to the Deutsche Sammlung von Mikroorganismen Zellkulturen GmbH (DSMZ), Braunschweig, Germany, and was identified as *Talaromyces wortmanii*. The sequence data have been submitted to GenBank with accession number HM807532.1.

Cultivation. Small pieces of medium from a Petri dish containing the pure fungus was transferred under sterile conditions to ten Erlenmeyer flasks (1L each) containing 100 g of rice and 100 mL of water (after having been autoclaved). Cultures were kept for 14 days at 22 °C under static conditions.

Extraction and purification. Cultures and culture media were exhaustively extracted with EtOAc and the crude extract (5 g) was further fractionated by vacuum liquid chromatography (VLC) using *n*-hexane/EtOAc and CH_2Cl_2/MeOH in 10% gradient steps as eluting solvents. Fraction 4 (500 mg), eluted with 100% CH_2Cl_2**,** was further separated using column chromatography on Sephadex LH-20 and purified by semi-preparative HPLC using MeOH/H_2O gradient as the mobile phase to yield compound **6** (wortmin; 8 mg), **7** (emodic acid; 1 mg), **8** (skyrin; 14 mg) and **9** (oxyskyrin; 1 mg). Fraction 9 (300 mg) eluted with 1:1 CH_2Cl_2:MeOH, was further separated by Sephadex LH-20 column continued by semi-preparative HPLC using MeOH/H_2O gradient as the mobile phase to yield compound **1** (biemodine; 3 mg). Fraction 10 (170 mg) eluted with 4:6 CH_2Cl_2:MeOH separated using column chromatography on Sephadex LH-20 to yield compound **2** (wortmannin B; 4 mg), **3** (wortmannin C; 31 mg) and **5** (wortmannin A, 30 mg). Fraction 12 (200 mg) eluted with 2:8 CH_2Cl_2:MeOH separated using column chromatography on Sephadex LH-20 continued purified by semi-preparative HPLC using MeOH/H_2O gradient as the mobile phase to yield compound **4** (wortmannin D; 11 mg). Fraction 13 (200 mg) eluted with 1:9 CH_2Cl_2:MeOH was separated using column chromatography on Sephadex LH-20 to yield compound **10** (rugulosin A; 4 mg) and **11** (rugulosin B; 3 mg).

Determination of Minimal Inhibitory Concentration: Tests were carried out according to the EUCAST (http://www.eucast.org) criteria in a dilution assay against the tested multidrug-resistant pathogens.

Biemodin (**1**): Orange amorphous powder. $[\alpha]_D^{20}$ -156 (*c* 0.02, $CHCl_3$). UV: λ_{max} = 450, 291, 255 and 223 nm. CD ($CHCl_3$, c = 3.71 10^{-3} M): λ_{max} ($\Delta\varepsilon$) = 263 (0.624), 291 (–1.80), 316 (–1.59), 374 (–1.08), 470 (–2.94), 507 (–2.38). MS (ESI, -ve): *m/z* = 537.3 $[M-H]^-$, HRESIMS: calcd. for $C_{30}H_{19}O_{10}$ $[M+H]^+$ 539.0978; found 539.0971 $[M+H]^+$ and for $C_{30}H_{18}O_{10}Na$ $[M+Na]^+$ 561.0798; found 561.0787. ^1H and ^{13}C NMR data, see Table 1.

Wortmannin B (**2**): Light brown amorphous powder. $[\alpha]_D^{20}$ + 18.8 (*c* 0.02, MeOH). UV: λ_{max} = 210, 259 and 300 nm. ESIMS (+ve): *m/z* = 386.8 $[M+H]^+$ and 794.9 $[2M+Na]^+$; (-ve): *m/z* 385.0 $[M-H]^-$ and 770.8 $[2M-H]^-$. HRESIMS: calcd. for $C_{21}H_{23}O_7$ $[M+H]^+$ 387.1444; found 387.1436 ^1H NMR data, see table 2.

Wortmannin C (**3**): Brown amorphous powder. $[\alpha]_D^{20}$ -40 (*c* 0.02, MeOH). UV: λ_{max} = 244, 312 and 398 nm. ESIMS (+ve): *m/z* 445.9 $[M+H]^+$ and 890.8 $[2M+H]^+$; (-ve): *m/z* 443.8 $[M-H]^-$ and 887.8 $[2M-2H]^-$. HRESIMS): calcd for $C_{23}H_{28}NO_8$ $[M+H]^+$ 446.1815; found 446.1802 $[M+H]^+$ and for $C_{23}H_{27}NO_8Na$ $[M+Na]^+$ 468.1634; found 468.1623 $[M+Na]^+$. ^1H and ^{13}C NMR data, see Table 3.

Wortmannin D (**4**): Light brown amorphous powder. $[\alpha]_D^{20}$ -70 (*c* 0.02, MeOH). UV: λ_{max} = 242, 302 and 390 nm. ESIMS(+ve): *m/z* 446.8 $[M+H]^+$, 468.9 $[M+Na]^+$ and 914.9 $[2M+Na]^+$. (-ve): *m/z* 444.9 $[M-H]^-$. HRESIMS: calcd for $C_{23}H_{27}O_9$ $[M+H]^+$ 447.1655; found 447.1648 $[M+H]^+$ and for $C_{23}H_{26}O_9Na$ $[M+Na]^+$ 469.1475; found 469.1467 $[M+Na]^+$. ^1H and ^{13}C NMR data, see Table 4.

Acknowledgment

This study was supported by grants of the BMBF awarded to P.P. and A.D. R.B. wishes to thank DAAD for a scholarship. B.-G. W. and P. P. acknowledge the support of a joint project from NSFC (30910103914). We are indebted to Robin Visse (Institut für Organische und Makromolekulare Chemie, HHU, Düsseldorf) for CD measurement.

References

Aly, A. H. Protein kinase inhibitors and other cytotoxic metabolites from the fungal endophyte Stemphylium botryosum isolated from Chenopodium album. Mycosphere. **2010**. 1. 2. 153

Aly, A. H., Debbab, A., Clements, C., Edrada-Ebel, R., Orlikova, B., Diederich, M., Wray, V., Lin, W. and Proksch, P. NF kappa B inhibitors and antitrypanosomal metabolites from endophytic fungus Penicillium sp. isolated from Limonium tubiflorum. Bioorg Med Chem. **2011**. 19. 1. 414-421

Aly, A. H., Debbab, A. and Proksch, P. Fungal endophytes: unique plant inhabitants with great promises. Appl Microbiol Biotechnol. **2011**. 90. 6. 1829-1845

Bacon, C. W. and White, J. F. Microbial endophytes. New York, Marcel Dekker, Inc.

Debbab, A., Aly, A. and Proksch, P. Bioactive secondary metabolites from endophytes and associated marine derived fungi. Fungal Divers. **2011**. 49. 1. 1-12

Debbab, A., Aly, A. and Proksch, P. Endophytes and associated marine derived fungi-ecological and chemical perspectives. Fungal Divers. **2012**. 57. 1. 45-83

Debbab, A., Aly, A. H., Edrada-Ebel, R., Wray, V., Müller, W. E. G., Totzke, F., Zirrgiebel, U., Schälchtele, C., Kubbutat, M. H. G., Lin, W. H., Mosaddak, M., Hakiki, A., Proksch, P. and Ebel, R. Bioactive metabolites from the endophytic fungus Stemphylium globuliferum isolated from Mentha pulegium. J Nat Prod. **2009**. 72. 4. 626-631

Debbab, A., Aly, A. H., Edrada-Ebel, R., Wray, V., Pretsch, A., Pescitelli, G., Kurtan, T. and Proksch, P. New Anthracene Derivatives – Structure Elucidation and Antimicrobial Activity. Eur J Org Chem. **2012**. 7. 1351-1359

Donadio, S., Monciardini, P., Alduina, R., Mazza, P., Chiocchini, C., Cavaletti, L., Sosio, M. and Puglia, A. M. Microbial technologies for the discovery of novel bioactive metabolites. J Biotechnol. **2002**. 99. 3. 187-198

Ebrahim, W., Aly, A. H., Mándi, A., Totzke, F., Kubbutat, M. H. G., Wray, V., Lin, W.-H., Dai, H., Proksch, P., Kurtán, T. and Debbab, A. Decalactone derivatives from Corynespora cassiicola, an endophytic fungus of the mangrove plant Laguncularia racemosa. Eur J Org Chem. **2012**. 18. 3476-3484

Fan, L., Qing, L., Hong, Y., Xiao-Ling, C., Xue-Kui, X., Sheng-Ping, C., Meng-Feng, L., Zhi-Gang, S. and Yong-Cheng, L. Structure elucidation of three diphenyl ether derivatives from the mangrove endophytic fungus SBE-14 from the South China Sea. Magn Reson Chem. **2009**.

Frisvad, J. C., Filtenborg, O., Samson, R. A. and Stolk, A. C. Chemotaxonomy of the genus Talaromyces. Antonie van Leeuwenhoek. **1990**. 57. 3. 179-189

Gill, M. and Morgan, P. M. Absolute stereochemistry of fungal metabolites: icterinoidins A1 and B1, and atrovirins B1 and B2. Arcivoc. **2004**. 152-165

Gill, M. and Steglich, W. Pigments of fungi (Macromycetes). Fortschr Chem Org Naturst. **1987**. 51. 1-317

Harada, N. and Nakanishi, K. (1983). Circularly dichroic spectroscopy-exciton coupling in organic stereochemistry, University Science Books: Mill Valley.

Klevens, R. M., Morrison, M. A., Nadle, J., Petit, S., Gershman, K., Ray, S., Harrison, L. H., Lynfield, R., Dumyati, G., Townes, J. M., Craig, A. S., Zell, E. R., Fosheim, G. E., McDougal, L. K., Carey, R. B. and Fridkin, S. K. Invasive methicillin-resistant Staphylococcus aureus infections in the United States. JAMA. **2007**. 298. 15. 1763-71

Knight, G. M., Budd, E. L., Whitney, L., Thornley, A., Al-Ghusein, H., Planche, T. and Lindsay, J. A. Shift in dominant hospital-associated methicillin-resistant Staphylococcus aureus (HA-MRSA) clones over time. J Antimicrob Chemother. **2012**. 67. 10. 2514-22

Liu, F., Cai, X.-L., Yang, H., Xia, X.-K., Guo, Z.-Y., Yuan, J., Li, M.-F., She, Z.-G. and Lin, Y.-C. The bioactive metabolites of the mangrove endophytic fungus Talaromyces sp. ZH-154 isolated from Kandelia candel (L.) Druce. Planta Med. **2010**. 76. 02. 185-189

MacDougall, C., Powell, J. P., Johnson, C. K., Edmond, M. B. and Polk, R. E. Hospital and community fluoroquinolone use and resistance in Staphylococcus aureus and Escherichia coli in 17 US hospitals. Clin Infect Dis. **2005**. 41. 4. 435-40

MacMillan, J., Vanstone, A. E. and Yeboah, S. K. Fungal products. Part III. Structure of wortmannin and some hydrolysis products. J. Chem. Soc., Perkin Trans. 1. **1972**. 2898-2903

Nakanishi, K. and Berova, N. (1994). The exciton Chirality method in circular dichroism, VCH: Weinheim & New York.

Nakanishi, S., Kakita, S., Takahashi, I., Kawahara, K., Tsukuda, E., Sano, T., Yamada, K., Yoshida, M., Kase, H., Matsuda, Y. and et al. Wortmannin, a microbial product inhibitor of myosin light chain kinase. J Biol Chem. **1992**. 267. 4. 2157-63

Norman, B. H., Shih, C., Toth, J. E., Ray, J. E., Dodge, J. A., Johnson, D. W., Rutherford, P. G., Schultz, R. M., Worzalla, J. F. and Vlahos, C. J. Studies on the mechanism of phosphatidylinositol 3-kinase Inhibition by wortmannin and related analogs. J Med Chem. **1996**. 39. 5. 1106-1111

Prelog, V. and Helmchen, G. Grundlagen des CIP-systems und vorschläge für eine revision. Angewandte Chemie. **1982**. 94. 8. 614-631

Pretsch, A., Proksch, P. and Debbab, A. (2010). Sealife. Austrian Pat. Appl. [Post-Grant]. CODEN: ATXXBE AT 507298 A4 20100415 CAN 153:254618 21 pp.

Pretsch, A., Proksch, P. and Debbab, A. (2010). Austrian Pat. Appl. [Post-Grant]. CODEN: ATXXBE AT 507999 A4 20101015 CAN 154:128299: 23 pp.

Proksch, P., Putz, A., Ortlepp, S., Kjer, J. and Bayer, M. Bioactive natural products from marine sponges and fungal endophytes. Phytochem Rev. **2010**. 9. 4. 475-489

Rao, J. U. M., Hanumaiah, T., Rao, B. K. and Rao, K. V. J. Emodin glycosides from Ventilago calyculata. J Nat Prod. **1986**. 49. 2. 343-345

Shiozawa, H., Takahashi, M., Takatsu, T., Kinoshita, T., Tanzawa, K., Hosoya, T., Furuya, K., Takahashi, S., Furihata, K. and Seto, H. Trachyspic acid, a new metabolite produced by Talaromyces trachyspermus, that inhibits tumor cell heparanase: taxonomy of the producing strain, fermentation, isolation, structural elucidation, and biological activity. J Antibiot (Tokyo). **1995**. 48. 5. 357-62

Vargas, F., Rivas, C., Zoltan, T., López, V., Ortega, J., Izzo, C., Pineda, M., Medina, J., Medina, E. and Rosales, L. Antioxidant and scavenging activity of skyrin on free radical and some reactive oxygen species. Av. Quím. **2008**. 3. 1. 7-14

Wakelin, S., Warren, R., Harvey, P. and Ryder, M. Phosphate solubilization by Penicillium spp. closely associated with wheat roots. Biol. Fert. Soils. **2004**. 40. 1. 36-43

Wang, S., Li, X.-M., Teuscher, F., Li, Diesel, A., Ebel, R., Proksch, P. and Wang, B.-G. Chaetopyranin, a benzaldehyde derivative, and other related metabolites from Chaetomium globosum, an endophytic fungus derived from the marine red alga Polysiphonia urceolata. J Nat Prod. **2006**. 69. 11. 1622-1625

Xu, J., Aly, A. H., Wray, V. and Proksch, P. Polyketide derivatives of endophytic fungus Pestalotiopsis sp. isolated from the Chinese mangrove plant Rhizophora mucronata. Tetrahedron Lett. **2011**. 52. 1. 21-25

Xu, J., Ebada, S. and Proksch, P. Pestalotiopsis a highly creative genus: chemistry and bioactivity of secondary metabolites. Fungal Diversity. **2010**. 44. 1. 15-31

Yuesheng, D., Jie, L., Xinhua, L., Zhihui, Z., Xiao, R., Hua, Z., Jiangong, H. and Junshan, Y. Cathepsin B inhibitory tetraene lactones from the fungus Talaromyces wortmannii. Helv. Chim. Acta. **2009**. 92. 3. 567-574

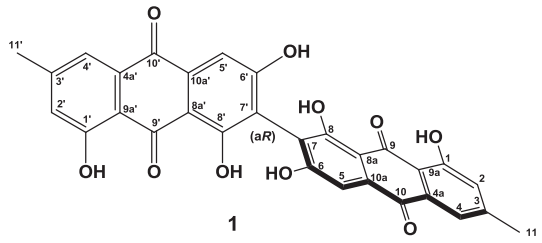

1

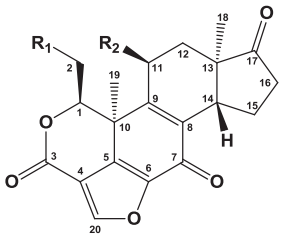

	R1	R2
2	OH	OCH_3
5	OMe	OAc

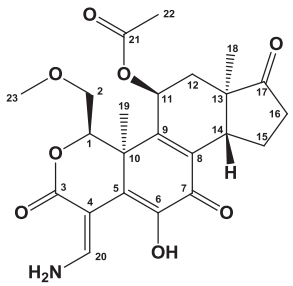

3

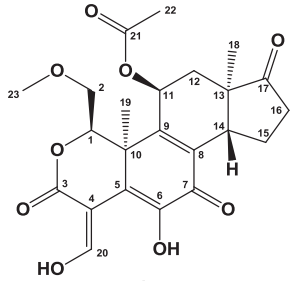

4

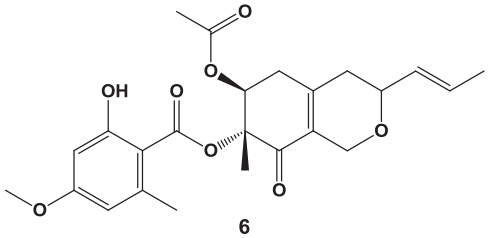

6

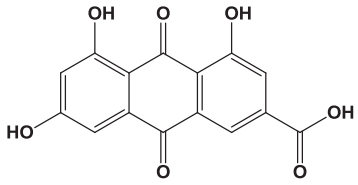

7

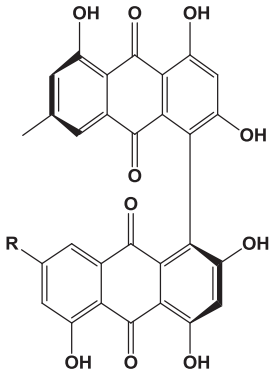

	R
8	CH_3
9	CH_2OH

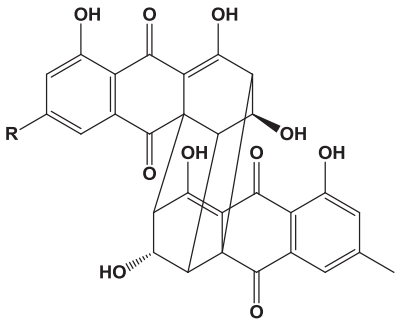

	R
10	CH_3
11	CH_2OH

Chart Structures of isolated compounds

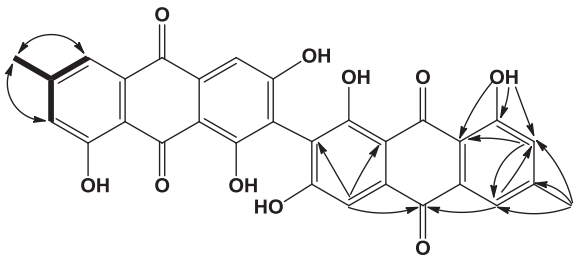

Figure 1. Key COSY (–), HMBC (→) and ROESY (↔) correlations of **1**.

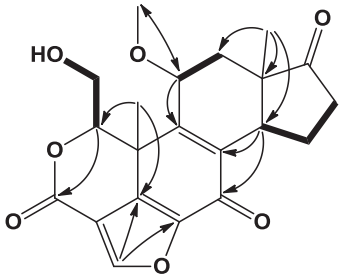

Figure 2. Key COSY (–) and HMBC (→) correlations of **2**.

Table 1. NMR spectroscopic data of **1** at 600 (^{1}H) and 150 (^{13}C) MHz ($CDCl_3$).

Nr.	**1**	
	δ_C [a]	δ_H
1/1′	164.0	-
2/2'	124.9	7.17 (1H; br s)
3/3'	150.0	-
4/4'	121.5	7.62 (1H; br s)
4a/4a'	134.2	-
5/5'	109.0	7.47 (1H; s)
6/6'	156.0	-
7/7'	114.1	-
8/8'	163.5	-
8a/8a'	110.1	-
9/9'	186.0	-
9a/9a'	115.0	-
10/10'	182.0	-
10a/10a'	137.0	-
11/11'	21.9	2.49
OH-1/1'		12.09
OH-8/8'		12.58

[a] Derived from HMBC spectrum

Table 2. NMR spectroscopic data of **2** at 600 (^{1}H) and 150 (^{13}C) MHz ($CDCl_3$).

Nr.	**2**	
	δ_C [a]	δ_H (J in Hz)
1	84.9	4.65 (1H; t; 4.0)
2	74.3	2.96 (1H; dd; 4.0, 10.5)
		3.07 (1H; dd; 4.0; 10.6)
3	160.7	
4	116.8	
5	136.6	
6	148.2	
7	174.2	
8	139.0	
9	149.1	
10	45.5	
11	53.7	5.11 (1H; br. d, 7.1)
12	35.4	1.44 (1H; br.d; 11.0)
		2.53 (1H; dd; 7.0; 11.0)
13	49.5	
14	45.5	2.98 (1H; m)
15	24.6	2.02 (2H; m)
16	38.3	2.25 (1H; m)
		2.61 (1H; m)
17	-	
18	18.8	1.01 (3H; s)
19		1.76 (3H; s)
20		8.23 (1H; s)
21	171.3	
22	-	
23	59.6	2.98 (3H; s)
OH-3		3.47 (1H; br.s)

[a] Derived from HMBC spectrum

Table 3. MIC values of isolated compounds against Gram negative and positive bacteria (μg/mL).

Gram negative	**1**	**2**	**3**	**4**	**5**	**6**	**8**	**10**	**11**
Escherichia coli	>64	>64	>64	>64	>64	>64	>64	>64	>64
Klebsiella pneumoniae	>64	>64	>64	>64	>64	>64	>64	>64	>64
Pseudomonas aeruginosa	>64	>64	>64	>64	>64	>64	>64	>64	>64
Acinetobacter baumannii	>64	>64	>64	>64	>64	>64	>64	>64	>64
Enterobacter sp.	>64	>64	>64	>64	>64	>64	>64	>64	>64
enterococcus cloacae	16	>64	>64	>64	>64	>64	32	16	32
Gram positive	**1**	**2**	**3**	**4**	**5**	**6**	**8**	**10**	**11**
MRSA	8	>64	>64	>64	>64	>64	8	8	32
Staphylococcus epidermidis	16	>64	>64	>64	>64	>64	4	8	32
Streptococcus pneumoniae	16	>64	>64	>64	>64	>64	4	8	32
Enterococcus faecalis	16	>64	>64	>64	>64	>64	16	16	32

= Chapter 4 =

Talaromins A and B, New Cyclic Peptides from the Endophytic Fungus *Talaromyces wortmannii*

Robert Bara[a], Amal H. Aly[a], Victor Wray[b], WenHan Lin[c], Peter Proksch[a], Abdessamad Debbab[a]*

[a] Institut für Pharmazeutische Biologie und Biotechnologie, Heinrich-Heine-Universität Düsseldorf, Universitätsstrasse 1, Geb. 26.23, 40225 Düsseldorf, Germany

[b] Helmholtz Centre for Infection Research, Inhoffenstraße 7, D-38124 Braunschweig, Germany

[c] National Research Laboratories of Natural and Biomimetic Drugs, Peking University, Health Science Center, 100083 Beijing, People's Republic of China

*Corresponding author, abdessamad.debbab@uni-duesseldorf.de

This chapter is adapted from a manuscript which has been submitted to *Tetrahedron Letters* as R. Bara, A. H. Aly, V. Wray, W. H. Lin, P. Proksch, A. Debbab. 2012. Talaromins A and B, new cyclic peptides from endophytic fungus *Talaromyces wortmannii*

The Impact factor of related journal is 2.683, overall participation on the paper is 70% as the first author. The first author involved to all laboratory works as well as the manuscript preparation.

Abstract

Chemical investigation of the endophytic fungus *Talaromyces wortmannii*, isolated from *Aloe vera* and grown on white beans in static culture yielded two new cyclic peptides, talaromins A (**1**) and B (**2**). Their structures were established on the basis of extensive NMR spectroscopic and mass spectrometric (ESI, HRESI and MALDI-TOF) analysis. Both compounds contain ring systems comprised of six α-amino acid residues connected to a *β*-amino acid (anthranilic acid), which provides the ring-closing template. The absolute configurations of the alpha-amino acids were determined by Marfey's method, which showed that all amino acids are present in the L-form, except for D-Val in **1** and D-Ile in **2**.

Keywords: *Talaromyces wortmannii*, endophyte, *Aloe vera*, cyclic peptide, structure elucidation, absolute configuration

Introduction

The term endophyte stands for “in the plant” (Greek: *endon* = within, *phyton* = plant), indicating microorganisms residing within plant tissues, rather than on the plant surface (Carroll 1988; Clay 1988). This term is not limited to bacteria and fungi inhabiting tissues of higher plants but extends to other potential hosts and inhabitants such as algae within algae (Schulz and Boyle 2006). Endophytes may be transmitted from one generation to the next through seeds of host plants or through vegetative propagules (Carroll 1988).

Mutualistic associations between host plants and their particular endosymbionts were found to confer a variety of benefits to both partners, such as, the production of bioactive secondary metabolites by the microbial partner which is involved in host plant protection against insects and parasites thereby representing an acquired chemical defense mechanism of the host (Carroll 1988; Clay 1988). However, endophytic microorganisms represent not only a vast reservoir of novel natural products involved in chemical ecology but offer also opportunities for exploitation in medicine, agriculture and industry as exemplified by the potent antimycotic substance cryptocandin A, the HIV-1 integrase inhibitors xanthoviridicatins E and F, and *Helicobacter pylori* inhibiting rhizotonic acid which were all obtained from fungal endophytes (Aly *et al.* 2011; Aly *et al.* 2011; Debbab *et al.* 2011; Debbab *et al.* 2012; Debbab *et al.* 2012). Taking into account the existence of approximately 300 thousand different species of higher plants, with each individual plant hosting one or more endophytes, a rich pool of fungal species and their bioactive constituents is to be discovered in the coming years (Strobel *et al.* 2004).

Species of the genus *Talaromyces* have been found in solitary as well as endophytic status surviving in various climates worldwide from terrestrial to marine environments (Shiozawa *et al.* 1995; Yuesheng *et al.* 2009). This genus attracted considerable attention of researchers since it produces a variety of interesting bioactive compounds ranging from antibiotics to cytotoxins (Frisvad *et al.* 1990; Wakelin *et al.* 2004; Liu *et al.* 2009; Yuesheng *et al.* 2009; Liu *et al.*). Examples of secondary metabolites produced by *Talaromyces* species include tetraene lactones (Yuesheng *et al.* 2009), diphenyl ether derivatives (Liu *et al.* 2009), episaustdiol and anthraquinones (Liu *et al.* 2010).

As part of our ongoing research focussing on the discovery of new natural products from endophytic fungal endophytes (Aly *et al.* 2011; Ebrahim *et al.* 2012), we studied the chemical constituents of *Talaromyces wortmanii*, which was isolated from the inner tissues of *Aloe vera*, collected in Alexandria, Egypt, and cultivated in static culture on white beans (*Phaseolus vulgaris*) which resulted in the isolation of two new cyclic peptides, talaromins A (**1**) and B (**2**). The structure elucidation of both compounds is described including the determination of the absolute configuration of their constituting amino acids. To the best of our knowledge, this is the first report on isolation and structure elucidation of peptides from the genus *Talaromyces*.

Results and discussion

The crude ethyl acetate extract of *T. wortmannii* cultured on white beans (*Phaseolus vulgaris*) was fractionated using vacuum liquid column chromatography on silica gel. Further purification of the resulting fractions was achieved on Sephadex LH-20 and with semi-preparative HPLC to yield compounds **1** and **2**. The structures of the isolated compounds were unambiguously determined using a combination of homo- and heteronuclear NMR techniques together with ESI and MALDI-TOF mass analysis.

Talaromin A (**1**) was obtained as a white amorphous powder and showed two UV maxima at λ_{max} 232 and 282 nm. The chemical formula of **1** was deduced as $C_{39}H_{53}O_9N_7$ from the prominent peak appearing at *m/z* 764.3959 $[M+H]^+$ in the HRESIMS. Extensive analysis of TOCSY and COSY data revealed the presence of eight spin systems. In the TOCSY spectrum, five characteristic spin systems were detected at low field (7.67-7.72 ppm) and were found to originate from the amidic protons of one Val, one Tyr, one Thr, one Ala and one Ile amino acid residue. In addition, one Pro unit was detected by close inspection of the high field region of the spectrum.The signal resonating at δ_H 7.68 ppm (NH), as well as signals corresponding to the ABCD spin system (δ_H 8.04 (H-2`), 7.55 (H-3`), 7.30 (H-4`), and 7.70 (H-5`) ppm) in association with their HMBC correlations to signals at δ_C 138.6 (C-1`) and 126.2 (C-6`), as well as to the carbonyl atom at δ_C 171.7 ppm indicated the presence of an unusual anthranilic acid (AA) moiety.

In the ^{13}C NMR spectrum, seven carbonyl carbons were detected at δ_C 171.7-175.6 ppm, and six α-carbons of amino acids in the region of 51.2-64.5 ppm, thus confirming the presence of

six amino acids along with an anthranilic acid residue. Accordingly, the structure fulfilled 17 of the double bond equivalents required by the molecular formula, whereas the cyclic structure of the molecule accounted for the remaining element of unsaturation. The sequence of amino acids and the location of anthranilic acid were established by detailed examination of ROESY and HMBC spectra (Figure 1). In the ROESY spectrum, diagnostic correlations were observed between H-α/H-β and NH of adjacent residues for the substructure Val-Tyr-Thr-Ala-Ile. H-α of Ile correlated to CH_2-δ of the Pro residue, thus extending the identified substructure to include Pro. The position of the AA residue was confirmed based on correlations of its aromatic doublet at 8.04 Hz with H-α and CH_2-β of the Pro residue. The amino acid sequence established from through space NOE correlations was confirmed by thorough inspection of the HMBC spectrum. Furthermore, H-5' of AA as well as H-α of Val correlated with the carbonyl carbon of AA indicating their adjacent position and hence the closure of the cyclic structure. The location of Pro between AA and Ile was confirmed from the observed correlations of H-α of Ile and CH_2-δ of Pro to the carbonyl carbon of Ile. Sequence evidence was also provided by MALDI-TOF-MS spectrum showing base peaks at *m/z* 400 and 434 (Figure 2), which corresponded to the substructures Ala-Ile-Pro-AA and Val-Tyr-Thr-Ala, repectively, thus confirming the cyclic nature of **1**.

The stereochemistry of the amino acid residues was determined by Marfrey's method after acid hydrolysis of **1** and subsequent derivatization to generate diastereomeric reaction products (Marfey 1984). Comparison of the resulting (N-(5-fluoro-2,4-dinitrophenyl)-L-leucinamide) amino acid derivatives with those of standard amino acids using LCMS indicated that all amino acids were of L-form except for the Val residue which was present in D-form. On the basis of the previous analysis, **1** was identified as cyclo-(D-Val-L-Tyr-L-Thr-L-Ala-L-Ile-L-Pro-AA) for which we propose the name talaromin A.

Compound **2** showed UV maxima at λ_{max} 235 and 283 nm in analogy to **1**. HRESIMS showed a prominent peak at *m/z* 778.4110 $[M+H]^+$ indicating a chemical formula of $C_{40}H_{55}O_9N_7$ with a 14 amu increase in molecular weight compared to **1**. Detailed comparison of ^1H NMR spectra of both compounds demonstrated a methyl signal appearing as a triplet at δ_H 0.81 ppm (CH_3-$\delta_{Ile\text{-}1}$), which is characteristic for the tertiary methyl group of Ile, whereas one secondary methyl group of Val was missing. Furthermore, two additional methylene protons were detected at δ_H 1.23 ppm and were assigned to CH_2-γ of Ile-1. Inspection of TOCSY and

COSY spectra revealed the presence of two Ile spin systems and the absence of a Val residue in **2**, hence in comparison to **1** Val was replaced by an additional Ile residue in **2**. Full assignment of ^{1}H and ^{13}C NMR data is given in table 2. The amino acid sequence of **2** was deduced from correlations observed in the ROESY and HMBC spectra as for **1** (Figure 1).
MALDI-TOF-MS analysis of **2** (Figure 3) indicated the presence of the substructures Ile-1-Tyr-Thr, Ala-Ile-5-Pro-AA, and AA-Ile-1-Tyr-Thr-Ala corresponding to the base peak at *m/z* 379, 400 and 567, respectively. As for **1**, the absolute stereochemistry of the amino acid residues in **2** was determined by Marfey's method, which revealed that all amino acid residues were of L-form except one Ile unit. Based on the fact that the structure of **2** was identical to that of **1** apart from the replacement of D-Val in the latter by Ile-1 in **2**, we assumed that Ile-5 was of L-form, in analogy to **1**, whereas the D-form was assigned to Ile-1. Thus, **2** was identified as cyclo-(D-Ile-L-Tyr-L-Thr-L-Ala-L-Ile-L-Pro-AA) and named talaromin B.

Both compounds showed no activity when evaluated for their cytotoxicity against L5178Y mouse lymphoma cells using the MTT assay. Furthermore, **1** and **2** were also tested for their antibacterial activity against a broad spectrum of bacterial strains, including antibiotic-susceptible reference strains and multi-resistant clinical isolates. Both compounds exhibited no antibacterial activity against the isolates up to a concentration of 64 μg/mL.

Acknowledgment

R.B. wishes to thank DAAD for a scholarship. This study was supported by grants of the BMBF awarded to P.P. and A.D. We wish to thank Prof. H. Brötz-Oesterhelt and Dr. I. Zerfass (both from University of Duesseldorf) for performing antibacterial assays and Prof. W.E.G. Müller (University of Mainz) for cytotoxicity assays.

Chart

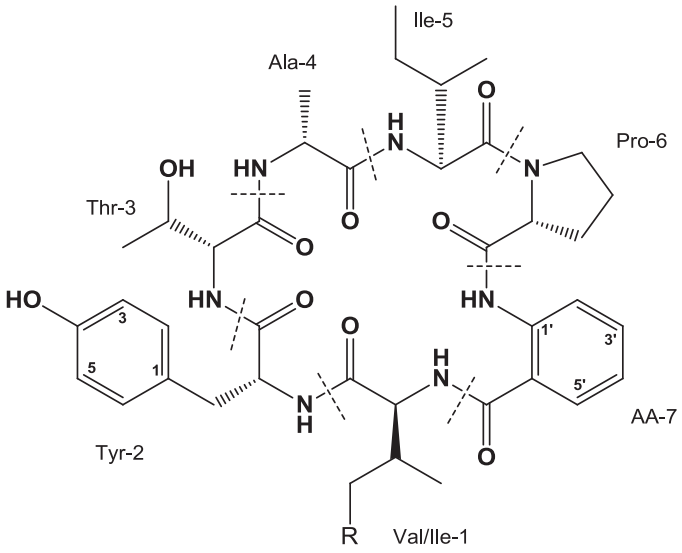

1 R: H
2 R: CH_3

Structures of talaromins A (1) and B (2)

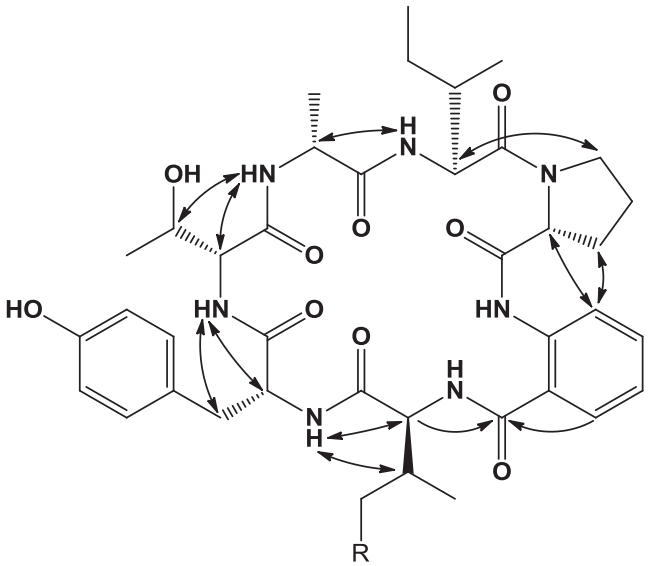

Figure 1: Key ROESY (⟷) and HMBC (⟶) confirming correlations the amino acid sequence of **1** and **2**.

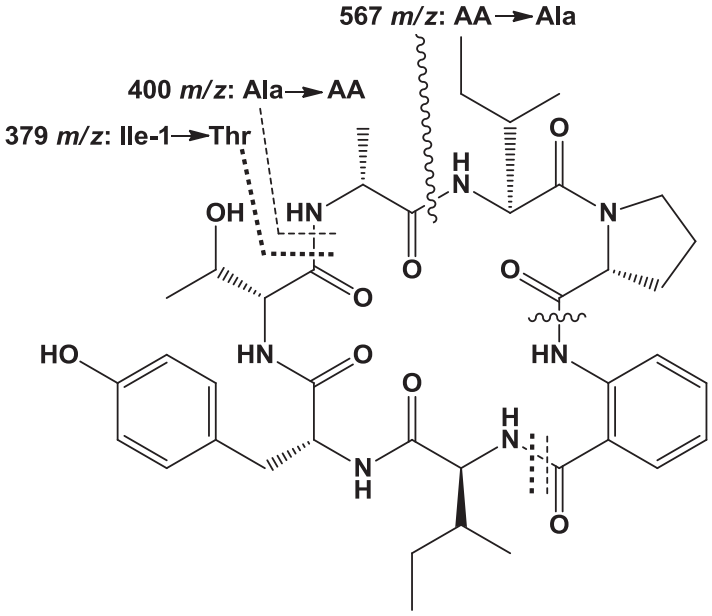

Figure 2: MALDI-TOF fragmentations of **1**.

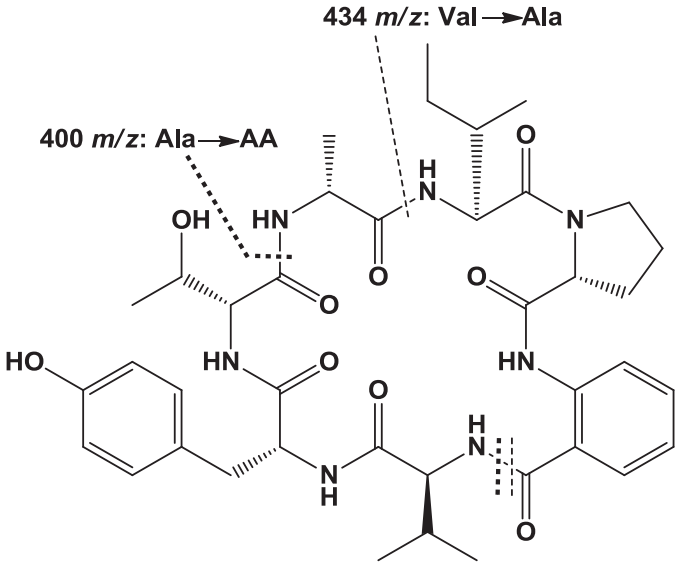

Figure 3: MALDI-TOF fragmentations of **2**.

Table 1. ^{1}H and ^{13}C NMR data of talaromin A (**1**) at 600 (^{1}H) and 150 (^{13}C) MHz ($CF_3CD_2OD:D_2O$ 1:1, δ in ppm, J in Hz)

Amino acid	Position	δ_C	δ_H
Val-1	NH		7.71*
	CO	174.9	
	α	60.6	4.64, dd (5.5, 8.7)
	β	33.5	2.05, m
	γ,γ`	18.3; 20.4	0.75, d (6.7); 0.80, d(6.7)
Tyr-2	NH		8.16, d (8.7)
	OH		10.98 s
	CO	175.6	
	α	57.7	4.80, ddd (4.9, 8.7, 10.4)
	β	38.6	2.99, dd(10.4, 14.2); 3.26, dd (4.9, 14.2)
	3/5	117.9	6.85, d (8.4)
	2/6	127.3	7.22, d (8.4)
	4	157.3	
Thr-3	NH		7.91, d (7.4)
	CO	173.2	
	α	62.5	4.19, dd (4.0, 7.4)
	β	69.4	4.35, m
	γ	20.3	1.40, d (6.9)
Ala-4	NH		7.69*
	CO	175.5	
	α	51.2	4.30, m
	β	20.3	1.20, d (6.4)
Ile-5	NH		7.72*
	CO	174.1	
	α	56.8	5.05, dd (5.8, 9.0)
	β	39.8	1.89, m
	γ	28.3	1.30, m; 1.40, m
	γ',δ	15.3; 12.7	0.9, d (6.7); 1.01, t (7.2)
Pro-6	CO	174.1	
	α	50.0	4.5, dd (4.2, 8.6)
	β	31.3	2.14, m, 2.31, m
	γ	26.1	2.05, m
	δ	64.5	3.70, ddd (7.3, 7.2, 8.0)
AA-7	NH		7.68*
	CO	171.7	
	1	138.6	
	2	125.8	8.04, d (7.8)
	3	134.8	7.55, t (7.8)
	4	127.3	7.30, t (7.6)
	5	130.4	7.70*
	6	126.2	

* Signals overlapped in the area between 7.67-7.73 ppm were extracted from HMQC, HMBC and TOCSY.

Table 2. ^{1}H and ^{13}C NMR data of talaromin B (**2**) at 600 (^{1}H) and 150 (^{13}C) MHz ($CF_3CD_2OD:D_2O$ 1:1, δ in ppm, J in Hz)

Amino acid	Position	δ_C	δ_H
Ile-1	NH		7.67*
	CO	174.9	
	α	60.1	6.67, dd (5.9, 8.7)
	β	39.7	1.8, m
	γ	26.1	1.23, m; 1.01 (ov. with CH_3-Ile-5)
	γ',δ	12.7; 15.3	0.80, d (6.8); 0.81, t (7.5)
Tyr-2	NH		8.1, d (8.8)
	OH		11.1
	CO	175.6	
	α	57.8	4.86, m
	β	38.5	2.26, dd (5.0, 14.4); 2.99, dd (10.4, 14.3)
	1	130.7	
	3/5	117.9	6.85, d (4.4)
	2/6	132.5	7.21, d (8.5)
	4	157.33	
Thr-3	NH		7.90, d (7.6)
	CO	173.1	
	α	62.4	4.20, dd (4.0, 7.6)
	β	69.4	4.37-4.31, m
	γ	20.8	1.20, d (6.4)
Ala-4	NH		7.70*
	CO	175.5	
	α	52.0	4.37-4.31, m
	β	20.3	1.4, d (7.0)
Ile-5	NH		7.71*
	CO	174.1	
	α	56.7	5.06, dd (5.6, 9.11)
	β	39.8	1.89, m
	γ	28.4	1.25, m; 1.38, m
	γ',δ	12.7; 16.5	0.92, d (6.8); 1.01, t (7.4)
Pro-6	CO	174.2	
	α	64.6	4.5, dd (4.0, 8.7)
	β	31.3	2,14, m; 2.32, m
	γ	26.0	2.03, m
	δ	50.0	3,70, br dt (7.5, 7.8); 3.90 (ov. with solvent)
AA-7	NH		7.23*
	CO	171.4	
	1	138.8	
	2	124.5	8.09, d (8.2)
	3	134.8	7.56, dt (1.1, 8.1)
	4	127.2	7.23, d (8.0)
	5	130.3	7.68*
	6	125.9	

* Signals overlapped in the area between 7.67-7.68 ppm were extracted from HMQC, HMBC and TOCSY.

SUPORTING MATERIAL

Talaromins A and B, New Cyclic Peptides from the Endophytic Fungus *Talaromyces wortmannii*

Robert Bara[a], Amal H. Aly[a], Victor Wray[b], WenHan Lin[c], Peter Proksch[a]* and Abdessamad Debbab [a]*

[a] Institut für Pharmazeutische Biologie und Biotechnologie, Heinrich-Heine-Universität Düsseldorf, Universitätsstrasse 1, Geb. 26.23, 40225 Düsseldorf, Germany.

[b] Helmholtz Centre for Infection Research, Inhoffenstraße 7, D-38124 Braunschweig, Germany.

[c] National Research Laboratories of Natural and Biomimetic Drugs, Peking University, Health Science Center, 100083 Beijing, People's Republic of China

Experimental Section

General experimental procedures. UV spectra were determined on a Dionex instrument with Chromeleon V6.3 as standard software programs. 1D and 2D NMR spectra were obtained on a AVANCE DMX 600 NMR spectrometers. Mass spectra were recorded using a LCMS HP1100 Agilent Finnigan LCQDecaXP Thermoquest. MALDI-TOF-MS spectra were determined on Bruker Microflex™ MALDI-ToF Mass Spectrometry System. HRESIMS were obtained with a FTHRMS-Orbitrap (Thermo-Finnigan) mass spectrometer. Vacuum and pressurized column chromatography was performed with Silica gel 60M (230-3400 mesh ASTM, Macherey-Nagel GmbH & Co.KG, Düren, Germany) and size exclusion chromatography was performed using Sephadex LH-20 (Sigma). TLC was carried out with precoated Silica gel plates (TLC silica gel 60 F-254, Merck KGaA, Darmstadt, Germany). Semi-preparative HPLC was carried out with Merck Hitachi L-7100 and L-7400 for pump and UV detector, respectively, using C-18 column (Knauer, Berlin, Germany).

Plant and fungal material. The *Aloe vera* plant was collected from the coastal region of Alexandria, Egypt, in June 2009. The endophytic fungus was isolated from the inner leaf tissues of the plant using previously described procedures (Debbab *et al.* 2009). A voucher strain (strain designation AVE 3.2) is kept in the authors' laboratory (P.P./A.D.).

Identification of fungal strain. The fungal strain was identified according to a molecular biological protocol by DNA amplification and sequencing of the ITS region as described previously (Wang *et al.* 2006). The BLAST search result showed that the sequence had 95-97% similarity to the sequence of *Talaromyces sp.* (AF285115.1). Identification to species level was achieved based on morphological and physiological characteristics at the Deutsche Sammlung von Mikroorganismen und Zellkulturen GmbH (DSMZ), Braunschweig, Germany. Accordingly, the fungal strain was identified as *Talaromyces wortmanii*. Sequence data have been submitted to GenBank with accession number HM807532.1.

Cultivation. Twenty Erlenmeyer flasks (1L each) containing 100 g of white beans (Phaseolus vulgaris) and 100 mL of distilled water were autoclaved. A small part of the medium from a Petri dish containing the purified fungus was transferred under sterile conditions to this solid medium and grown at room temperature (22 °C) for 40 days.

Extraction and purification. Cultures were exhaustively extracted with EtOAc and the dried crude extract (4.3 g) was subjected to vacuum liquid chromatography (VLC) using n-hexane/EtOAc followed by CH_2Cl_2/MeOH gradient as eluting solvent. Fraction 13 (90 mg), eluted with CH_2Cl_2:MeOH (2:8), was further purified using sephadex LH-20 (100% MeOH) and semi-preparative HPLC (MeOH/H_2O gradient) to yield compounds **1** (14.3 mg) and **2** (5.4 mg).

Talaromin A (1) white amorphous powder; $[\alpha]_D^{20}$–12.6 (*c* 1.0, MeOH); UV λ_{max} (PDA) 232, 282 nm; ^1H and ^{13}C spectroscopic data, see Table 1; ESIMS *m/z* (positive) 764.2 $[M+H]^+$, (negative) 762.3 $[M-H]^-$; HRESMS calcd for $C_{39}H_{54}O_9N_7$ 764.3983 $[M+H]^+$, found 764.3959.

Talaromarin B (2). White amorphous powder; $[\alpha]_D^{20}$–10.7 (*c* 1.0, MeOH); UV λ_{max} (PDA) 235, 283 nm; ^1H and ^{13}C spectroscopic data, see Table 2. ESIMS *m/z* (positive) 778.2 $[M+H]^+$, (negative) 776.3 $[M-H]^-$; HRESIMS calcd for $C_{40}H_{56}O_9N_7$ 778.4140 $[M+H]^+$, found 778.4110.

Cell proliferation assay. Cytotoxicity was tested against L5178Y mouse lymphoma cells using a microculture tetrazolium (MTT) assay and compared to that of untreated controls as described previously (Carmichael *et al.* 1988; Ashour *et al.* 2006). Experiments were repeated three times and carried out in triplicates. Media with 0.1% EGMME/DMSO were included in the experiments as negative controls. The depsipeptide kahalalide F, isolated from *Elysia grandifolia* (Ashour *et al.* 2006), was used as a positive control.

Antibacterial activity. Antibacterial activity was tested against a panel of antibiotic-susceptible CLSI (CLSI 2008) quality control strains including *Staphylococcus aureus* ATCC 29213, *Streptococcus pneumoniae* ATCC 49619, *Escherichia coli* ATCC 25922, *Klebsiella pneumoniae* ATCC 27799 , a standard laboratory strain (*Bacillus subtilis* 168) (Burkholder and Giles 1947), a high-level quinolone-resistant laboratory mutant (*Escherichia coli* WT-3-1 MB2, Prof. Dr. Peter Heisig, University of Hamburg, Germany) and the following (multi)drug-resistant clinical isolates: *Staphylococcus aureus* Mu50 (Hiramatsu *et al.* 1997), *Staphylococcus aureus* 25697 (AiCuris, Wuppertal, Germany), *Streptococcus agalactiae* 013761 and *Streptococcus pyogenes* 014327 (Prof. Dr. Hans-Georg Sahl, University of Bonn, Germany), *Enterococcus faecalis* UW 2689 (Prof. Dr. Wolfgang Witte, Robert Koch Institute,

Wernigerode, Germany), *Enterococcus faecium* 6011 (Klare *et al.* 1995), and *Pseudomonas aeruginosa* B 63230 (Henrichfreise *et al.* 2005). The MIC (Minimal Inhibitory Concentration) for each bacterial strain was determined by the broth microdilution method according to the recommendations of the Clinical and Laboratory Standards Institute (CLSI 2008) . For preparation of the inoculum the direct colony suspension method was used.

S 1. ^{1}H NMR spectrum of talaromin A (**1**) 600 MHz

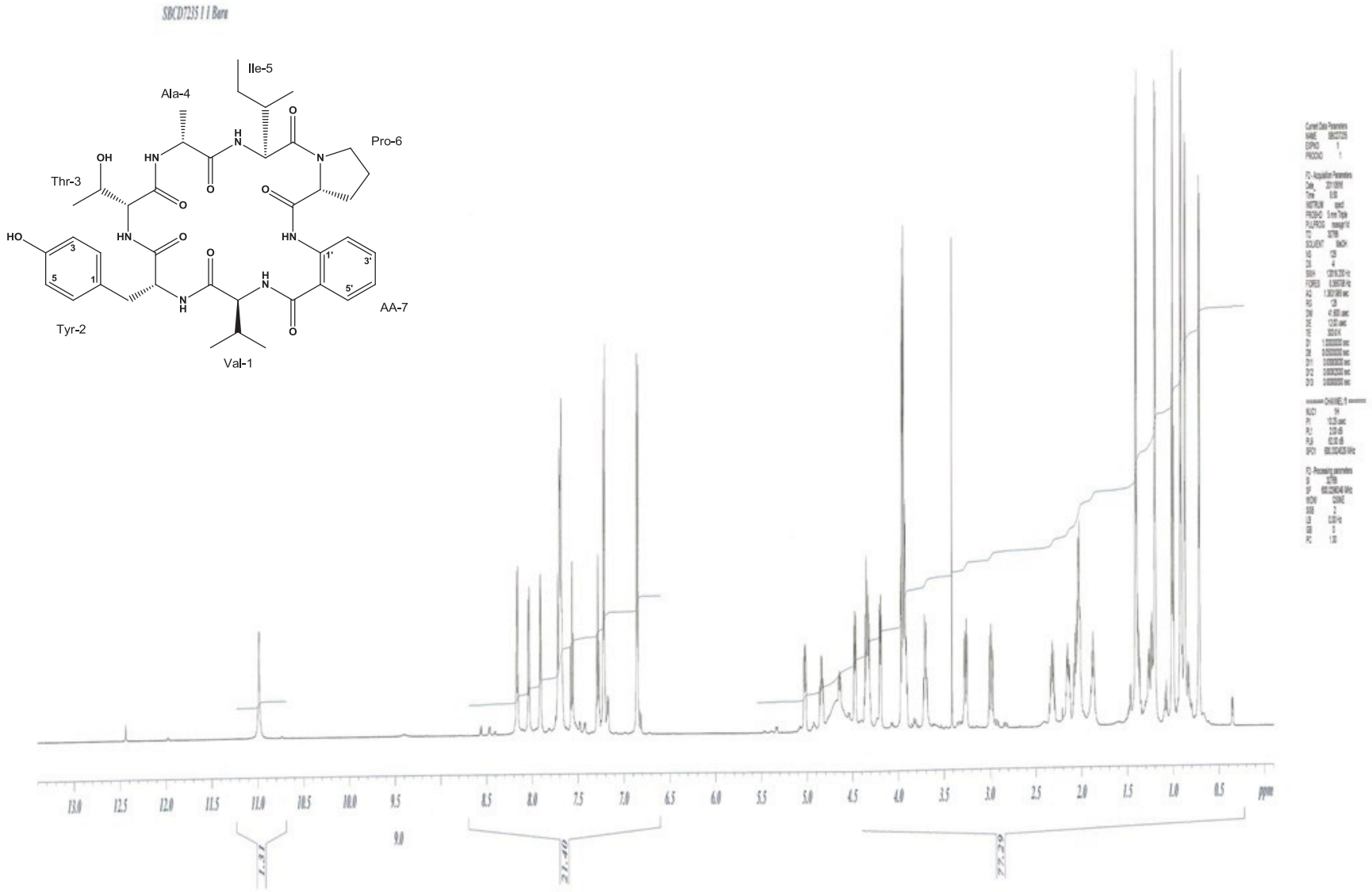

S 2. ^{13}C NMR spectrum of talaromin A (**1**) 150 MHz

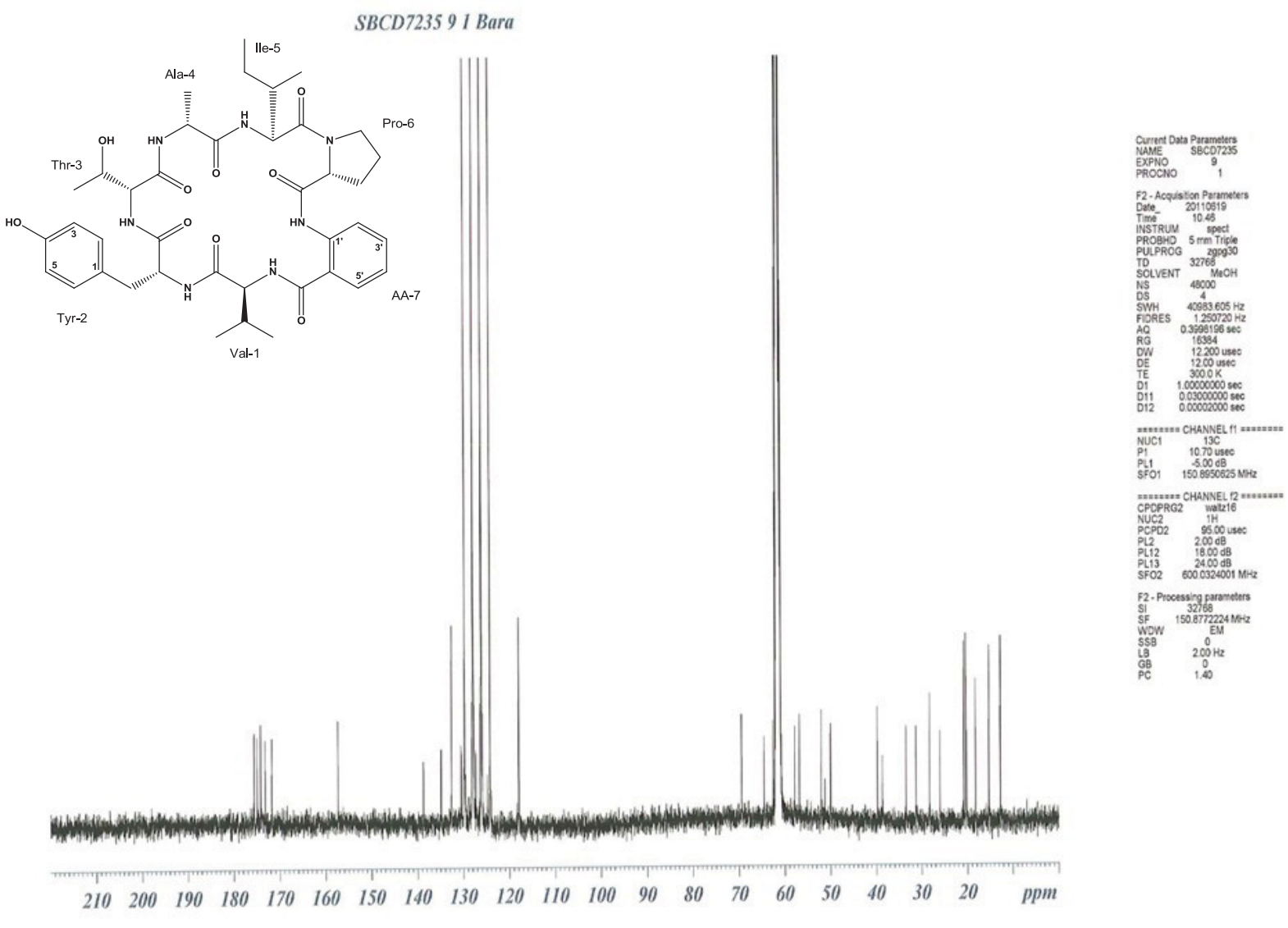

S 3. DEPT spectrum of talaromin A (**1**) 150 MHz

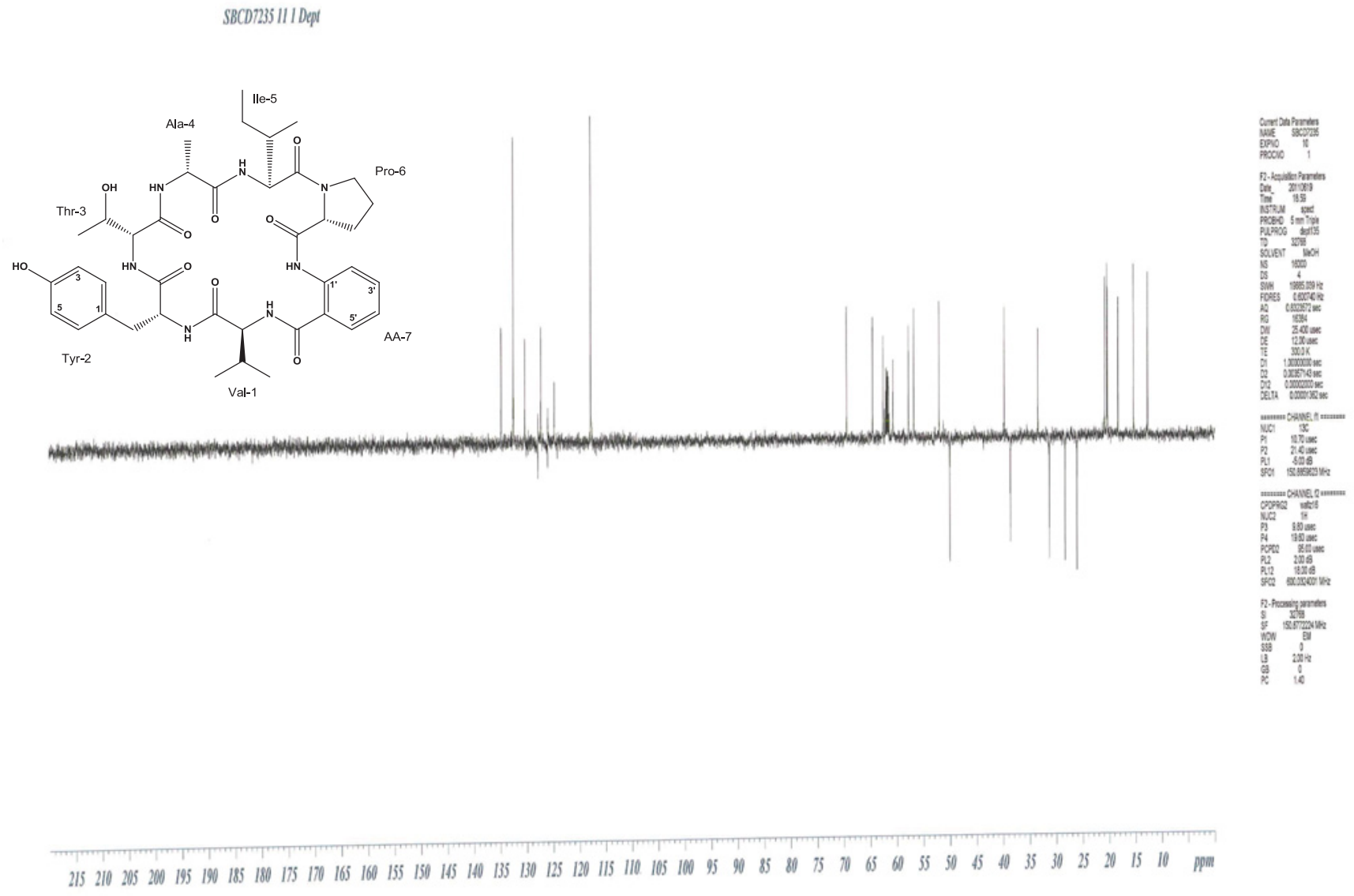

S 4. COSY spectrum of talaromin A (**1**)

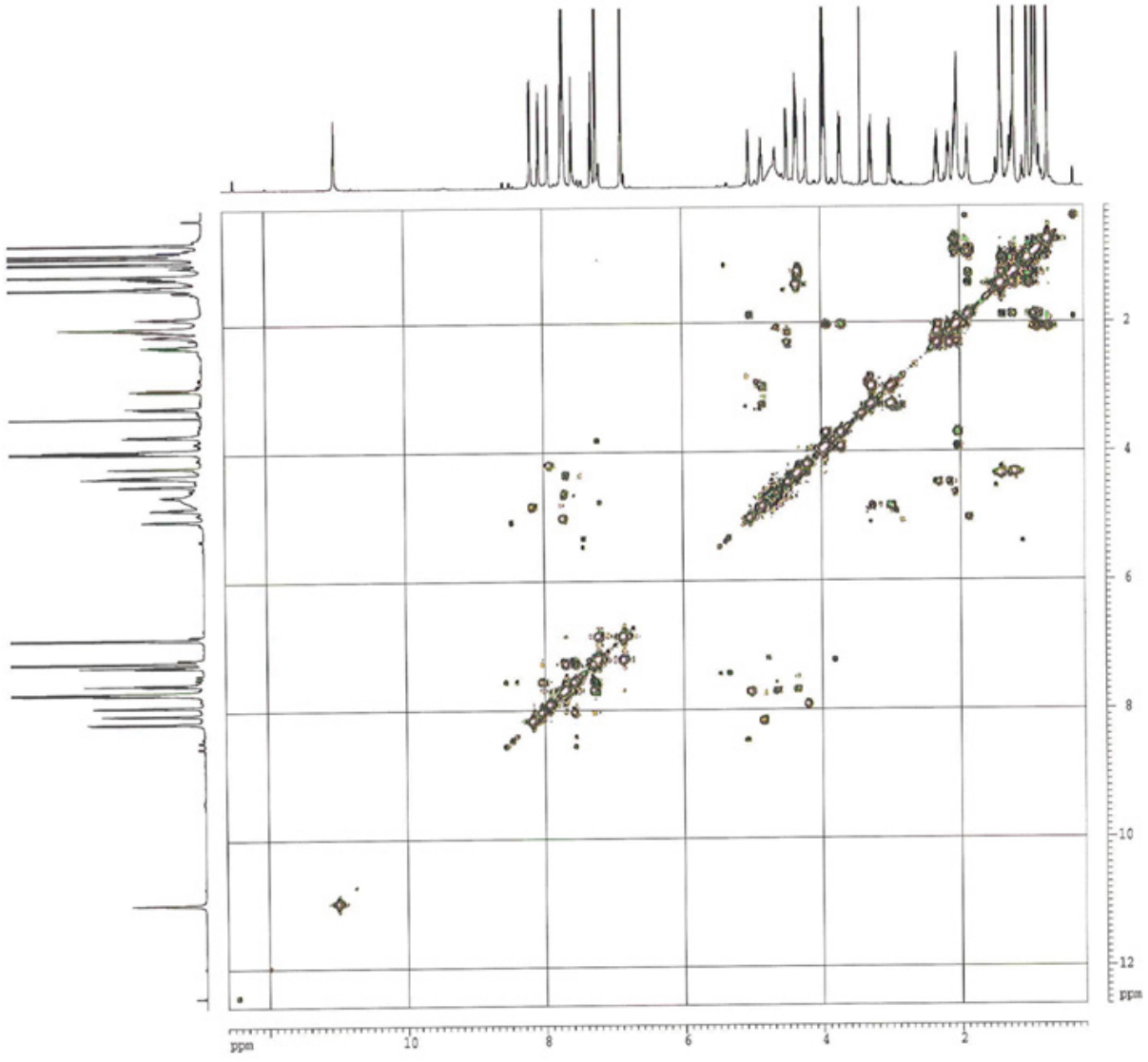

Current Data Parameters

NAME	SBCD7235
EXPNO	2
PROCNO	1

F1 - Acquisition parameters

ND0	1
TD	256
SFO1	600.0325 MHz
FIDRES	38.752480 Hz
SW	16.533 ppm

F2 - Processing parameters

SI	2048
SF	600.0296349 MHz
WDW	SINE
SSB	0
LB	0.00 Hz
GB	0
PC	1.00

F1 - Processing parameters

SI	1024
MC2	QF
SF	600.0296349 MHz
WDW	SINE
SSB	0
LB	0.00 Hz
GB	0

2D NMR plot parameters

CX2	20.00 cm
CX1	20.00 cm
F2PLO	12.600 ppm
F2LO	7560.37 Hz
F2PHI	0.200 ppm
F2HI	120.01 Hz
F1PLO	12.600 ppm
F1LO	7560.37 Hz
F1PHI	0.200 ppm
F1HI	120.01 Hz
F2PPMCM	0.62000 ppm/cm
F2HZCM	372.01837 Hz/cm
F1PPMCM	0.62000 ppm/cm
F1HZCM	372.01837 Hz/cm

S 5. TOCSY spectrum of talaromin A (**1**)

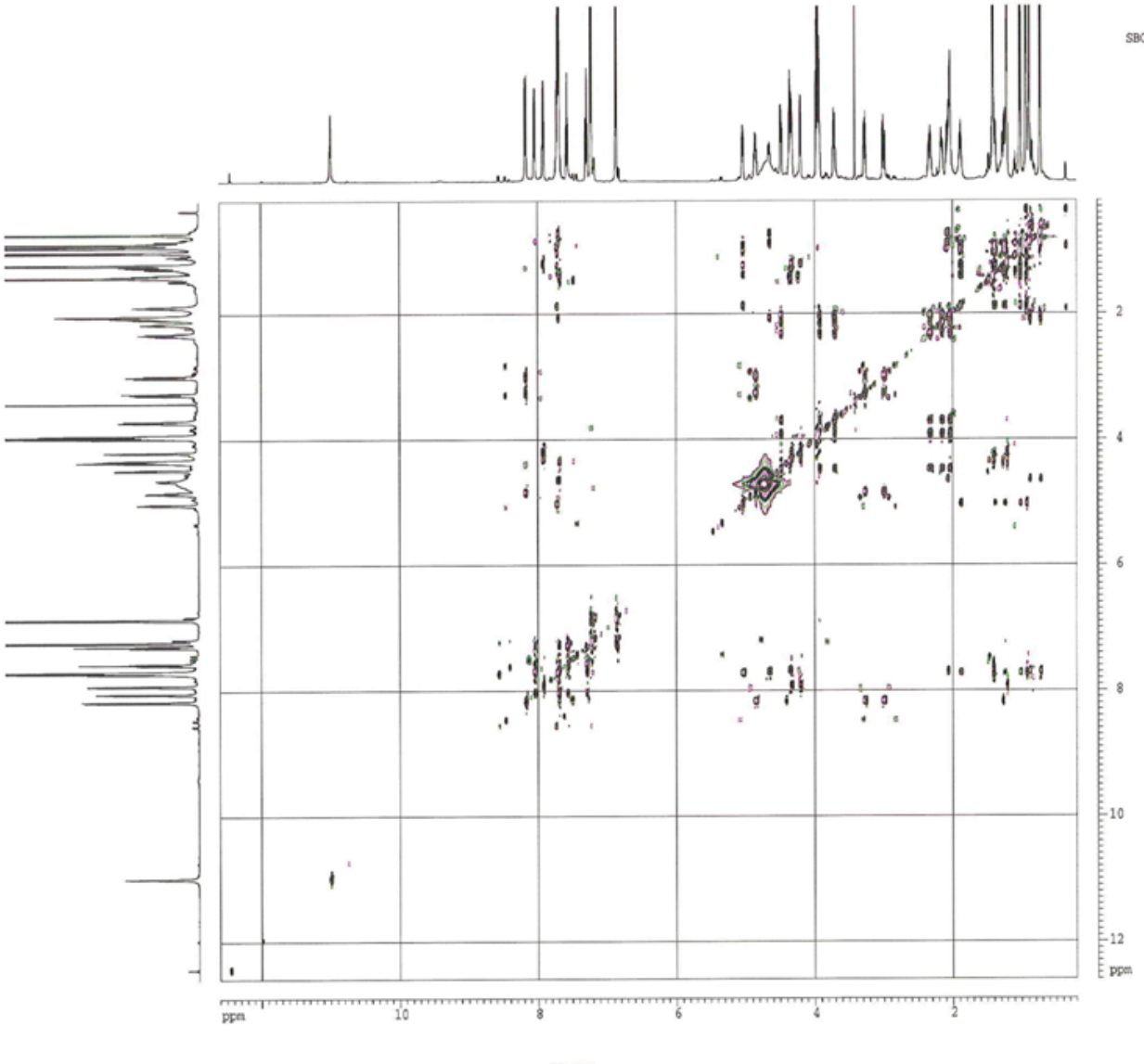

Current Data Parameters

NAME	SBCD7235
EXPNO	3
PROCNO	1

F1 - Acquisition parameters

ND0	2
TD	256
SFO1	600.0325 MHz
FIDRES	38.752480 Hz
SW	16.533 ppm

F2 - Processing parameters

SI	2048
SF	600.0296349 MHz
WDW	GM
SSB	0
LB	-13.00 Hz
GB	0.3
PC	1.40

F1 - Processing parameters

SI	1024
MC2	TPPI
SF	600.0296349 MHz
WDW	QSINE
SSB	2
LB	0.00 Hz
GB	0

2D NMR plot parameters

CX2	20.00 cm
CX1	20.00 cm
F2PLO	12.600 ppm
F2LO	7560.37 Hz
F2PHI	0.200 ppm
F2HI	120.01 Hz
F1PLO	12.600 ppm
F1LO	7560.37 Hz
F1PHI	0.200 ppm
F1HI	120.01 Hz
F2PPMCM	0.62000 ppm/cm
F2HZCM	372.01837 Hz/cm
F1PPMCM	0.62000 ppm/cm
F1HZCM	372.01837 Hz/cm

S 6. ROESY spectrum of talaromin A (**1**)

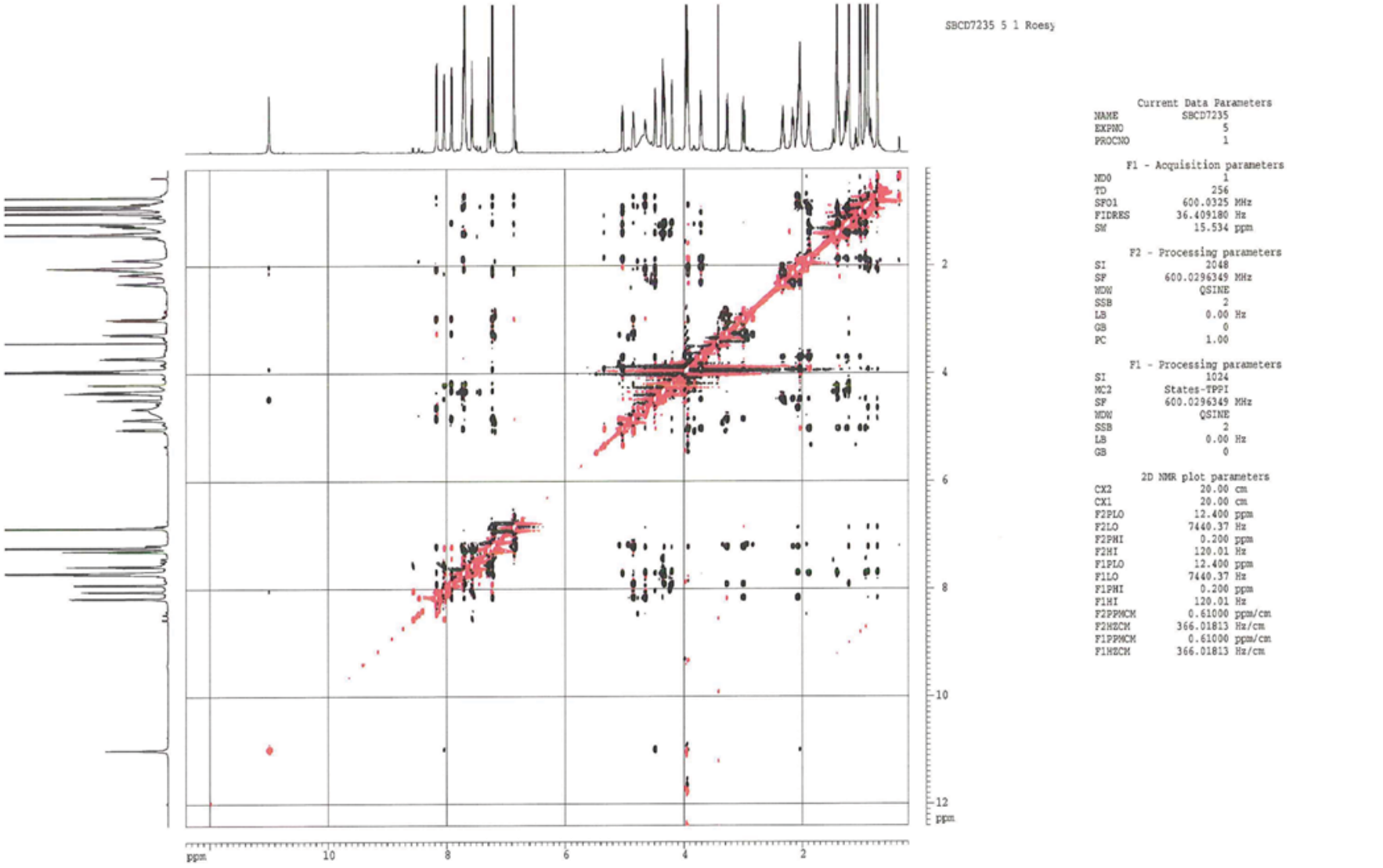

S 7. HMBC spectrum of talaromin A (**1**)

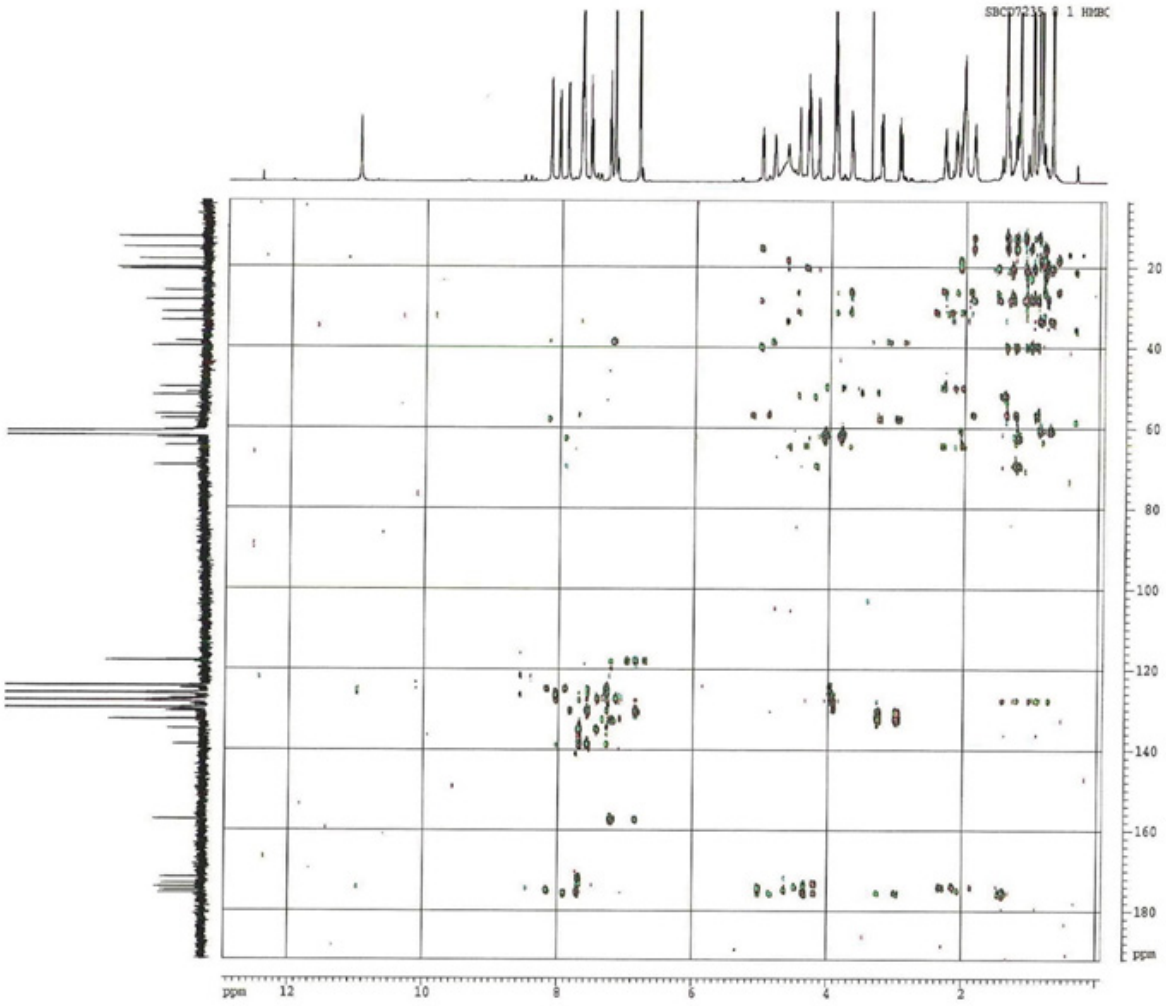

Current Data Parameters

NAME	SBCD7235
EXPNO	8
PROCNO	1

F1 - Acquisition parameters

ND0	2
TD	256
SFO1	150.8946 MHz
FIDRES	147.405655 Hz
SW	250.081 ppm

F2 - Processing parameters

SI	2048
SF	600.0296349 MHz
WDW	SINE
SSB	0
LB	0.00 Hz
GB	0
PC	1.00

F1 - Processing parameters

SI	1024
MC2	QF
SF	150.8772132 MHz
WDW	SINE
SSB	0
LB	0.00 Hz
GB	0

2D NMR plot parameters

CX2	20.00 cm
CX1	20.00 cm
F2PLO	12.947 ppm
F2LO	7768.60 Hz
F2PHI	-0.083 ppm
F2HI	-49.71 Hz
F1PLO	192.144 ppm
F1LO	28990.22 Hz
F1PHI	3.585 ppm
F1HI	540.93 Hz
F2PPMCM	0.65149 ppm/cm
F2HZCM	390.91565 Hz/cm
F1PPMCM	9.42796 ppm/cm
F1HZCM	1422.46472 Hz/cm

S 8. HMQC spectrum of talaromin A (**1**)

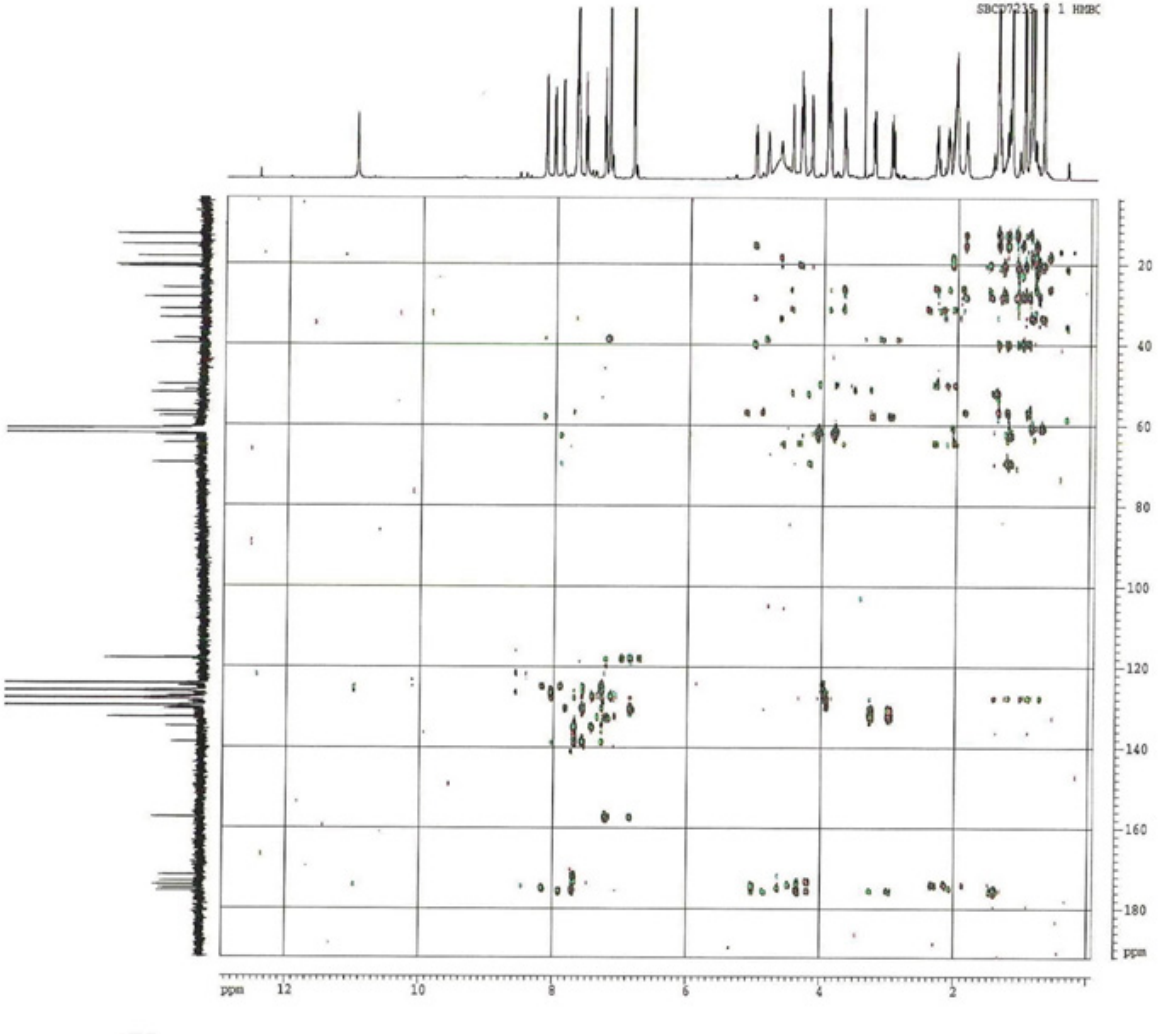

Current Data Parameters

NAME	SBCD7235
EXPNO	8
PROCNO	1

F1 - Acquisition parameters

ND0	2
TD	256
SFO1	150.8946 MHz
FIDRES	147.405655 Hz
SW	250.081 ppm

F2 - Processing parameters

SI	2048
SF	600.0296349 MHz
WDW	SINE
SSB	0
LB	0.00 Hz
GB	0
PC	1.00

F1 - Processing parameters

SI	1024
MC2	QF
SF	150.8772132 MHz
WDW	SINE
SSB	0
LB	0.00 Hz
GB	0

2D NMR plot parameters

CX2	20.00 cm
CX1	20.00 cm
F2PLO	12.947 ppm
F2LO	7768.60 Hz
F2PHI	-0.083 ppm
F2HI	-49.71 Hz
F1PLO	192.144 ppm
F1LO	28990.22 Hz
F1PHI	3.585 ppm
F1HI	540.93 Hz
F2PPMCM	0.65149 ppm/cm
F2HZCM	390.91565 Hz/cm
F1PPMCM	9.42796 ppm/cm
F1HZCM	1422.46472 Hz/cm

S 9. ^{1}H NMR spectrum of talaromin B (**2**) 600 MHz

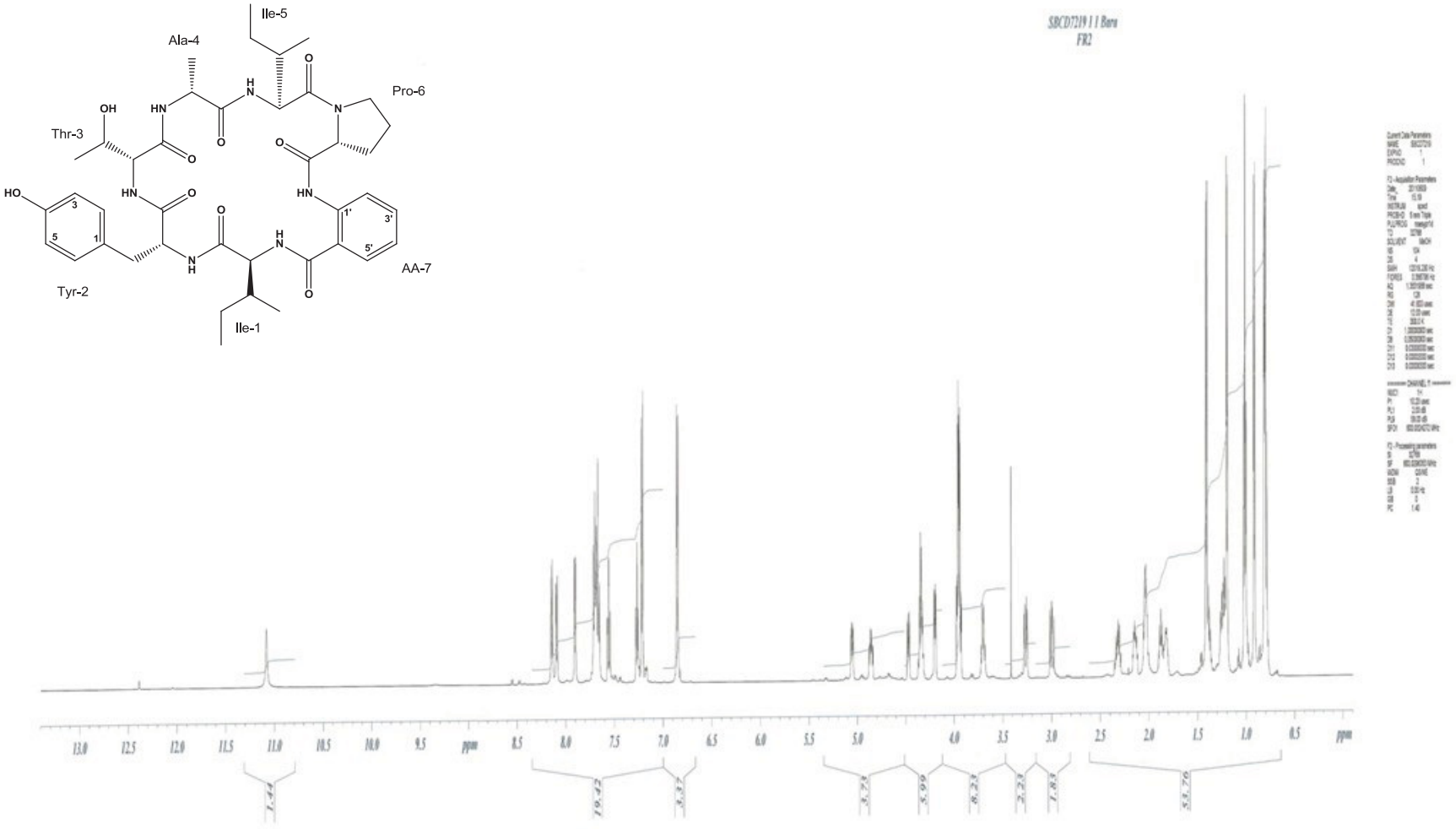

S 10. ^{13}C NMR spectrum of talaromin B (**2**) 150 MHz

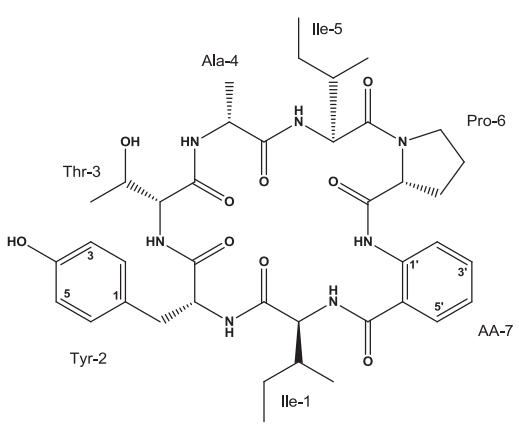


```
Current Data Parameters
NAME            SBCR7219
EXPNO                 21
PROCNO                 1

F2 - Acquisition Parameters
Date_              500000
Time                 9.44
INSTRUM           arx400
PROBHD     5 mm QNP  1H
PULPROG           zgpg30
TD                 32768
SOLVENT           Aceton
NS                384019
DS                     2
SWH            33333.332 Hz
FIDRES          1.017253 Hz
AQ              0.4915700 sec
RG                 32768
DW                15.000 usec
DE                21.43 usec
TE                300.0 K
D12            0.00002000 sec
DL6               18.00 dB
D1             1.00000000 sec
CPDPRG            waltz16
P31               100.00 usec
D11            0.03000000 sec
DL5               16.00 dB
P1                10.70 usec
DE                21.43 usec
SFO1       100.5726241 MHz
NUCLEUS             13C

F2 - Processing parameters
SI                 32768
SF         100.5596699 MHz
WDW                   EM
SSB                    0
LB                  2.00 Hz
GB                     0
PC                  1.40

1D NMR plot parameters
CX                30.00 cm
F1P              220.000 ppm
F1             22123.13 Hz
F2P                0.000 ppm
F2                 0.00 Hz
PPMCM           7.33333 ppm/cm
HZCM          737.43756 Hz/cm
```

S 11. DEPT spectrum of talaromin B (**2**) 150 MHz

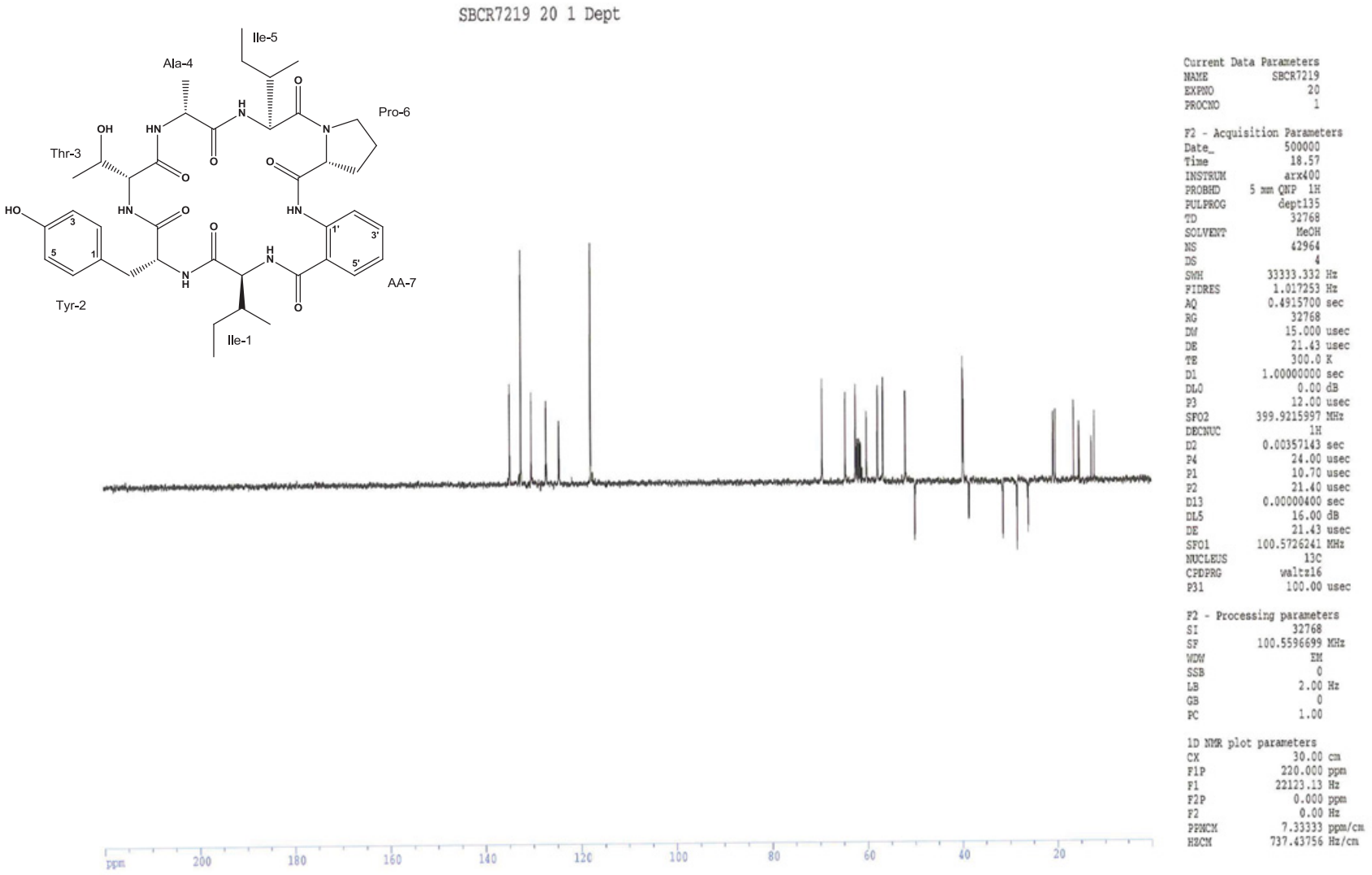

S 12. COSY spectrum of talaromin B (**2**)

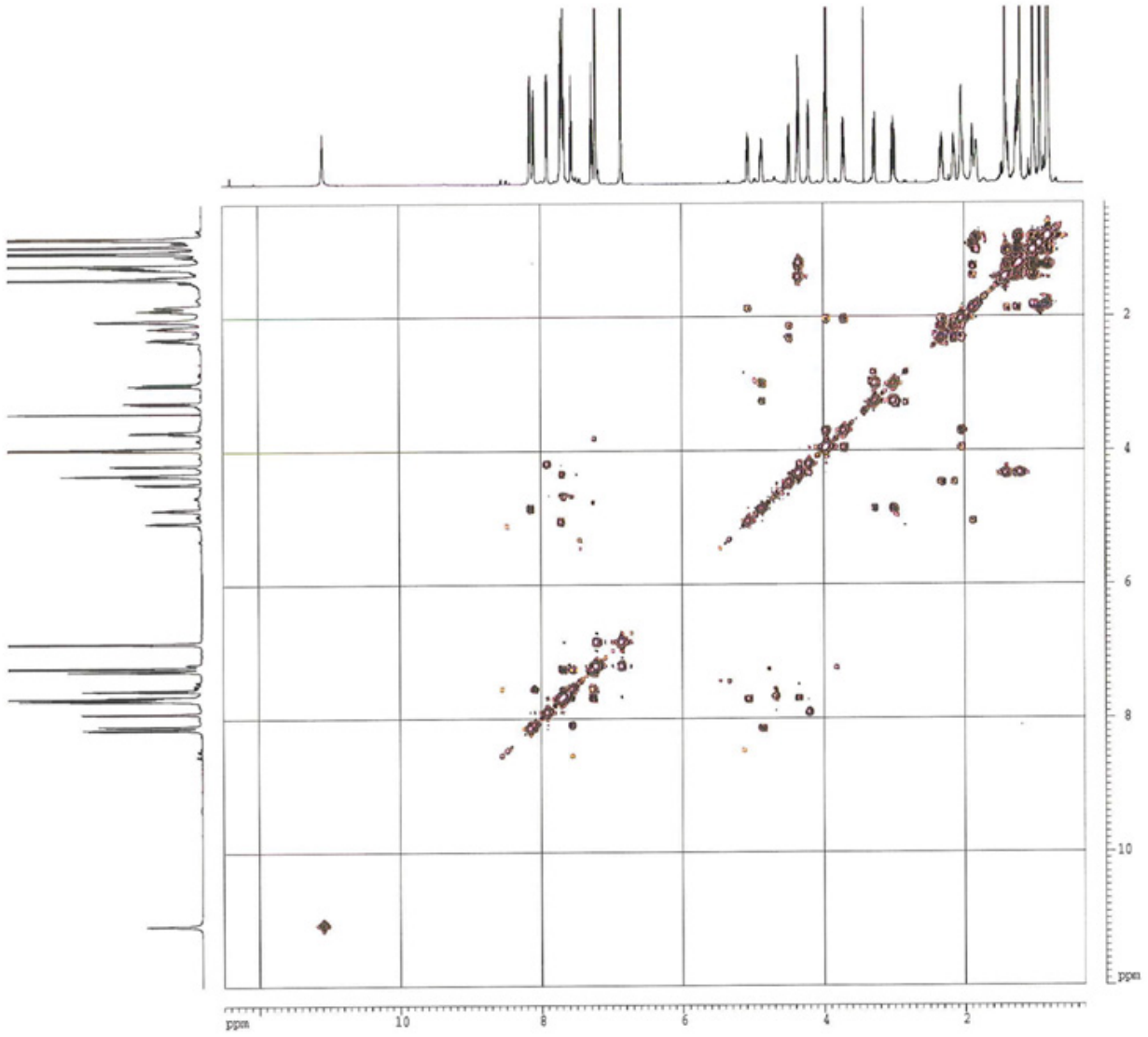

Current Data Parameters

NAME	SBCD7219
EXPNO	2
PROCNO	1

F1 - Acquisition parameters

ND0	1
TD	256
SFO1	600.0324 MHz
FIDRES	38.752480 Hz
SW	16.533 ppm

F2 - Processing parameters

SI	2048
SF	600.0296353 MHz
WDW	SINE
SSB	0
LB	0.00 Hz
GB	0
PC	1.40

F1 - Processing parameters

SI	1024
MC2	QF
SF	600.0296353 MHz
WDW	SINE
SSB	0
LB	0.00 Hz
GB	0

2D NMR plot parameters

CX2	20.00 cm
CX1	20.00 cm
F2PLO	12.500 ppm
F2LO	7500.37 Hz
F2PHI	0.300 ppm
F2HI	180.01 Hz
F1PLO	12.000 ppm
F1LO	7200.36 Hz
F1PHI	0.300 ppm
F1HI	180.01 Hz
F2PPMCM	0.61000 ppm/cm
F2HZCM	366.01813 Hz/cm
F1PPMCM	0.58500 ppm/cm
F1HZCM	351.01733 Hz/cm

S 13. TOCSY spectrum of talaromin B (**2**)

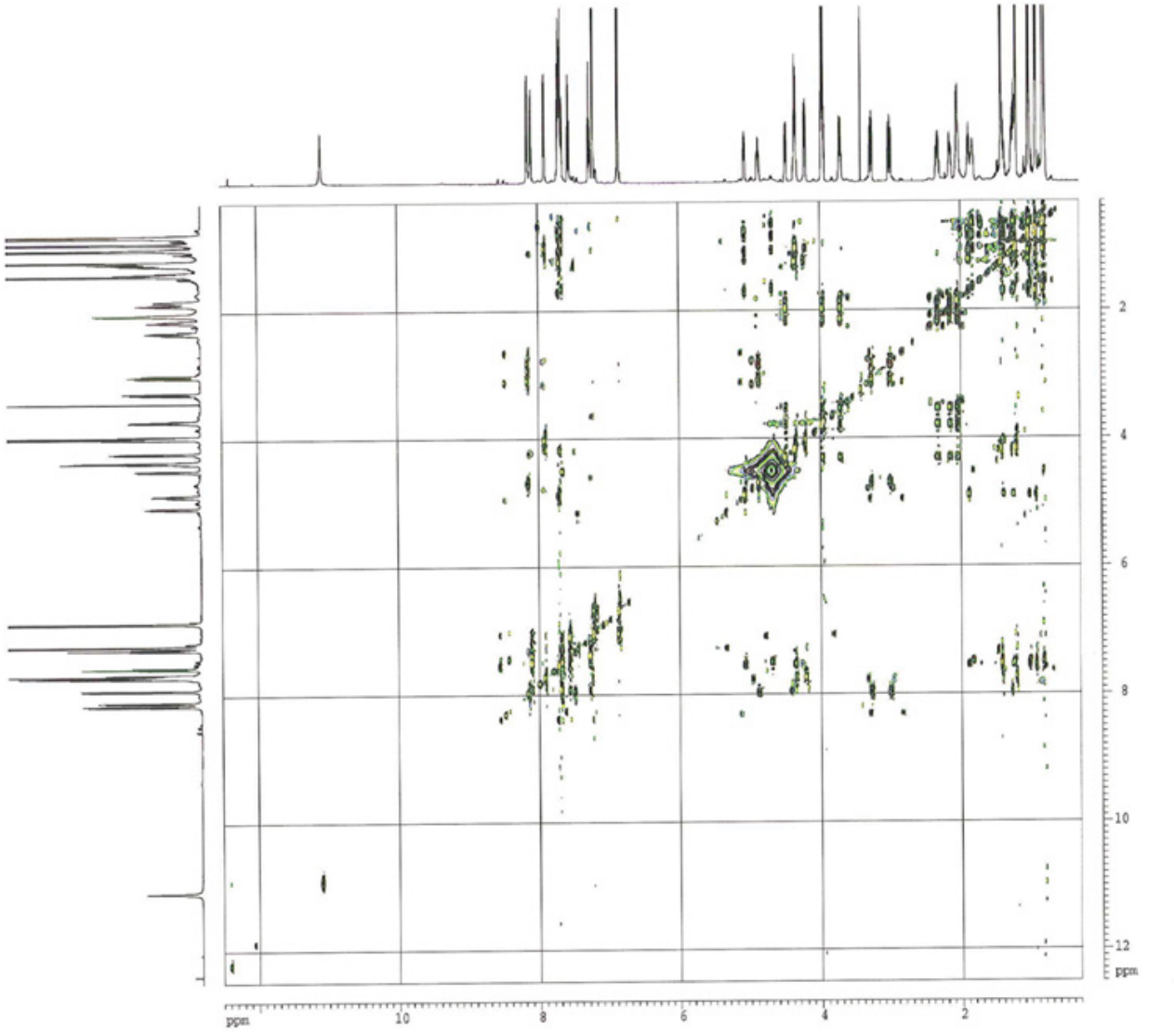

Current Data Parameters

NAME	SBCD7219
EXPNO	3
PROCNO	1

F1 - Acquisition parameters

ND0	2
TD	256
SFO1	600.0324 MHz
FIDRES	38.752480 Hz
SW	16.533 ppm

F2 - Processing parameters

SI	2048
SF	600.0296353 MHz
WDW	GM
SSB	0
LB	-13.00 Hz
GB	0.3
PC	1.40

F1 - Processing parameters

SI	1024
MC2	TPPI
SF	600.0297353 MHz
WDW	QSINE
SSB	2
LB	0.00 Hz
GB	0

2D NMR plot parameters

CX2	20.00 cm
CX1	20.00 cm
F2PLO	12.500 ppm
F2LO	7500.37 Hz
F2PHI	0.300 ppm
F2HI	180.01 Hz
F1PLO	12.500 ppm
F1LO	7500.37 Hz
F1PHI	0.300 ppm
F1HI	180.01 Hz
F2PPMCM	0.61000 ppm/cm
F2HZCM	366.01813 Hz/cm
F1PPMCM	0.61000 ppm/cm
F1HZCM	366.01816 Hz/cm

S 14. ROESY spectrum of talaromin B (**2**)

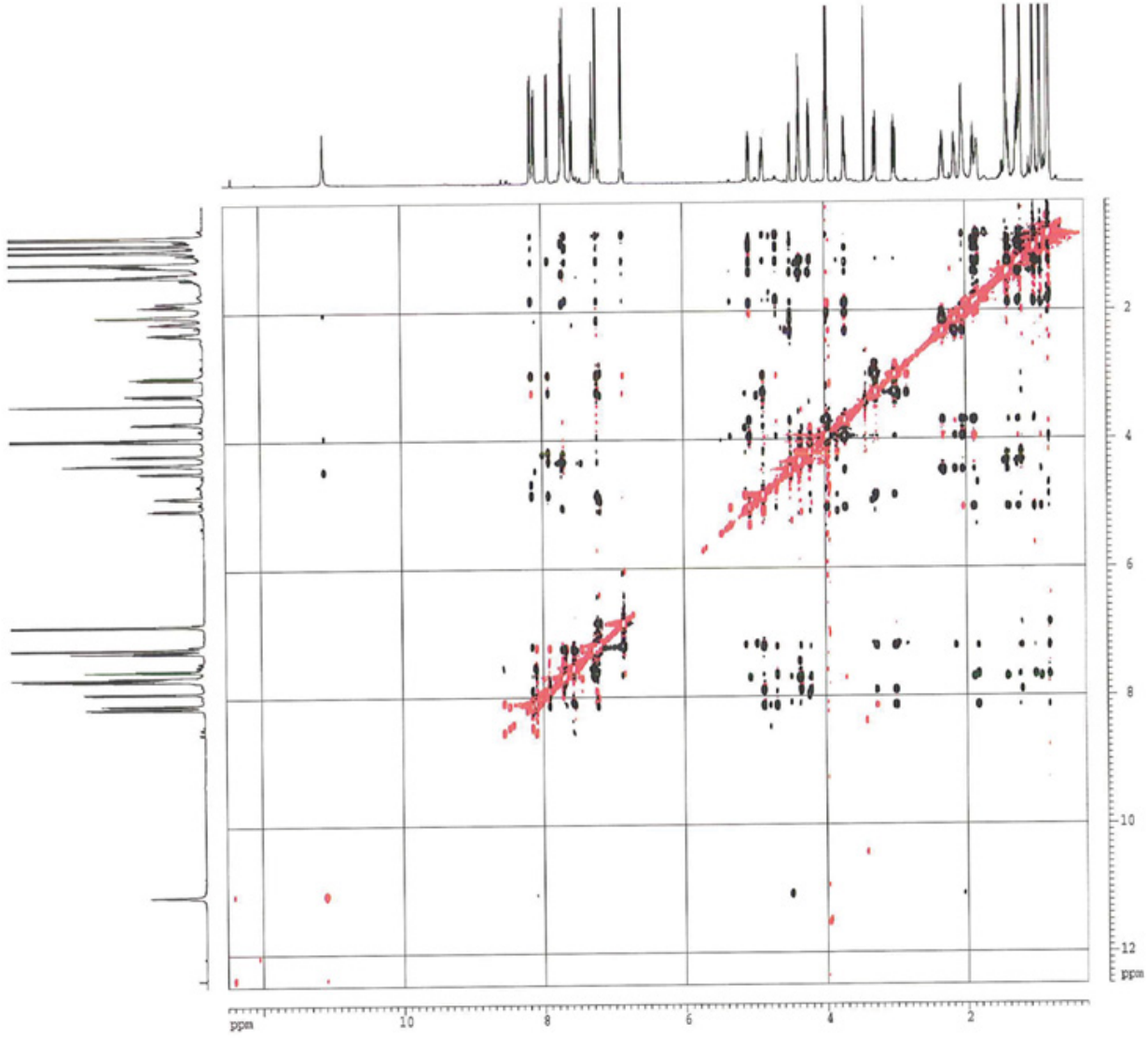

Current Data Parameters

NAME	SBCD7219
EXPNO	5
PROCNO	1

F1 - Acquisition parameters

ND0	1
TD	256
SFO1	600.0324 MHz
FIDRES	38.752480 Hz
SW	16.533 ppm

F2 - Processing parameters

SI	2048
SF	600.0296353 MHz
WDW	QSINE
SSB	2
LB	0.00 Hz
GB	0
PC	1.40

F1 - Processing parameters

SI	1024
MC2	States-TPPI
SF	600.0296353 MHz
WDW	QSINE
SSB	2
LB	0.00 Hz
GB	0

2D NMR plot parameters

CX2	20.00 cm
CX1	20.00 cm
F2PLO	12.500 ppm
F2LO	7500.37 Hz
F2PHI	0.300 ppm
F2HI	180.01 Hz
F1PLO	12.500 ppm
F1LO	7500.37 Hz
F1PHI	0.300 ppm
F1HI	180.01 Hz
F2PPMCM	0.61000 ppm/cm
F2HZCM	366.01813 Hz/cm
F1PPMCM	0.61000 ppm/cm
F1HZCM	366.01813 Hz/cm

S 15. HMBC spectrum of talaromin B (**2**)

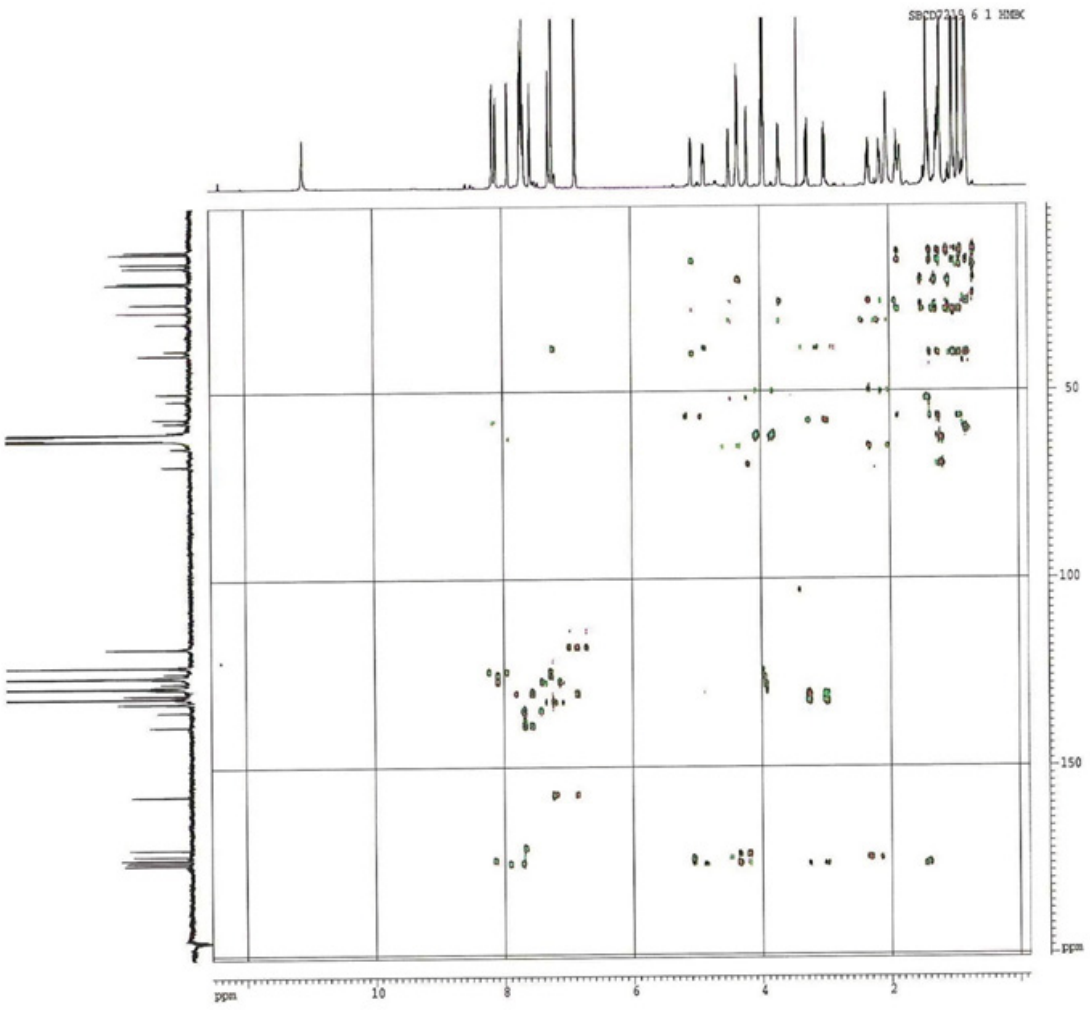


```
Current Data Parameters
NAME          SBCD7219
EXPNO                6
PROCNO               1

F1 - Acquisition parameters
ND0                  2
TD                 256
SFO1         150.8946 MHz
FIDRES     147.405655 Hz
SW           250.081 ppm

F2 - Processing parameters
SI                2048
SF        600.0296353 MHz
WDW               SINE
SSB                  0
LB                0.00 Hz
GB                   0
PC                1.00

F1 - Processing parameters
SI                1024
MC2                 QF
SF        150.8772104 MHz
WDW               SINE
SSB                  0
LB                0.00 Hz
GB                   0

2D NMR plot parameters
CX2              20.00 cm
CX1              20.00 cm
F2PLO            12.540 ppm
F2LO           7524.59 Hz
F2PHI            -0.150 ppm
F2HI             -90.28 Hz
F1PLO            200.956 ppm
F1LO           30319.66 Hz
F1PHI              0.673 ppm
F1HI             101.58 Hz
F2PPMCM          0.63454 ppm/cm
F2HZCM         380.74313 Hz/cm
F1PPMCM         10.01413 ppm/cm
F1HZCM        1510.90369 Hz/cm
```

S 16. HMQC spectrum of talaromin B (**2**)

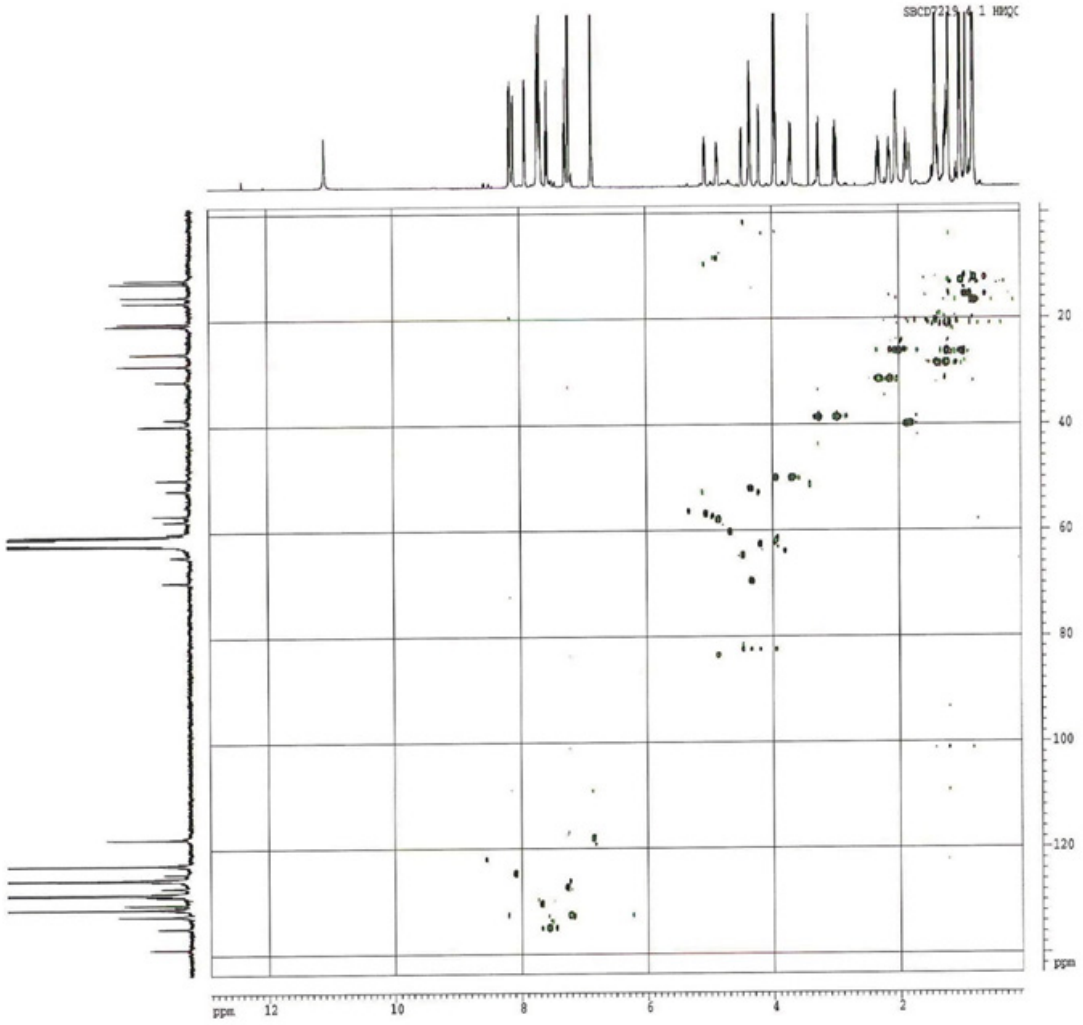


```
      Current Data Parameters
NAME          SBCD7219
EXPNO                4
PROCNO               1

      F1 - Acquisition parameters
ND0                  2
TD                 256
SFO1        150.8897 MHz
FIDRES      117.924530 Hz
SW          200.071 ppm

      F2 - Processing parameters
SI                2048
SF          600.0296353 MHz
WDW               QSINE
SSB                  3
LB                0.00 Hz
GB                   0
PC                1.40

      F1 - Processing parameters
SI                1024
MC2         States-TPPI
SF          150.8771981 MHz
WDW               QSINE
SSB                  3
LB                0.00 Hz
GB                   0

      2D NMR plot parameters
CX2              20.00 cm
CX1              20.00 cm
F2PLO            12.920 ppm
F2LO           7752.26 Hz
F2PHI            0.059 ppm
F2HI             35.67 Hz
F1PLO            143.758 ppm
F1LO           21689.83 Hz
F1PHI            -1.423 ppm
F1HI           -214.65 Hz
F2PPMCM          0.64302 ppm/cm
F2HZCM         385.82941 Hz/cm
F1PPMCM          7.25904 ppm/cm
F1HZCM        1095.22412 Hz/cm
```

References

Aly, A. H., Debbab, A., Clements, C., Edrada-Ebel, R., Orlikova, B., Diederich, M., Wray, V., Lin, W. and Proksch, P. NF kappa B inhibitors and antitrypanosomal metabolites from endophytic fungus Penicillium sp. isolated from Limonium tubiflorum. Bioorg Med Chem. **2011**. 19. 414-421.

Aly, A. H., Debbab, A. and Proksch, P. Fungal endophytes: unique plant inhabitants with great promises. Appl Microbiol Biotechnol. **2011**. 90. 1829-1845.

Ashour, M., Edrada, R., Ebel, R., Wray, V., Watjen, W., Padmakumar, K., Muller, W. E., Lin, W. H. and Proksch, P. Kahalalide derivatives from the Indian sacoglossan mollusk Elysia grandifolia. J Nat Prod. **2006**. 69. 1547-53.

Burkholder, P. R. and Giles, N. H., Jr. Induced biochemical mutations in Bacillus subtilis. Am J Bot. **1947**. 34. 345-8.

Carmichael, J., Mitchell, J. B., DeGraff, W. G., Gamson, J., Gazdar, A. F., Johnson, B. E., Glatstein, E. and Minna, J. D. Chemosensitivity testing of human lung cancer cell lines using the MTT assay. Br J Cancer. **1988**.57(6): 540-7.

Carroll, G. Fungal endophytes in stems and leaves: from latent pathogen to mutualistic symbiont. Ecology. **1988**. 69. 2-9.

Clay, K. Fungal endophytes of grasses: a defensive mutualism between plants and fungi. Ecology. **1988**. 69. 10-16.

CLSI, M.-A. Methods for dilution antimicrobial susceptibility tests for bacteria that grow aerobically. Approved standard. **2008**. Clinical and Laboratory Standards Institute.

Debbab, A., Aly, A. and Proksch, P. Bioactive secondary metabolites from endophytes and associated marine derived fungi. Fungal Divers. **2011**. 49. 1-12.

Debbab, A., Aly, A. and Proksch, P. Endophytes and associated marine derived fungi-ecological and chemical perspectives. Fungal Divers. **2012**. 57. 45-83.

Debbab, A., Aly, A. H., Edrada-Ebel, R., Wray, V., Müller, W. E. G., Totzke, F., Zirrgiebel, U., Schälchtele, C., Kubbutat, M. H. G., Lin, W. H., Mosaddak, M., Hakiki, A., Proksch, P. and Ebel, R. Bioactive metabolites from the endophytic fungus Stemphylium globuliferum isolated from Mentha pulegium. J Nat Prod. **2009**. 72. 626-631.

Debbab, A., Aly, A. H., Edrada-Ebel, R., Wray, V., Pretsch, A., Pescitelli, G., Kurtan, T. and Proksch, P. New Anthracene Derivatives – Structure Elucidation and Antimicrobial Activity. Eur J Org Chem. **2012.** 1351-1359.

Ebrahim, W., Aly, A. H., Mándi, A., Totzke, F., Kubbutat, M. H. G., Wray, V., Lin, W.-H., Dai, H., Proksch, P., Kurtán, T. and Debbab, A. Decalactone derivatives from Corynespora cassiicola, an endophytic fungus of the mangrove plant Laguncularia racemosa. Eur J Org Chem. **2012**. 3476-3484.

Frisvad, J. C., Filtenborg, O., Samson, R. A. and Stolk, A. C. Chemotaxonomy of the genus Talaromyces. Antonie van Leeuwenhoek. **1990**. 57. 179-189.

Henrichfreise, B., Wiegand, I., Sherwood, K. J. and Wiedemann, B. Detection of VIM-2 metallo-beta-lactamase in Pseudomonas aeruginosa from Germany. Antimicrob Agents Chemother. **2005**, 49. 1668-9.

Hiramatsu, K., Hanaki, H., Ino, T., Yabuta, K., Oguri, T. and Tenover, F. C. Methicillin-resistant Staphylococcus aureus clinical. strain with reduced vancomycin susceptibility. J Antimicrob Chemother. **1997**. 40. 135-6.

Klare, I., Heier, H., Claus, H., Bohme, G., Marin, S., Seltmann, G., Hakenbeck, R., Antanassova, V. and Witte, W. Enterococcus faecium strains with vanA-mediated high-level

glycopeptide resistance isolated from animal foodstuffs and fecal samples of humans in the community. Microb Drug Resist. **1995**. 1. 265-72.

Liu, F., Cai, X.-L., Yang, H., Xia, X.-K., Guo, Z.-Y., Yuan, J., Li, M.-F., She, Z.-G. and Lin, Y.-C. The bioactive metabolites of the mangrove endophytic fungus Talaromyces sp. ZH-154 isolated from Kandelia candel (L.) Druce. Planta Med. **2010**. 76. 185-189.

Liu, F., Li, Q., Yang, H., Cai, X.-L., Xia, X.-K., Chen, S.-P., Li, M.-F., She, Z.-G. and Lin, Y.-C. Structure elucidation of three diphenyl ether derivatives from the mangrove endophytic fungus SBE-14 from the South China Sea. Magn Reson Chem. **2009**. 47. 453-455.

Marfey, P. Determination ofD-amino acids. II. Use of a bifunctional reagent, 1,5-difluoro-2,4-dinitrobenzene. Carlsberg Research Communications. **1984**. 49. 591-596.

Schulz, B. and Boyle, C. What are Endophytes? Microbial Root Endophytes.**2006**. 1-13.

Shiozawa, H., Takahashi, M., Takatsu, T., Kinoshita, T., Tanzawa, K., Hosoya, T., Furuya, K., Takahashi, S., Furihata, K. and Seto, H. Trachyspic acid, a new metabolite produced by Talaromyces trachyspermus, that inhibits tumor cell heparanase: taxonomy of the producing strain, fermentation, isolation, structural elucidation, and biological activity. J Antibiot (Tokyo). **1995**. 48. 357-62.

Strobel, G., Daisy, B., Castillo, U. and Harper, J. Natural Products from endophytic microorganisms. J Nat Prod. **2004**, 67. 257-268.

Wakelin, S., Warren, R., Harvey, P. and Ryder, M. Phosphate solubilization by Penicillium spp. closely associated with wheat roots. Biol. Fert. Soils. **2004**. 40. 36-43.

Wang, S., Li, X.-M., Teuscher, F., Li, Diesel, A., Ebel, R., Proksch, P. and Wang, B.-G. Chaetopyranin, a benzaldehyde derivative, and other related metabolites from Chaetomium globosum, an endophytic fungus derived from the marine red alga Polysiphonia urceolata. J Nat Prod. **2006.** 69. 1622-1625.

Yuesheng, D., Jie, L., Xinhua, L., Zhihui, Z., Xiao, R., Hua, Z., Jiangong, H. and Junshan, Y. Cathepsin B inhibitory tetraene lactones from the fungus Talaromyces wortmannii. Helv. Chim. Acta. **2009**. 92. 567-574.

= Chapter 5 =

General Discussion

Within the last three decades, endophytic fungi have gained tremendous importance in the field of drug discovery and development, as both producers and as sustainable sources of unique and diverse bioactive compounds which can be used as powerful drugs in order to combat major global diseases (Strobel and Daisy 2003; Aly *et al.* 2011; Núñez-Trujillo *et al.* 2012).

However, large yields of selected bioactive compounds are needed for preclinical and clinical trials and their concentrations in the endophytes are often very low. For example, the concentration of flavomannin B (**2**) which is the most active antibiotic metabolite of *Talaromyces wortmannii* – encountered in this study – is only one tenth of that of the less active flavomannin A (**1**). Thus, methods must be developed in order to enhance the production of such interesting and potent compounds. At first one needs to gain knowledge on biosynthetic pathways which includes factors that can induce or alter production of metabolites

It is generally assumed that endophytes serve their host by secreting compounds to combat pathogenic intruders (Carroll 1988; Clay 1988), to compete for space with other organisms, or to prevent fouling by other organisms as it is usually seen in algae. Living in a highly competitive environment such as the tropical rainforest ultimately results in high frequencies of toxic or deterrent metabolites. For instance, the chemical deterrence was found to be significantly higher for an extract of endophytic fungi obtained from a tropical rainforest area as compared to a temperate area (Strobel and Daisy 2003). Predation pressure, threat of diseases and space competition thus increases investment into chemical defense.

There are several examples that support the theory of a possible induction of metabolite production. For example, adding epigenetic modifier compounds or plant-derived metabolites can trigger silent biosynthetic pathways within the investigated fungi. Co-

cultivation of two endophytic fungi or different growth media can also induce metabolite productions.

Growth media

Endophytic fungi are a group of eukaryotic spore bearing, achlorophyllous organisms that generally reproduce asexually and sexually. Due to their competitive ability expressed by fast mycelia growth, spores production and presence of efficient and extensive systems of powerful enzymes fungi are able to utilise complex polysaccharides and proteins as carbon and nitrogen sources. A culture medium is defined as any material in which microorganisms find nourishment and can reproduce themselves. Therefore, for a microbiological medium to fulfill its specific purpose, it must contain all substances and compounds which are necessary for the organism to grow and to reproduce. Therefore an optimal medium must contain sufficient amounts of nitrogen and carbon sources as well as vitamins and dietary minerals. Already minor changes in the composition of the culture medium can negatively affect the growth of the fungus. Hence, an optimal nutrient medium should not only provide adequate growth, but the best possible growth in order to allow fungi to grow without restriction. The dramatic effect of changing of growth media with regard to metabolite production became visible in this thesis when *T. wortmannii* was grown on white beans instead of rice. Whereas dimeric anthraquinones and hydroanthraquinones (flavomannins and talaromannins) were the major compounds produced on rice medium, the bean medium provoked the production of peptides talaromins as dominant compounds instead.

Co-cultivation experiments

Rediscovery of known secondary metabolites is a constant problem in natural products chemistry suggesting that new approaches must be adopted to induce production of novel compounds or at least enhance the production of minor compounds. Another cultivation method which has been explored in the attempt to access silent biosynthetic pathways (SBP) is based on the fact that fungi naturally live in complex communities which involve a wide range of chemical interactions. It has been proposed that cohabitating microorganisms might serve as a signal for the production of natural products. Consequently, it was thought

that agents capable of triggering SBP production might include a variety of undefined signaling molecules making co-culture a highly promising approach for natural product discovery.

Several co-cultivation approaches have been reported (Bigelis *et al.* 2006; Oh *et al.* 2007; Pettit 2009; Pettit *et al.* 2010). For instance, cultivation of the cyanobacterium *Scytomena ocellatum*, with added elicitors, such as fungal wall polysaccharides, increased the production of the previously known metabolite tolytoxin (Patterson and Bolis 1997). Another example is the production of new analogues of the well-known chaetoglobosins (Christian *et al.* 2005) by the marine-derived fungus *Phomopsis asparagi*, when cultured in the presence of the sponge metabolite jasplakinolide. Co-culture experiments with the fungus *Libertella* sp. and the bacterial strain used in the previously mentioned pestalone case induced the production of new cytotoxic diterpenoids, which are not produced in either microorganism in single cultivation (Pettit 2009). Given that microbes interact with each other in the natural habitat and that these interactions are, debatably, the leading force to produce required secondary metabolites, simulating microbial habitats by cultivating two different microbial strains in one culture vessel seems to be an effective way to produce new active compounds.

Epigenetic modifier experiments

Epigenetics is defined as heritable changes in gene activity and expression that occur without alteration in DNA sequence. It is known that these non-genetic alternations are tightly regulated by two major epigenetic modifications: chemical modifications of the cytosine residues of DNA (DNA methylation) and histone proteins associated with DNA (histone modifications). In this case, the use of small molecule epigenetic modifying agents which inhibit histone deacetylase and DNA methyltranferase/histone methyltransferase functions will lead to the transcriptional up regulation of SBPs resulting in the production of novel secondary metabolites.

It has been recognized that under standard laboratory conditions most microbial biosynthetic gene clusters are either silent or expressed at very low levels. The culture manipulation of fungi in the presence of DNA methyltransferase and/or HDAC inhibitors led

to the enhanced expression of biosynthetic pathways and further production of new secondary metabolites.

Williams *et al* (2008), demonstrated that eleven of the studied endophytic fungi were responsive to one or more epigenetic treatments based on the production of new natural products and/or enhanced accumulation of constitutive secondary metabolites. Exposure of selected *Aspergillus, Cladosporium, Clonostachys, Diatrype* and *Penicillium* species to added elicitors confirmed that many of the new natural products were exclusively obtained following the use of epigenetic modifying treatments. Furthermore, introduction of epigenetic modifiers e. g. sodium butyrate, suberohydroxamic acid, valproic acid and hydralazine, into the culture of *Nigrospora sphaeritica* induces the production of additional compounds in comparison to the culture without epigenetic modifiers (Lopes *et al.* 2012).

The success of inducing the production of new natural products from fungi by administering small-molecule epigenetic modifiers indicates that this technique is a very promising and rational approach for the native expression of silent biosynthetic pathways. This method has several significant benefits : first, it provides a needed tool for fast accessing potential pools of cryptic fungal natural products in their native hosts. Second, this methodology can be readily implemented in most labs without extensive retooling, giving it a wide scope of utilization. Third, this approach will significantly reduce the cost and effort of acquiring the products of silent secondary metabolic pathways since fungi do not need to be pre-screened using a multitude of culture conditions.

It then seems that in the future both co-cultivation experiments and studies with epigenetic modifiers can enhance the chemical diversity of *T. wortmannii* giving rise to a broaden and structurally more diverse pattern of bioactive natural products.

References

Aly, A. H., Debbab, A. and Proksch, P. (2011). Fungal endophytes: unique plant inhabitants with great promises. Applied Microbiology and Biotechnology 90(6): 1829-1845.

Bigelis, R., He, H., Yang, H. Y., Chang, L. P. and Greenstein, M. (2006). Production of fungal antibiotics using polymeric solid supports in solid-state and liquid fermentation. J Ind Microbiol Biotechnol 33(10): 815-26.

Carroll, G. (1988). Fungal endophytes in stems and leaves: from latent pathogen to mutualistic symbiont. Ecology 69(1): 2-9.

Christian, O. E., Compton, J., Christian, K. R., Mooberry, S. L., Valeriote, F. A. and Crews, P. (2005). Using jasplakinolide to turn on pathways that enable the isolation of new chaetoglobosins from Phomospis asparagi. Journal of Natural Products 68(11): 1592-1597.

Clay, K. (1988). Fungal endophytes of grasses: a defensive mutualism between plants and fungi. Ecology 69(1): 10-16.

Lopes, A. A., da Silva, D. B., Lopes, N. P. and Pupo, M. T. (2012). Epigenetic modulation changed the secondary metabolite profile in the endophyte Nigrospora sphaerica SS67. Planta Med 78(14): PL38.

Núñez-Trujillo, G., Cabrera, R., Burgos-Reyes, R. L., Da Silva, E., Giménez, C., Cosoveanu, A. and Brito, N. (2012). Endophytic fungi from Vitis vinifera L. isolated in Canary Islands and Azores as potential biocontrol agents of Botrytis cinerea Pers. Journal of Horticulture, Forestry and Biotechnology 16(1): 1-6.

Oh, D.-C., Kauffman, C. A., Jensen, P. R. and Fenical, W. (2007). Induced production of emericellamides A and B from the marine-derived fungus Emericella sp. in competing co-culture. Journal of Natural Products 70(4): 515-520.

Patterson, G. M. L. and Bolis, C. M. (1997). Fungal cellwall polysaccharides elicit an antifungal secondary metabolite (phytoalexin) in the cyanobacterium Scytonema ocelutum. Journal of Phycology 33(1): 54-60.

Pettit, R. K. (2009). Mixed fermentation for natural product drug discovery. Appl Microbiol Biotechnol 83(1): 19-25.

Pettit, R. K., Pettit, G. R., Xu, J. P., Weber, C. A. and Richert, L. A. (2010). Isolation of human cancer cell growth inhibitory, antimicrobial lateritin from a mixed fungal culture. Planta Med 76(5): 500-1.

Strobel, G. and Daisy, B. (2003). Bioprospecting for microbial endophytes and their natural products. Microbiol. Mol. Biol. Rev. 67(4): 491-502.

Williams, R. B., Henrikson, J. C., Hoover, A. R., Lee, A. E. and Cichewicz, R. H. (2008). Epigenetic remodeling of the fungal secondary metabolome. Org Biomol Chem 6(11): 1895-7.

Summary

Mutualistic associations between host plants and their particular endosymbionts were found to confer a variety of benefits to both partners, such as, the production of bioactive secondary metabolites by the microbial partner which is involved in host plant protection against insects and parasites thereby representing an acquired chemical defense mechanism of the host. However, endophytic microorganisms represent not only a vast reservoir of novel natural products involved in chemical ecology but offer also opportunities for exploitation in medicine, agriculture and industry.

In chapter two, six new bisdihydroantracene atropisomers are described. Five of them are new natural products named as flavomannins B-D (**2**-**4**) and talaromannins A (**5**) and B (**6**), together with a known compound flavomannin A (**1**). Their structures were determined on the basis of spectroscopic methods including 1D (^{1}H, ^{13}C and DEPT) and 2D (COSY, HMQC, HMBC, ROESY) NMR experiments and by mass spectroscopic measurements data. The absolute stereochemistry of Flavomannin A (**1**) and B (**2**) was studied by solution ECD measurements. The ECD spectrum of Flavomannin A (**1**) was dominated by a positive exciton couplet centered around 277 nm, while Flavomannin B (**2**) showed the other way around as it recorded as a negative exciton couplet. Besides these opposite couplets, their ECD spectra showed also near mirror image relationship suggesting that they are diastereomeric homodimers with different axial chirality and identical central chirality. These types of atropisomers are really interesting for further studies since they have not only interesting type of structures but also their activity against pathogenic bacteria, including broad-spectrum antibacterial activity against multi-resistant clinical isolates of pathogenic bacteria including *Staphylococcus aureus* and *Pseudomonas aeruginosa*, Noteworthy, the compounds showed no activity when tested against eukaryotic THP-1 cells (leukemia cell line) and BALB cells (mouse embryonic fibroblasts), with IC_{50} value for both cell lines was >32 µg/ml, indicating that the flavomannins and talaromannins displayed specificity for prokaryotes in the concentration range tested, making those putative new starting points for antibacterial drug development.

For orienting studies on the mode of action of the flavomannins and talaromannins, *B. subtilis* was chosen as a model organism, reporter gene assays were performed using *B. subtilis* strains that carry the firefly luciferase or β-galactosidase reporter gene fused to six different antibiotic-inducible promoters. Response of the biomarkers *yor*B, *hel*D, *bmr*C, *lia*I and *rec*A in the presence of increasing concentrations of flavomannin A-D (**1**-**4**) and talaromannin A (**5**) and B (**6**). Flavomannin B, D and talaromannin B specifically induced the *yor*B and the *rec*A promotor. Flavomannin B showed the strongest induction, followed by flavomannin D and talaromannin B in decreasing order. Furthermore, analysis of an effect of flavomannin B (**2**) on the cell morphology and chromosomal organization of *B. subtilis* 168 trpC2 resulted in filamentation of *B. subtilis*, indicating cell division inhibition and defects in nucleoid segregation.

In chapter three, one atropisomer named biemodin and three wortmannin derivatives, including one new wortmannin B and two new as natural product, in addition to eight known compounds including wortmannin A, wortmin, skyrin, oxyskyrin, emodic acid, rugulosin A and B. Their structures were determined on the basis of NMR spectroscopic methods including 1D (^{1}H, ^{13}C and DEPT) and 2D (COSY, HMQC, HMBC and ROESY) and by mass spectrometry data (ESI and HRESI-MS). The axial chirality of biemodin was determined by CD experiment. When tested against pathogenic bacteria, only biemodin, skyrin and rugulosin A showed strong inhibition, especially against gram positive bacteria with MIC values ranging between 4 and 16 μg/mL.

In chapter four, other interesting isolated compound from *T. wortmanni* are 2 cyclic peptides named Talaromin A and B. The absolute of their amino acids content within the peptides were determined by using Marfrey's Methods. Both compounds were cyclic peptides containing a ring system with 6 amino acids linked to anthranilic acid. In chapter four, two other compounds from *T. wortmanni* which are two cyclic peptides named Talaromarin A and B containing six amino acids are presented. The absolute configuration of their amino acids was determined by using Marfrey's Methods. Both compounds are cyclic peptides containing a ring system with 6 amino acids linked to anthranilic acid. The only difference of both peptides is the exchange of D-Val in one compound for D-Ile in the second peptide. Even though no biological activities have been recorded so far for both

peptides after they have been tested against pathogenic bacteria as well as against the mouse lymphoma cell line (L5178Y), both represent new structures and are still interesting for further studies.

In chapter five, a comprehensive overview and a future prospect on enhancing the production of secondary metabolites compounds and inducing silent biosynthetic pathways within the investigated fungi were explained. This can be achieved by adding epigenetic modifier compounds, co-cultivation between endophytic fungi or/and with bacteria as well as utilizing different diets.

Zusammenfassung

Die Natur hat die Menschheit seit jeher mit einer großen und strukturell diversen Vielfalt pharmakologisch aktiver Verbindungen versorgt, die im Weiteren genutzt werden als hoch effektive Arzneistoffe im Kampf gegen eine Vielzahl tödlicher Krankheiten oder als Leitstrukturen für die Entwicklung neuer synthetisch generierter Arzneistoffe, die als Spiegelbilder ihrer natürlichen Vorbilder dienen. Wechselseitige Vergesellschaftungen zwischen einer Wirtspflanze und ihren bestimmten Endosymbionten gewähren nachweislich eine Vielzahl an Vorteilen für beide Partner, wie beispielsweise die Produktion an bioaktiven Sekundärmetaboliten durch den mikrobiellen Partner, welche zum Schutz der Wirtspflanze gegenüber Insekten und Parasiten beiträgt und dadurch einen erworbenen chemischen Verteidigungsmechanismus darstellt. Wie auch immer repräsentieren endophytische Mikroorganismen nicht nur ein enormes Reservoir neuer Naturstoffe mit Einfluß auf die chemische Ökologie, sondern bieten auch Möglichkeiten für die Verwendung in Medizin, Agrikultur und Industrie. In Anbetracht der Existenz von schätzungsweise 300.000 verschiedenen Arten hoher Pflanzen, jede als potentieller Wirt für ein oder mehr Endophyten, ist ein großer Pool an Pilzspezien und ihren bioaktiven Inhaltsstoffen in den kommenden Jahren zu entdecken.

In Kapitel zwei werden die fünf neuen Bisdihydroantracen-Atropisomere Flavomannine B-D (**2-4**) und Talaromannins A (**5**) und B (**6**) beschrieben, die zusammen mit dem bereits bekanten Flavomannin A (**1**) aus dem endophytischen Pilz *Talaromyces wortmannii* isoliert wurden. Die Ihre Strukturen wurden mithilfe verschiedener spektroskopischer Methoden wie 1D (^{1}H, ^{13}C and DEPT) und 2D (COSY, HMQC, HMBC, ROESY) NMR Experimenten und Massenspektrometrie aufgeklärt. Die absolute Konfiguration von Flavomannin A (**1**) und (**B**) wurde mittels ECD Messungen untersucht. Das ECD Spektrum von Flavomannin A (**1**) wurde geprägt von einem positiven Exziton-Couplet um 277 nm, wohingegen Flavomannin B (**2**) im Gegensatz dazu ein negatives Exziton-Couplet zeigt. Neben den gegensätzlichen Couplets bildeten die beiden ECD Spektren nahezu ein spiegelbildliches Verhältnis, was indiziert, dass es sich hier um diastereomere Homodimere mit unterschiedlicher axialer, aber identischer zentraler Chiralität handelt. Diese Formen von Atropisomeren sind sehr interessant für

weitergehende Studien, da sie nicht nur strukturell von hohem Interesse sind, sondern auch aufgrund ihrer Aktivität gegen pathogene Bakterien, einschließlich breiter antibakterieller Aktivität gegen multi-resistente klinische Isolate pathogener Bakterien wie *Staphylococcus aureus* and *Pseudomonas aeruginosa*. Nennenswert ist weiterhin, dass die Verbindungen im Test gegen eukaryotische THP-1 (leukämische Zelllinie) und BALB Zellen (murine embryonische Fibroblasten) mit IC_{50} Werten für beide Zelllinien von >32 μg/ml keine Aktivität zeigten, was besagt, dass Flavomannine und Talaromannine Spezifität für Prokaryoten im getesteten Konzentrationsbereich zeigen und somit mutmaßliche neue Ansatzpunkte für die Entwicklung neuer antibakterieller Arzneistoffe darstellen.

Für Orientierungsstudien zum Wirkmechanismus der Flavomannine und Talaromannine wurde *B. subtilis* als Modelorganismus ausgewählt und Reportergen Assays wurden mit *B. subtilis* Stämmen durchgeführt, die das Leuchtkäfer Luciferase- oder β-Galactosidase Reportergen gebunden an sechs verschiedene Antibiotika-induzierbare Promotoren tragen. Ein Ansprechen auf die Biomarker *yor*B, *hel*D, *bmr*C, *lia*I and *rec*A in Gegenwart von steigenden Konzentrationen an Flavomannin A-D (**1**-**4**) und Talaromannin A (**5**) und B (**6**) wurde registriert. Flavomannin B, D, und Talaromannin B induzierten besonders die *yor*B und *rec*A Promotoren. Flavomannin B zeigte die stärkste Induktion, gefolgt von Flavomannin D und Talaromannin B in abfallender Reihenfolge. Im Weiteren führte eine Analyse des Effektes von Flavomannin B (**2**) auf die Zell Morphologie und die chromosomale Organisation von *B. subtilis* 168 trpC2 zu einer Filamentation von *B. subtilis*, was auf eine Hemmung der Zellteilung und Defekte in der Nucleosid-Segregation hindeutet.

In Kapitel drei werden Biemodin und drei neue Wortmanninderivate Wortmannin B, C und D, wobei von letzteren beiden bereits synthetische Verbindungen existieren, beschrieben, die zusammen mit den sieben bekannten Verbindungen Wortmannin A, Wortmin, Skyrin, Oxyskyrin, Emodinsäure, Rugulosin A und B isoliert wurden. Ihre Strukturen wurden auf der Grundlage der NMR-spektroskopischen Methoden einschließlich 1D (^{1}H, ^{13}C und DEPT) und 2D (COSY, HMQC, HMBC und ROESY) und Massenspektrometrie-Daten (ESI und HRESI-MS) aufgeklärt. Die axiale Chiralität von Biemodin wurde durch CD-Spektroskopie bestimmt. In einem Bioaktivitätsassay gegen pathogene Bakterienstämme zeigten nur Biemodin, Skyrin und Rugulosin A, vor allem gegen gram-positive Bakterien mit MHK-Werten zwischen 4 und 16 μg /mL.

In Kapitel vier sind zwei weitere interessante Verbindungen aus *T. wortmanni* aufgeführt: Talaromin A und B. Es handelt sich um zyklische Peptide, die aus jeweils sechs Aminosäuren und einer peptidisch gebundenen Anthranilsäure bestehen. Die absolute Konfiguration der Aminosäuren wurde mittels der Methode nach Marfey bestimmt. Talaromin A unterscheidet sich nur von Talaromin B durch einen Austausch von D-Val gegen D-Ile. Auch wenn bisher keine biologischen Aktivitäten für beide Peptide verzeichnet wurden, nachdem sie sowohl gegen pathogene Bakterien wie auch gegen murine Lymphomzellen (L5178Y) getestet wurden, sind beide dennoch interessant für weitere Bioaktivitätsstudien.

In Kapitel fünf werden eine umfassende Übersicht und Zukunftsperspektiven dargestellt, wie man die Produktion von sekundären Metaboliten Verbindungen erhöhen und „stille“ Biosynthesewege innerhalb der zu untersuchenden Pilze induzieren kann. Dies kann durch die Zugabe von „epigenetic modifiers“, Co-Kultivierung von mehreren endophytischen Pilzen miteinander oder mit Bakterien oder auch durch Verwendung verschiedener Nährmedien erreicht werden.

= Appendices =

Aloe vera sampling point in Alexandria, Egypt (red arrow);©googlemaps[tm]

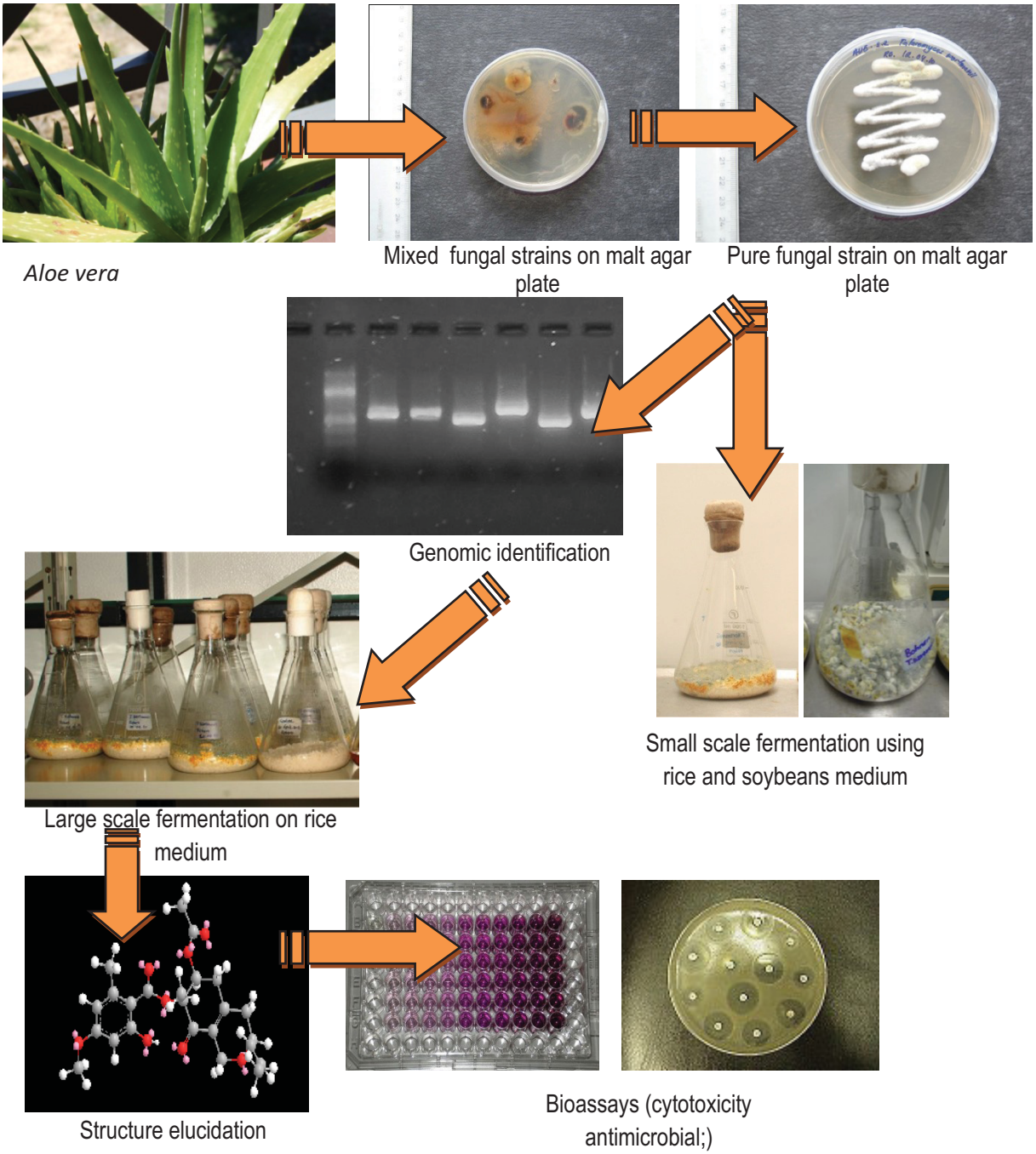

Flow chart of isolation of endophytic fungi, structural elucidation and bioactivity analysis.

Acknowledgements

When I visited Germany on 2006 for the very first time, I could never imagine that this country specially this city, Düsseldorf, would be my second home in the coming years. I still remember how all this have happened. One thing I know for sure, on this journey I have met many people who helped me to find my way and to whom I would like to express my gratitude.

First of all, I would like to thank to my daily supervisor and Promotor Prof. Dr. Peter Proksch, for offering me the valuable opportunity to purse the doctoral research and excellent working facilities in the Institute of Pharmaceutical Biology and Biotechnology, Heinrich-Heine University, Düsseldorf. I would also like to express my sincere gratitude and deep thanks for his kindness, friendly supervision, venerable guidance, productive discussions, charitable considerations and memorable supports during my study in Düsseldorf. You have been a very inspiring mentor to me through the year. Your optimisms, humor and enthusiasm help me to stay on track. Thank you very much!

I would like to acknowledge Prof. Dr. Matthias U. Kassack for conducting cytotoxicity assays and estimating my PhD study as second referee.

I would also thank for Deutscher Akademischer Austauschdienst (DAAD) for providing generous financial support up till the end of my study, here in Germany.

Then I would like to thank to Prof. Dr. Bin Gui Wang (Laboratory of Experimental Marine Biology; Institute of Oceanology, Chinese Academy of Science) for his valuable suggestions, constructive discussions and continuous encouragement. I will never forget how you help me through my difficulties.

I am deeply grateful to Dr. Abdessamad Debbab, my daily supervisor, for all the techniques and knowledge you showed me, together with your valuable help and scientific advices, writing manuscripts, as well as correcting this thesis.

I would also like to thank to Prof. Dr. H. Brötz-Oesterhelt, for very productive discussion regarding antibiotic assay of the isolated compounds of me. Using the facilities of lab lab, performing antibacterial and cytotoxicity assays I appreciated your advised to present my Poster in DGHF seminar in Hamburg. It still remains in my ears what you said "if I attended a conference I will be upset if I saw empty blackboard of a poster which is should be there. Your abstract has been chosen among anyone, so I want you go there and present the poster!". Thank you for a very good discussion we made so far.

Dr. Ilka Zerfass, my God, I cannot express anything except a thank you so much for your help during my experiments a very constructive discussions. you help me to conduct antibacterial assay of most of my isolated compounds as well as their mechanism of actions, I was really enjoy our coffee pause during the day as well as our journey to Uni-Bonn. I hope the best for you future career.

I would like to express my appreciation to Prof. Weihan Lin (National Research Laboratories of Natural and Biomimetic Drugs, Peking University, Health Science Center) and Dr. Victor Wray (Helmholtz Centre for Infection Research) for the distinguished NMR measurements and his significant opinion on the structure elucidation of compounds, Prof. W. E. G. Müller (University of Mainz) for conducting the cytotoxicity assays. I am also thankful to Dr. Peters and his colleagues (HHU-Düsseldorf) for 200 and 500 MHz NMR measurement as well as Dr. Keck and Dr. Tommes (HHU-Düsseldorf) for EI-mass spectra measurements.

I am grateful to Dr. Tibor Kurtán (Department of Organic Chemistry, University of Debrecen, Hungary) and his coworkers for their splendid CD calculation, as well as Dr. Amal Hassan for valuable advices and NMR.

I would like to deeply thank them for the pleased conversations. Thank you to Dr. Weeam Ebrahim and David Rönsberg , for showing me how to do the experiments, sending samples to HPLC-Dionex, preparing VLC column and many others at the very beginning of my study. I would like to write my thank you as well to Mustapha El Amrani, for showing me to isolate the endophytes from natural sources as well as how to isolate their DNA. My grateful to Dr. Daowan Lai as well for helping me to get through my problem solving some NMR spectra.

I am indebted to Mrs. Claudia Eckelskemper for her kind and generous help of administration, and the technical staff Mrs. Waltraud Schlag and Mrs. Katja Friedrich and Mrs. Simone Miljanovic, for their geniality and for supplying laboratory materials. My thanks are also to Mr. Klaus Dieter Jansen, Mrs. Eva Müller and Mrs. Heike Goldbach-Gecke for their help. Heike, thank you for performing antibacterial and cytotoxicity assay as well.

I would like to extend my sincere thanks to my past and present colleagues Dr. M. Bayer, Dr. Peter Sass, Cong-Dat Pham, Bartoz Lipowicz, Lena Hammerschmidt, Georgeos Daletos, Fatima Kabbaj, Dr. Festus Okoye, Mousa Tarabeen, Mona Elnekity, Mathias Onyebuchi, Gideon Alade, Justina Nwondo, Ilias Marmouzi, Liu Yang, Mi-Young Chung, Huiqin Chen, Kirsten Famulla, Andreas Marmann, Catherine Schumacher, Dhana Thomy, Ingo Kolb, Imke Form, Tatiana Medvedeva and Nihal Aktas and Rini Muharini for the very warm multicultural time I spent with them, for their help and assistance whenever I need. My thanks Hendrik Niemann for his help in writing and revising the German summary in this study, hey, we need to play tennis once more! As well as to Dat and Catalina for proof reading the thesis. Dhana, thanks for the preparing the bacteria!

I am also thankful to Prof. Dr. Claus Paßreiter for his safety instruction, and discussions about research as well.

My special thanks to my Erasmus friends all over Europe Marcella Chechova, for your hospitality your warm house every time I visited you in Praha, Czech. Praha 7 times, It is quite a lot! makes me know Praha as well as Düsseldorf. Maria Szasko (Budapest, Hungary), thank you for travelling me around Budapest, enjoying almost all hot spring basins around the city of Budapest, Arnold Kuzniar (Koralovo, Slowakia), Michaela Sava (Cluj-Napoca, Romania), Paulina Kurnicka (Poznan, Poland), Robert Kitchko, Jitka Simkova, Pavlina Sekaninová (Praha, Czech), Lenka Adamondyová (Barjedov, Slowakia), Jimmy Perdana, Audrey Jacky and Meliana Jonathan (Wageningen, the Netherlands), Tuncay Aydemir (Turkey) thank you for your friendship that you all offer to me genially. To Elsbieta Rhone (Warsaw, Poland), thank you for your kindness, attention, nice chatting and about every discussions during you're stayed in Düsseldorf. I rather enjoyed our tennis time.

Daniela Ackermann, you encourage me to stand and never surrender during my difficulties. Thanks for sharing knowledge and story sometimes during years past, I rather enjoy our coffee time in Hbf.

I would like to impress my special thank you to Antonius Ola and his family, Maria Renny and “die Kleine” Greis. You make me feel so welcome and enjoying your hospitality every time I visited you. I will never forget how Greis was always crying whenever she delivered me home…”ich bin sehr traurig wenn om Robert nach Hause gehen!”. Saya bersyukur dapat berbicara dengan bahasa ibu dengan kalian. To Csiska Wuwung, I finally found you at the end! Thank you for accompanying me from apart, when I am in writing. Thank you for your hope and discussion. Looking forward to see you soon!

At the end, I would like to express my deepest thanks and gratitude to my family, my father and mother, my sister Veronica and Fransisca, for encouraging and supporting me always in good and bad times until I am able to finish my study.

To all of you, thank you very much!

Curriculum vitae

PERSONAL INFORMATION:

Name : Robert Bara
Date and Place of Birth : 09.02.1976, Malang East Java, Indonesia
Nationality : Indonesia
Sex : Male
Marital Status : Single
Address : Studentwohnheim Campussüd
Universitätsstraβe 74; Zi. 67-00-20
40225 Düsseldorf, Germany
Mobile phone : +4915784329299
E-mail : Robert.bara@uni-duesseldorf.de
Robertbara@yahoo.com

EDUCATIONAL BACKGROUND:

Level	Date	Institute	Department	Place
PhD	October 2009-December 2012	Institute of Pharmaceutical Biology and Biotechnology Heinrich-Heine University Düsseldorf	Faculty of Mathematic and Natural Science	Düsseldorf, Germany
MSc	September 2005-September 2007	Wageningen University	Biotechnology	Wageningen-The Netherlands
BSc	July 1994-March 1998	Sam Ratulangi University	Marine Science specialized in marine pharmacology	Manado-North Sulawesi Indonesia

HONORS AND AWARDS:

Netherland Fellowship Programme (NFP-Scholarship) holder August 2005- September 2007
Deutscher Akademischer Austauschdienst (DAAD) scholarship holder September 2009-November 2012

WORK EXPERIENCE:

2001-2002 **Laboratory Assistant** Manado, North Sulawesi Indonesia
2002-2004 **Junior Scientist** Manado, North Sulawesi-Indonesia

- Secondary metabolites as hepatoprotector from *Nypa fruticans.*
- Screening Antimicrobial/antifungal from *Jatropha curcas* Linn.
- Antibacterial analysis from marine algae *Laurencia papillosa* and *Padina australis* collected from Tongkeina Bay North Sulawesi Indonesia

2004-date Lecturer Manado, North Sulawesi-Indonesia

- Marine Toxicology and Pharmaceutics Dept.

August 2006 – March 2007 Thesis (Wageningen Univ., The Netherlands)

- Study metabolic rate and metabolism in the sponges using ^{13}C labelled substrates for feeding (*ex-situ*)

January 2007-March 2007 Molecular Biology Toolbox (Wageningen Univ., The Netherlands)

- Marker development for detection of nodule senescence in plant symbiotic-nitrifying bacteria

April 2007- September 2007 Thesis (Wageningen Univ., The Netherlands)

- Nutrient_cycling genes in soil; PCR primer sets for quantification of amoA, nirK and nirS genes in organic soils.

April 2010 (HHU-Düsseldorf)

Isolation, identification and bioactivity screening endophytic fungi from Marroco and mangroves from Hainan Province, P.R. China

October 2011-November 2011 (HHU-Düsseldorf)

Isolation, identification and bioactivity screening endophytic fungi mangrove and teresterial plants growing in Bali island, Indonesia

February 2012-March 2012 (HHU-Düsseldorf)

Application of epigenetics compounds to enhance silence biotranformation pathway within fungal endophyte *T. wortmannii.*

2-3 March 2012

Youth Research Meeting, Muenster, Germany; Poster presentation

March 2012 (HHU-Düsseldorf)

Effect of co-culture growth of *T. wortmannii-F.tricintum* to enhance production of their new secondary metabolites.

April 2012 (HHU-Düsseldorf)

Effect of co-culture growth of *F.tricintum* with 3 different Streptomyces species to enhance production of their new secondary metabolites.

June 2012 (HHU-Düsseldorf)

Application of epigenetics compounds to enhance silence biotranformation pathway within fungal endophyte *F.tricintum*

30 September-3 October 2012

Jahrestagung der Deutschen Gesellschatft für Hyegine und Microbiologie (DGHM), Hamburg, Germany; poster presentation

ACTIVITIES AND MEMBERSHIP:

December 2005-December 2006
Member of International Student Panel at Wageningen University

December 2005-December 2006
Member of Wageningen Electronic Student Plaza (WESP) at Wageningen University

January 2006-January 2007
Treasurer of Indonesian Student Association at Wageningen University

August 2006
International Excursion Biotechnology in Switzerland

LABORATORY EXPERIENCE:

Laboratory courses at university:

Immunotechnology, Molecular Virology, Microbial Ecology, Applied Molecular Microbiology, Marine and Animal Cell Biotechnology, Cellular and Molecular Biology, Pharmacology, Toxicology, General Pathology, Genetics, Marine Microbiology, Genetic Design, Methods of Marine Natural Product Analysis, Biochemistry, Biology I and II, Chemistry I and II.

Laboratory techniques:

- NMR data analysis both ss-NMR/liquid-NMR (1D and 2D)
- Mass spectroscopic analysis (MALDI; ESI-MS; EI-MS)
- Antibacterial and antifungal assays (agar diffusions and MIC)
- Fungal endophytes cultivation from natural resources (both teresterial and marine source)
- PCR, qPCR (Real Time PCR) analysis
- Gel electrophoresis, ELISA, SDS-PAGE, Western Blotting
- Protein assays, protein isolation, immuno precipitation
- RNAi; gene regulation, gene knockdown.
- Cloning DNA/DNA Library construction
- Primer design.
- Animal cell culture
- Animal laboratory handling such as mice (*Mus musculus*), rats (*Rattus rattus*), guinea pig (*Cavia* sp.) and rabbits.
- Tissue preparation (fixation; slicing, staining etc) for histopathology analysis
- Viral vector delivery systems such as Vaccinia system, Bacmid system, etc.

Courses taken

M.Sc at Wageningen University

- Bioinformation Technology
- Microbial Ecology
- Applied Molecular Microbiology
- Molecular Virology
- Marine and Animal Cell Biotechnology

- Advance Practical Course of Microbiology
- General Medicine
- Bioprocess Design
- Immunotechnology
- Toolbox Molecular Biology

German language preparation course:

- March 2009-April 2009 German language course at Goethe Institute, Jakarta
- June 2009-September 2009 German language course at Speak + Write, Marburg, Germany

Journals:

Dihydroanthracenones from the Endophytic Fungus *Talaromyces wortmanii* with activity against multi-resistant *Staphylococcus aureus*
(*submitted to Journal of Medicinal Chemistry*)

Talaromins A and B, New Cyclic Peptides from the Endophytic Fungus *Talaromyces wortmannii* *(submitted to Tetrahedron letters*)

Bioactive metabolites from *Talaromyces wortmannii*, an endophyte of *Aloe vera* *(submitted to Journal of antibiotics)*

LANGUAGE SKILLS:

Indonesian: native
English: fluent in reading, writing, speaking
Germany: good in speaking writing and reading.
Dutch: intermediate

COMPUTER SKILLS:

MS-Office (Word; Excel; Power Point), Adobe Photoshop (design graphic)
Statistical analysis programs: SAS; SPSS.
Computer Installation; hardware and software.

HOBBIES:

- Sports: tennis, squash, badminton
- Reading
- Photography
- Nature and travelling